The Role of Emx1 and Emx2 in the developing chick telencephalon

Dissertation

Zur Erlangung des Doktorgrades

der Naturwissenschaften (Dr.rer.nat.)

der Fakultät für Biologie

der Ludwig-Maximilian-Universität München

Angefertigt am Max-Planck-Institut für Neurobiologie

in der Arbeitsgruppe Neuronale Spezifizierung

und in der GSF am Institut für Stammzellforschung

Julia von Frowein

München, Dezember 2004

If the brain were so simple we could understand it, we would be so simple we couldn't.

Lyall Watson

1 Table of content

2 Abstract

The forebrain is generated by distinct sets of precursor cells that express specific transcription factors as well as secreted signaling factors in a time- and region-dependent manner. The distribution of these factors is similar in the avian and mammalian forebrains.

In this work I aimed to examine the molecular mechanisms regulating telencephalic patterning. Therefore, I first compared the expression pattern of homeobox transcription factors, known to play crucial roles in regionalization of the forebrain, such as Emx1 and Emx2. This analysis showed particularly intriguing domains in the developing telencephalon expressing either only Emx2, such as the dorso-ventricular ridge (DVR) and the cortical hem, both genes, such as the hippocampus and the pallium or none, such as the subpallium and the choroid plexus (ChP). Taken together with other expression patterns I could conclude that the DVR, the nature of which was debated for a long period of time, displays a dorsal nature and that the pallial/subpallial boundary is located between DVR and subpallium.

Next, I aimed to examine the role of Emx1 and Emx2 in the specification of these distinct regions. Therefore, I used a misexpression approach targeting Emx1 and Emx2 into the anlage of the choroid plexus (ChP) where these transcription factors are normally not expressed. In this region normal development was disturbed. The normally non-neuronal, thin morphology of the ChP with a low rate of proliferation and the characteristic expression of Otx2 and Bmp7 was lost. Instead, the rate of proliferation and the thickness of the tissue were increased and rather displayed "hem-like" properties. Instead, the Otx2-positive region of the ChP was shifted beside the region of ectopic Emx1/2-expression and exhibited intermediate properties, with features of ChP-tissue like Otx2 and Bmp7-expression, but also features of the cortical hem with a higher rate of proliferation and increased thickness of tissue.

Thus, Emx1 and Emx2 play a key role in instructing dorsal neuroepithelium to proliferate. The misexpression of these genes is sufficient to convert non-neuronal ChP-tissue into neuroepithelium. Ectopic expression of Emx1/2 in the dorsal pallium, its normal region of expression, also displayed alterations. Ectopic Emx-expression blocked the expression of the neurogenic transcription factor Pax6 and suppressed neuronal differentiation. This change of neuronal differentiation could be caused by reduction of Pax6.

Taken together, Emx1 and Emx2 are two potent factors that can change regional identity, enhance proliferation and block neuronal differentiation.

3 Zusammenfassung

Das Vorderhirn wird von bestimmten Populationen von Vorläuferzellen gebildet, die unterschiedliche Transkriptionsfaktoren und morphogenetische Faktoren in einem charakteristischen räumlichen und zeitlichen Muster exprimieren. Diese Transkriptionsfaktoren sind im Vorderhirn von Maus und Huhn ähnlich verteilt.

Ziel dieser Arbeit war die Untersuchung von molekularen Mechanismen welche die Musterbildung im Telencephalon regulieren. Dafür habe ich zunächst die Expressionsmuster von Homeobox Transkriptionsfaktoren, wie Emx1 und Emx2, verglichen, die eine entscheidende Rolle bei der Regionalisierung des Vorderhirns spielen. Die Analyse zeigte eine regionsabhängige Expression von Emx1 und Emx2. Im Dorso-ventricular ridge (DVR) und im kortikalen Saum wurde ausschließlich Emx2 exprimiert, während im Hippocampus und im Pallium Emx1 und Emx2 exprimiert wurden. Im Subpallium oder Choroiden Plexus (ChP) hingegen wurde weder Emx1- noch Emx2- Expression detektiert. Die Region des DVR, dessen Zuordnung lange umstritten war, konnte aufgrund von Expressionsanalysen weiterer Transkriptionsfaktoren dem Pallium zugeordnet werden. Die palliale/supalliale Grenzregion des Hühnchenvorderhirns befindet sich somit zwischen DVR und Subpallium.

Neben der Analyse der Expressionsmuster von Emx1 und Emx2 wurde auch deren Rolle bei der Spezifizierung dieser speziellen Gehirnregionen untersucht. Dafür habe ich Misexpressions-Experimente durchgeführt. Emx1 und Emx2 wurden in die Anlage des Choroiden Plexus (ChA) eingebracht, eine Region im Telencephalon, die normalerweise keines dieser Gene exprimiert. Die anschließende Untersuchung zeigte, dass die normale Entwicklung des ChP nicht mehr stattfinden konnte. Der ChP, ein nicht-neuronales, schwach proliferierendes Gewebe, in dem unter anderem Otx2 und Bmp7 exprimiert werden, konnte durch die Überexpression von Emx1 und Emx2 missspezifiziert werden. Die Expression von Otx2 und Bmp7 wurde unterdrückt, die Proliferationsrate stieg an und die Dicke des Gewebes nahm zu, was den Eigenschaften des kortikalen Saums entsprach. Die Otx2-positive ChP-Region wurde neben die ektopisch Emx1/2-exprimierenden Region verschoben. Dort zeigte sich ein intermediärer Phänotyp, der sowohl durch Eigenschaften von ChP-Gewebe (Otx2- und Bmp7-Expression) wie auch von Saumgewebe (erhöhte Proliferationsrate und Gewebedicke) charakterisiert war.

Somit konnte gezeigt werden, dass Emx1 und Emx2 eine Schlüsselrolle bei der Instruktion zur Proliferation von dorsalem Neuroepithelium spielen. Die Misexpression dieser Gene ist ausreichend um nicht-neuronales ChP-Gewebe in Neuroepithelium umzuwandeln.

Weiterhin konnte durch Überexpression von Emx1 und Emx2 im Pallium, wo diese Gene normalerweise exprimiert werden, eine Suppression des dorsalen neurogenen Transkriptionsfaktors Pax6 erzielt werden. Der Verlust von Pax6 ist die mögliche Ursache für die verminderte Differenzierung zu Neuronen. Die Ergebnisse dieser Arbeit zeigen, dass Emx1 und Emx2 zwei potente Faktoren sind, die die Regionalisierung beeinflussen, die Proliferation erhöhen und außerdem einer neuronalen Differenzierung entgegenwirken.

4 Introduction

The vertebrate forebrain is one of the most complex but also most fascinating biological structures and we are still far away from understanding how its complicate organization is achieved during development. However, the molecular mechanisms underlying its formation are very similar in all developing tissues.

4.1 General development of the regions of the central nervous system

The central nervous system (CNS) develops from the neural plate, a structure of ectodermal origin receiving inductive signals from the mesoderm. The edges of this neural plate fold up and close to form the neural tube (Fig.1). The neural tube then starts to develop along the anterior/posterior axis. From the anterior (rostral) pole, the differentiation proceeds to the posterior (caudal) pole. At the rostral end three primary vesicles develop that will later give rise to the forebrain (prosencephalon), midbrain (mesencephalon) and hindbrain (rhombencephalon; Fig.2). The forebrain further differentiates into the diencephalon and the telencephalon at the most rostral position with its characteristic two hemispheres.

4.2 Patterning and regionalization

The formation of the nervous system has to be strictly controlled to allow a temporally and spatially correct generation of different cell types. Thus, the nervous system develops along two axes: the anterior/posterior (A/P) and the dorso/ventral (D/V) axis. Regionalization along the A/P axis divides the neural tube into four major divisions: forebrain, midbrain, hindbrain and spinal cord, which can already be detected at neural plate stage. Later in development D/V patterning establishes distinct regions that develop dorsally and become delineated from those differentiating ventrally. In this way cells acquire a distinct regional identity. The specification of regions along the A/P and D/V axis is controlled by the action of organizing signals (Fig.3; Jessell, 2000; Lumsden and Krumlauf, 1996; Rubenstein et al., 1998; Stern, 2001; Wolpert, 1969).

These organizing signals are secreted molecules belonging to the families of Fibroblast growth factors (Fgfs), Sonic hedgehog (Shh), Wingless-Int proteins (Wnts) and Bone morphogenic proteins (Bmps):

Wnt-molecules are cysteine-rich secreted glycoproteins that regulate multiple processes during development, like proliferation and cell fate in the dorsal neural tube (Ikeya et al., 1997; Lee and Jessell, 1999; Megason and McMahon, 2002; Wodarz and Nusse, 1998). Nineteen Wnt-genes have been identified so far (Cadigan and Nusse, 1997; Nelson and Nusse, 2004).

Bmps belong to the transforming growth factors-β (TGF-β) superfamily and are known to be important mediators for the development of the nervous system. They are involved in processes like cell proliferation, differentiation and apoptosis. By structural similarities the vertebrate Bmps are subdivided into the dpp family (Bmp2, 4) and the 60A family (Bmp5-8) and the more distant activin (Zhao, 2003). Several Bmps are detectable in the non-neural ectoderm adjacent to the neural plate and later on in the dorsal midline of the neural tube (Tanabe and Jessell, 1996).

Fgfs constitute a large family of polypeptide growth factors and are involved in diverse processes, such as cell proliferation, migration, differentiation, cell survival, chemotaxis and apoptosis (Bottcher and Niehrs, 2004; Dono, 2003; Ford-Perriss et al., 2001).

Shh, a member of the Hedgehog family of intercellular signaling molecules has been shown to regulate cell fate specification, cell proliferation and cell survival mainly in the ventral neural tube (Ingham and McMahon, 2001).

At neural plate stage two local signaling centers have been identified to play a role for A/P patterning: the anterior neural ride (ANR) and the mid/hindbrain junction (isthmus; Houart et al., 1998; Joyner, 1996; Joyner et al., 2000; Shimamura and Rubenstein, 1997). The ANR controls forebrain development and the isthmus is involved in the formation of midbrain and cerebellum. Fgf3, 8 (Fig.3A; Crossley et al., 2001), Chordin and Noggin are factors that are secreted from the ANR (Fig.3A) and promote anterior fate by regulating the expression of transcription factors (TFs) like Bf1, Nkx2.2, Nkx2.1, Otx1 and Emx2 that are involved in the specification of the anterior forebrain (Fig.3C; Rubenstein et al., 1998; Shimamura et al., 1995). The graded expression of several other Wnt- and Bmp-antagonists allows stronger Wnt- and Bmp-signaling in the caudal region (Chapman et al., 2004; Chapman et al., 2002; Wilson and Houart, 2004).

As development proceeds, the neural plate folds up and gives rise to the neural tube. Regions located medially in the neural plate are now located ventrally and regions located at the lateral edge move into the dorsal region, giving rise to two new signaling centers the roof plate dorsally and the floor plate ventrally (Fig.3B,D). Roof plate and floor plate regionalize the neural tube into discrete domains along the D/V axis through the action of secreted morphogenetic factors (Fig.3B). In the forebrain this results in the formation of the subpallium ventrally and the pallial domains dorsally.

The expression of members of the Bmp- and Wnt-gene family (Altmann and Brivanlou, 2001; Furuta et al., 1997; Lee and Jessell, 1999) from the roof plate have been suggested to play roles in the specification of dorsal fate by inducing transcription factors like Emx-genes and Ngn2 (Fig.3D; Wilson and Rubenstein, 2000). Signals secreted from the floorplate, like Shh induce ventral characteristics by regulating the expression of Nkx 2.1, Dlx-genes and Mash1 (Fig.3D; Lumsden and Krumlauf, 1996; Tanabe and Jessell, 1996).

Thus, by signaling from those organizing centers a distinct pattern of transcription factors is established that controls the generation of distinct regions in the forebrain. This finally results in an architecture, axonal connectivity and a distribution of cell types characteristic for this area. The precise molecular mechanisms being involved in this multi-step process are still not fully understood and need to be further analyzed. The telencephalic signaling centers, which are involved in regulating the basic patterning, are very similar in mouse and chick and therefore hint to a general mechanism in both species.

4.3 Regions of the forebrain

In this way the distinct regions of the forebrain are specified and delineated from each other. In vertebrates each cerebral hemisphere of the forebrain consists of the dorsal pallium (avian wulst/mammalian cortex), the ventral subpallium (mammalian striatum: composed of medial ganglionic eminence (MGE) and lateral ganglionic eminence (LGE)) and midline-structures that bifurcate the brain into two hemispheres. Birds possess an additional structure called the dorso-ventricular ridge (DVR; ventral pallium) located between the pallium (avian wulst) and the subpallium (Fig.4, 5).

While the main structure for information processing resides in mammals and birds in the telencephalon, these vertebrate classes use different telencephalic regions of which the homology is not clear. The mouse forebrain mainly consists of two major parts, the layered pallium (cortex), which processes sensory and motor information and the nuclear subpallium (striatum), which controls the motor system. The avian DVR is involved in processing visual, somatosensory and auditory information, while the avian wulst is referred to as the telencephalic visual area (Fig.4; Deng and Rogers, 2000). Former analyses have already described the dual role of the DVR, which shows dorsal as well as ventral features and one could allocate this structure to the pallium (Puelles et al., 2000), subpallium (Ariëns Kappers, 1936) or characterize it as an intermediate structure like

an enlarged boundary-region (Fernandez et al., 1998). On the one hand it processes cortical functions and expresses dorsal markers, but on the other hand it is organized in patch (nuclear cell clusters) and matrix (surrounding grey matter) like the subpallium (Striedter, 1997). To obtain clearer evidence for a dorsal, ventral or intermediate nature of the DVR, I analyzed the expression of several dorsal and ventral markers.

These regions of the avian and mammalian forebrains are generated in a similar way: Cells located in the ventricular zone (VZ), the layer directly lining the ventricular surface, strongly proliferate and produce large amounts of precursor cells as well as differentiating neurons that migrate outward to form distinct layers or structures of the brain. Precursor cells either remain in the VZ or move to the adjacent subventricular zone (SVZ), a second proliferative layer (Fig.4; Boulder Committee, 1970; Noctor et al., 2004; Smart, 1976), which is most prominent in the subpallium of both species.

In mammals the six-layered cortex develops in a strict inside-out mode, which means that cells generated later in development accumulate on top of earlier born neurons (McConnell, 1989). Neurons are generated between E12-18, while first astrocytes start to be detectable at E16 (Cameron and Rakic, 1991; Chenn and McConnell, 1995; Qian et al., 1998; Qian et al., 2000). The avian pallium is generated similarly compared to the mammalian cortex. Neurogenesis of the avian wulst of the chick takes place between E4 and E9, while most neurons are born on E6 and E7 (Tsai et al., 1981a). Most of the glial cells are born after E10 (Tsai et al., 1981a). According to Tsai et al., (1981a; 1981b) the avian telencephalon develops in an outside-in mode, where young neurons usually accumulate below older ones. Contradicting the findings of an "outside-in" generation of the avian brain, are the observations made by Striedter and Keefer (2000), who demonstrated that many cells in the avian wulst migrate past older ones, which is proposed to be accomplished along radial glial fibers (Medina and Reiner, 2000; Striedter and Beydler, 1997). However, the regions in the avian and mammalian forebrain develop into slightly different structures, of which the affiliation of homology has not been completely clarified yet.

The most medial part of the mammalian and avian forebrain is called midline-region and it is composed of the hippocampus (HC), located closest to the medial pallium, the cortical hem (CH) intermediately and the choroid plexus (ChP) and choroidal roof (r) developing most medially in the midline-region. The hippocampal complex composed of the dentate gyrus and CA fields is an important structure for learning and memory (Abel and Lattal, 2001; Martin et al., 2000). The

cortical hem has been proposed to serve as a signaling center by expressing several members of the Wnt-family (Wnt2b, Wnt3a, Wnt5a, Wnt7b, Wnt8b; Garda et al., 2002; Grove et al., 1998). Some studies have provided evidence that Wnt is important for the development of the medial pallium (Roelink, 2000). The mature choroid plexus, a non-neuronal epithelium secretes the cerebrospinal fluid (CSF; Fig.5) and thus might be responsible for maintaining a proper pressure in the ventricles. Furthermore, it serves as a source for Bmps (Furuta et al., 1997).

This midline-region develops from the medial region of the telencephalic vesicle. In the chick forebrain around embryonic day 4 (E4) the tissue located most medially already appears distinct from the adjacent tissue by a slightly thinner morphology. This thin tissue will later give rise to the choroid plexus and choroidal roof and therefore I will refer to it as choroidal anlage (ChA). Already at this stage the tissue adjacent to this choroidal anlage exhibits characteristics of the cortical hem.

4.4 Migration

The development of these distinct regions in the forebrain is also characterized by distinct modes of cell migration. Neurons, born in the VZ, either migrate radially to form the different cortical layers or they move tangentially, orthogonal to the direction of radial migration, and in this way manage to migrate over long distances e.g. from the subpallium to the pallium. Both modes of migration have been described in mouse and chick (Anderson et al., 1997; Cobos et al., 2001a; Marin and Rubenstein, 2003; Medina and Reiner, 2000; Murakami and Arai, 2002; Striedter and Beydler, 1997; Striedter and Keefer, 2000).

4.4.1.1 Radial migration

The development of the cortical layers involves at least two different modes of radial migration. At early stages of corticogenesis, cells migrate via somal translocation to form the preplate (PP), the first layer generated above the VZ (Morest, 1970). This mechanism seems to be independent of radial glia cells (Miyata et al., 2001; Nadarajah and Parnavelas, 2002). These cells extend a long process that terminates at the pial surface and a short ventricular process attached to the ventricular surface (Brittis et al., 1995; Marin and Rubenstein, 2003; Miyata et al., 2001; Morest, 1970; Nadarajah et al., 2001). The translocating cells loose their contact to the ventricular surface and their leading process becomes progressively shorter, lifting the soma basally in an apparently continuous movement (Nadarajah et al., 2001). The second mode of radial migration is used for the

formation of the cortical plate (CP; see Fig.4). Neurons, born in the VZ, use radial glial cells to migrate to their final destination. These cells have a short leading process and migrate forward in a short and rapid way which alternates with a longer stationary phase (Nadarajah et al., 2001).

4.4.1.2 Tangential migration

Three different types of tangential migration can be observed dependent on the substrate the cells migrate through. *In vitro* precursor cells from E14 MGE and LGE explants migrate through matrigel arranged in chains (Wichterle et al., 1999). This homotypic chain migration, also observed when neural precursor cells are grown as neurospheres was demonstrated to be regulated by integrins, a group of adhesion molecules (Hynes, 1992; Jacques et al., 1998).

Other tangentially migrating neurons use growing axons to find their final position, which is e.g. the case for neurons expressing Gonadotropin-releasing hormone (GnRH). These cells are derived from the nasal placode and reach the forebrain by following the nasal septum, crossing the cribiform plate under the olfactory bulb and finally migrate into the forebrain along vomeronasal (VMN) axons (Marin and Rubenstein, 2003; Wray, 2001).

A large number of cells rather migrate individually, not following any cellular substrates or following substrates that have not been identified so far. This type of tangential migration can be observed when cells move from the subpallium to the pallium. The subpallium, specifically the MGE in the mouse and the pallidum (PA) in the chick, is the main source of GABAergic interneurons migrating into the cortex and hippocampus (Cobos et al., 2001a; Lavdas et al., 1999; Sussel et al., 1999; Wichterle et al., 1999; Wichterle et al., 2001). The interneurons migrate along restricted routes towards the cortex. In the forebrain of the mouse they migrate superficially through the marginal zone (MZ), intermediately through the subplate (SP) and deeply through the SVZ (Fig.6B; DeDiego et al., 1994; Denaxa et al., 2001; Lavdas et al., 1999; Marin and Rubenstein, 2001). In the chick, neurons also take three different routes, through the MZ, the mantel zone (M) and the SVZ (Fig.6A; Cobos et al., 2001a). Semaphorins have been suggested to play a role in directing the migration of neurons (Polleux et al., 1998; Polleux et al., 2000).

However, cell migration is not occurring without restraints. Boundaries along the A/P and D/V axis have been described in the hindbrain between the rhombomeres (Guthrie and Lumsden, 1991) and in the diencephalon (Zona Limitans Intrathalamica, ZLI; Figdor and Stern, 1993; Zeltser et al., 2001), which exhibit lineage restriction and prevent cell mixing. In the forebrain of mice a dorso-ventral boundary forms, restricting dorsal cells from migrating into the ventral direction, while it

allows a prominent cell migration from the subpallium into the pallium (Chapouton et al., 1999; Chapouton et al., 2001; Sussel et al., 1999; Wichterle et al., 1999). In mammals this boundary is composed of a radial glia fascicle (Matsunami and Takeichi, 1995; Stoykova et al., 1996; Stoykova et al., 1997). Since the avian and mammalian forebrains exhibit structural differences, such as the region of the DVR, it is interesting to investigate the question if the boundaries in different vertebrates are located at homologous regions.

4.5 Emx1 and Emx2, two homeobox transcription factors

My research mainly concentrated on the homeobox transcription factors Emx1 and Emx2, which have been shown - together with Otx homeobox genes - to be crucial regulators of forebrain development (Acampora et al., 1998; Acampora et al., 1997; Acampora et al., 1995; Crossley et al., 2001; Simeone et al., 1992a; Simeone et al., 1992b). Emx1 and Emx2 also seem to specify the dorsal region of the forebrain (Bishop et al., 2002; Mallamaci et al., 2000b; Muzio and Mallamaci, 2003). Both genes are expressed from early stages in overlapping regions in the dorsal telencephalon, including the midline-structures such as cortical hem and hippocampal anlage, but excluding the midline-structure that develops into the ChP and roof. In particular there are small territories adjacent to the Emx1/2 double-positive region that lack Emx1-expression. These are the regions of the pallial/subpallial boundary (Muzio et al., 2002) and the medial part of cortical hem (Tole et al., 2000; Yoshida et al., 1997). Emx1 and Emx2 represent homologues of the *Drosophila empty spiracles* (ems) head-gene and share an identity of 80% at the amino-acid level with the ems homeodomain. In Drosophila, mutations in the ems-gene lead to a loss of the anterior cephalic segments, where this gene is normally expressed (Hirth et al., 1995).

4.5.1 Expression pattern of Emx1 and Emx2 in the forebrain of the mouse

In the mouse, Emx1 and Emx2 are expressed in a subset of precursor cells located in the VZ of the dorsal telencephalon. These two TFs are expressed in a descending caudo/medial to rostro/lateral gradient and thus show their strongest expression caudally in the midline-structures (Boncinelli, 1999; Finkelstein and Boncinelli, 1994; Gulisano et al., 1996; Mallamaci et al., 1998; Simeone et al., 1992a; Simeone et al., 1992b). Their expression starts prior to neurogenesis at E9 in the mouse telencephalon, immediately after the neural tube has closed and the expression covers most of the cortex. A subset of precursor cells as well as postmitotic pyramidal neurons express Emx1 (Chan et al., 2001). Emx2 is already detectable at E8, in the latero/caudal forebrain primordium and later it

covers the entire cortex. The expression of Emx2 peaks at E12 and disappears until E17 (Simeone et al., 1992a). Emx2 is not only expressed in the VZ but also in the nuclei of Cajal-Retzius (CR) cells and in the most marginally located cortical plate neurons, where expression is only detected in the apical dendrites (Mallamaci et al., 2000a). In few adult regions Emx2 is still detectable, like the adult SVZ of the lateral ventricles and the dentate gyrus of the hippocampus, notably the only zones where neurogenesis continues lifelong (Gangemi et al., 2001).

4.5.2 The role of Emx1 and Emx2 during forebrain development

4.5.2.1   Emx1-, Emx2-, Emx1/2- mutant mice

The inactivation of the Emx2-gene has demonstrated important contribution to corticogenesis (Pellegrini et al., 1996; Yoshida et al., 1997). Already at E12 the cerebral hemispheres and the olfactory bulbs are reduced in size. The hippocampus is smaller and the dentate gyrus is missing. Emx2-mutants also lack the uro-genital tract at this age and die at birth (Fig.7). Only subtle defects could be detected in the adult Emx1-mutant, which might be attributable to its later expression (Yoshida et al., 1997).

In the Emx1/2 double-mutants the defects are much stronger than in the single mutants. Emx1/2 double-mutant mice show small cerebral hemispheres, no hippocampus, cortical hem or ChP and the remaining tissue of the medial wall does not invaginate (Fig.7; Bishop et al., 2003; Pellegrini et al., 1996; Shinozaki et al., 2002; Yoshida et al., 1997). This suggests a redundancy between Emx1 and Emx2 in most of the cortical region. The small size of the ventricles could be due to a loss of CSF, normally secreted by the choroid plexus. This loss of the midline-structures seems to be compensated by an extension of the telencephalic roof. Since the cortical hem signaling center and the ChP do not develop, two major signaling sources for Wnt and Bmp are lost (Shinozaki et al., 2004). The loss of the hem also leads to a lack of Cajal-Retzius cells because the hem has recently been discovered as the main source for this cell type (Shinozaki et al., 2002; Takiguchi-Hayashi et al., 2004).

4.5.2.2   Emx1/2-overexpression *in vitro*

Heins et al. (2001) investigated the role of Emx1 and Emx2 in cell division and proliferation *in vitro*. He showed that Emx2-overexpression promotes symmetric cell division in the cortex, thus enhancing the number of multipotent cells. In contrast, Emx2-overexpression had no effect on the

proliferation of striatal cells (Heins et al., 2001). The effect in the cortex was most prominent in the rostral region at E16, which normally contains fewer Emx2-positive cells than the caudal part. Here, a 4-fold increase of the clonal size, the progeny generated by a single precursor cell, was observed at E16. In his studies Emx1 did not effect the proliferation but kept the cells in a rather undifferentiated state. However, if Emx1 and Emx2 influence cell proliferation *in vivo* is not known yet. To answer this important question, I overexpressed Emx1 and Emx2 in the developing telencephalon in chick embryos *in ovo*.

The main aim of my thesis was to study the role of Emx1 and Emx2 during chick forebrain development. Several studies of Emx1-, Emx2-mutant and Emx1/2 double-mutant mice have already described several functions of these genes during telencephalic development. However, mutant analyses reveal not all functions of the genes knocked out, but can be studied in overexpression or misexpression experiments. I performed these overexpression studies *in vivo* using *in ovo* electroporation of chick embryos. This is a very efficient tool to analyze the influence of a gene on regions where it is normally not or only weakly expressed. Even regions that express this gene can show alterations by ectopic overexpression. In my studies I focused on the influence of Emx1 and Emx2 on regionalization of certain forebrain areas and on their role in cell proliferation and differentiation.

5 Abbreviations

Ab	antibody
ANR	anterior neural ridge
A/P	anterior/posterior
bHLH	basic helix-loop-helix
Bmp	bone morphogenic protein
bp	base pairs
BrdU	5'-Bromo-2'deoxy-Uridine
ChA	choroidal anlage
ChP	choroid plexus
CH	cortical hem
ctx	cortex
Dkk	Dickkopf
DNA	desoxyribonucleic acid
DVR	dorso-ventricular ridge
Cad	Cadherin
CNS	central nervous system
CP	cortical plate
CSF	cerebrospinal fluid
di	diencephalon
DLHP	dorso/lateral hinge point
DMEM	Dulbecco's modified eagle medium
D/V	dorso/ventral
E	embryonic day
E1	early region1
EGFP	enhanced green fluorescent protein
FCS	fetal calf serum
Fgf	fibroblast growth factor
Fig.	figure
fp	floor plate
GE	ganglionic eminence
GFP	Green fluorescent protein
GnRH	gonadotropin-releasing hormone

H	hour
HC	hippocampus
HH	Hamburger Hamilton stage
IgF-II	Insulin-like growth factor II
Ig	immunglobulin
IRES	internal ribosome entry site
is	isthmus
IZ	intermediate zone
LGE	lateral ganglionic eminence
LV	lateral ventricle
mAb	monoclonal antibody
M	mantel zone
me	mesencephalon
MGE	medial ganglionic eminence
MHP	medial neural hinge point
MP	medial pallium
M-Phase	mitoses phase of the cell cycle
mRNA	messenger ribonucleic acid
MZ	marginal zone
n	number of samples
NE	neuroepithelium
NP	neopallium
Oc	optic cup
P	pallium
PA	pallidum
pAb	polyclonal antibody
PBS	phosphate buffered saline
PDL	poly-D-lysine
pfu	plaque forming unit
PP	preplate
pr	prosencephalon
r	choroidal roof
r1	rhombomer1

rh	rhombencephalon
RMS	rostral migratory stream
RNA	ribonucleic acid
RT	room temperature
SEM	standard error of the mean
Sfrp	secreted frizzled related protein
Shh	sonic hedgehog
SP	subplate
sp	secondary prosencephalon
S-Phase	DNA-synthesis phase of the cell cycle
Stdev	standard deviation
SVZ	subventricular zone
TF	transcription factor
TGF-β	transforming growth factors-β
VMN	vomeronasal
V	ventricle
VZ	ventricular zone
Wnt	wingless Int protein
WT	wildtype
ZLI	zona limitans intrathalamica
'	minute

6   Materials and Methods

6.1   Animals

Fertilized eggs (White Leghorn, Rhode Island Red, White Rock, Araucana) were obtained weekly from Firma Hölzl in Moosburg (Blütenstraße 22) and kept at 4°C. To start the development they were incubated horizontally at 37.8°C with a humidity of 55%. The first day of incubation was considered as embryonic day 0 (E0). The experiments were performed between E2 and E10. Chicken embryos can be staged precisely with the developmental table of Hamburger and Hamilton (Hamburger, 1951). For experimental analysis the embryos were decapitated and dissected immediately in Hanks Balanced Salt Solution (HBSS) containing 1% HEPES.

6.2   EGFP-adenovirus production

The EGFP-adenovirus was constructed by A.Gärtner (Chapouton et al., 1999). This adenovirus is lacking the "Early" region1 (E1) and is therefore replication incompetent. Infected cells cannot generate new virus. The EGFP-transgene is driven by the CMV-promotor and has been inserted into the viral vector by homologous recombination.

For virus production 293 cells, that stably express E1a and E1b (Graham, 1991) were grown until confluency. Virus (10^9 pfu) was added to the 293 cells. After 2-3 days, about 70% of the cells were detached from the culture plates. Cells were centrifugated (172 x g, 5 min, 4°C) and 10ml of medium, containing 10% glycerol, were added to the pellet, which could then be stored at –80°C. Freezing and thawing was performed three times. A following homogenizing step mechanically cracked the membranes of the cells. Debris was centrifugated (1550 x g, 15 min, 4°C) and homogenized again. The supernatant was then purified and concentrated using a CsCl-gradient: A 12ml ultracentrifugation tube was filled with 1.5ml of a 1.45g/cm^3 CsCl-solution, 2.5ml of a 1.32g/cm^3 and overlayed with the cell extract. The probes were centrifugated at 90.000 x g for 3-4 hours at 4°C. Adenovirus with a normal density of 1.34g/cm^3 forms a visible layer, which can be removed with a syringe. This solution containing the virus was applied onto a second CsCl-gradient (10mM Tris pH8) and centrifugated for 16-24 hours. The layer containing the adenovirus is easily recognizable and removable. CsCl was taken away by gelfiltration using an NAP-25 column. 10mM Tris/10% glycerol was used for elution. The virus was frozen in 10µl aliquots on dry ice and then stored at -80°C.

6.3   EGFP-adenovirus injections and migration analysis

To infect slices with an adenovirus, brain hemispheres of E7 chick embryos were cut frontally with a tissue chopper at 300µm thickness. The slices were collected in DMEM-medium with 5% FCS. For washing, the filter inserts were incubated in DMEM/FCS-medium and afterwards, 3-4 slices were transferred close to the centre of each Millipore insert of the 6-well plate, containing 1.5 ml DMEM/FCS-medium.

Different regions of the slices, like pallium, DVR and subpallium were stereotactically infected with the EGFP-adenovirus using capillaries with an opening of about 1mm. At different time points (24h, 48h, 72h) after infection, pictures of migrating, EGFP-positive cells were taken at the binocular.

To analyze the specificity of the infected site, tests with Cytochalasin D, a poison that inhibits actin polymerization and therefore disables cells to migrate (Cooper, 1987), were performed. Slices treated with Cytochalasin D should not show cells far away from the infected site, otherwise it would indicate a contamination of the medium with virus.

6.4   Construction of plasmids for electroporation

6.4.1   Pmes-Emx2

Emx2 was removed from the bluescript vector pBSKEmx2EP1 (4245pb) by digestion with XhoI and EcoRI. Additionally, DraI and SapI were used to cut the backbone of the bluescript vector to minimize the possibility for contamination with the bluescript. The size of Emx2 is 1326bp. Since PMES (5727bp) contains two SalI sites, it was partially digested with SalI for 30min. SalI and XhoI produce the same overlapping ends. In this way two fragments with the size of 3999bp and 1728bp appeared. The intention of the short incubation period was to disable a complete digest and produce a greater fraction of linerized plasmid when the enzyme only cut at one restriction site. 0.6µl of 0.5M EDTA were used to stop the restriction digest. The linerized band (5727bp) was removed from a 1% agarose gel and cleaned with the Qiagen gel extraction kit. Pmes was then digested with EcoRI for 3 hours, to cut away a small band of 10bp. The right band (5717bp) was separated in an agarose gel and afterwards cleaned with the gel extraction kit. For ligation the Pmes-vector and the Emx2-insert were mixed in 1:3-5 ratios and incubated with ligation buffer and T4 DNA ligase at 17°C over night. In order to decrease the volume for transformation I precipitated the DNA. The transformation was conducted with 50µl of TOP10 bacteria, plated and incubated over night. For

testing the colonies, Minipreps were performed and test-digestions with BamHI, AccI and EagI. To increase the amount of Pmes-Emx2 plasmid Midipreps were prepared (Fig.8A).

6.4.2 Pmes-Emx1

To remove Emx1 from the Pgem3-vector, Pgem3-Emx1 was digested with EcoRI and XbaI. PvuI was added to digest the backbone of the plasmid to minimize contamination with the bluescript vector. Pmes was first digested with XbaI for 3h for allowing a complete digest and then separated on an agarose gel. I cut out the higher band (5727bp) which resembled the linarized plasmid in comparison to the lower uncut supercoiled plasmid and purified the DNA by gel extraction.

Next, this band was enzymatically digested with EcoRI for 2h and the DNA was purified with the PCR Purification Set, to gain a higher amount of DNA. The ligation mix, that contained Pmes-vector and the Emx1-insert in a ratio 1:3-5, ligation buffer and T4 DNA ligase were incubated at 17°C over night. The transformation was performed with 25µl of TOP10 bacteria, 5µl of the ligation mix and SOB medium. To test the ligation, the amount of plasmid was increased by Minipreps and tested by digestion with BamHI. The correct band showed a size of 820bp. The amount of Pmes-Emx1 plasmid was increased by the preparation of Midipreps (Fig.8B).

6.5 Plasmid "preparation"

Plasmids received on filter paper were soaked in 50µl TE buffer or water for 30 minutes and subsequently centrifuged for 5 minutes at maximum speed. For transformation, 1µl of the elution or 10ng of plasmid DNA were added to 25µl of chemically competent TOP10 cells or to 100µl self made Dh5α E.coli and incubated on ice for 30 minutes. After a heat shock of 45 seconds at 42°C cells could recover for 10 minutes on ice. 1ml of LB-medium was added to the cells, which were then placed in a bacterial shaker at 37°C for 45 minutes. 50-100µl of the suspension were plated on LB-Agar plates containing antibiotics e.g. Ampicillin (50µg/µl) depending on the resistance gene encoded by the plasmid at 37°C over night. The next day one colony was picked and incubated for about 4 hours in 3-5ml LB-medium containing antibiotics (e.g. Ampicillin 50µg/µl). The preculture was added to 50ml of LB-medium containing antibiotics and over night incubated in the bacterial shaker at 37°C. Bacteria were harvested and plasmid DNA was purified following the Qiagen Midiprep protocol using a midi Tip100 column. The DNA pellet was dissolved in 200µl H_2O_{bidest} and the concentration was measured with the photometer at 260nm.

6.6 *In ovo* electroporation

The technique of *in ovo* electroporation is a method to efficiently transfer genes into developing chick embryos in order to analyze gene regulation, function and expression. The efficiency of expression of a reporter gene is enhanced by 10-1000 fold, using electroporation compared to DNA injection only (Jaroszeski et al., 1999; Mir et al., 1998; Somiari et al., 2000). The exposure to pulsed electric fields enhances the permeability of cell membranes and enables plasmids to cross cytoplasmic membranes. Different models try to explain the structural rearrangements of the lipid bilayer (Neumann, 1999; Weaver, 1996). The Neumann model proposes that the application of an electric field alters the distribution of ions at the inner surface of the cell membrane, which leads to a difference in the transmembrane potential. This induces electroporative deformations of the cell that elongates along the axis of the field. Thus, small hydrophobic pores are formed which enable the DNA to enter (Fig.9; Neumann, 1999).

Different parameters like thickness of tissue, conductivity of the environment and architecture of electrodes have to be combined and optimized with the parameters of the applied electric pulses like voltage, duration, frequency and total number of pulses to minimize cell damage and maximize the amount of gene delivery (Somiari et al., 2000).

6.7 Procedure for electroporation

6.7.1 Preparation of the embryos

The horizontally incubation of the eggs allows the embryo to be nested on the highest point on top of the yolk. A small amount of albumin has to be removed from the flat side of the egg at E2 (HH: 9-13) to enable the embryo to sink. A small piece of adhesive tape on the eggshell allows to easily cut a small window into the eggshell. If it is difficult to recognize the embryo or to count somites it is useful to underlay the embryo with Font India ink diluted 1:6 in PBS by using a syringe.

6.7.2 Injection of DNA-solution

The DNA-solution (2-5µg/µl) was mixed with Fast Green (0.1%), an indicator to color the DNA for the injection. Glass capillaries without filament were pulled (settings: heat 575; pull 255; velocity 50; time 120). Using a pulse generator I gave pulses with a pressure of 20-30psi and injected 0.2-1µl of the DNA solution into the telencephalic vesicle until the whole vesicle appeared to be green.

6.7.3   Electroporation

Platin covered gold electrodes were placed parallel to the tissue and 4-6 pulses were given by the stimulator in order to transfer the DNA to the side of the positive pole. For enlarging the region of misexpression the electrodes were slightly rotated after some pulses.

My optimized parameters of the stimulator were:

Frequency: 5Hz

Mode: 1/manual

Delay: 50ms

Width: 10ms

Voltage: 20-30V

Number of pulses: 4-6

The area of electroporation was determined according to the fate map analysis performed by (Cobos et al., 2001b). Since the pallial and midline-regions are not located dorsally at these early developmental stages, it is difficult to hit these regions, which are located more posterior along the neural ridge (Fig.10; Cobos et al., 2001b).

6.7.4   Post-electroporation treatment

The manipulated embryos were covered with 70µl of Penicillin/Streptomycin to minimize the risk of infection and the eggshell was carefully sealed with a piece of adhesive tape to prevent them from drying. Afterwards, the eggs were incubated again in order to let the embryos develop further. Two or four days later (which equals E4 or E6), depending on the experiment, the eggs were opened and the embryos were taken out, decaptured, tested for fluorescence and fixed for 2-4 hours in 4% PFA. Afterwards the heads or brains were cryoprotected by over night treatment with 20% sucrose at 4°C. Then the tissue was frozen in TissueTek and afterwards cut with a cryostat in 20µm thick sections collected on Superfrost Plus slides.

6.8   BrdU-Labeling

5-Bromo-2-deoxyuridin (BrdU); (Nowakowski et al., 1989) is a DNA base analogon, which is incorporated into the DNA during DNA synthesis (S-phase of cell cycle). In this way proliferating cells can be labeled. Therefore, 14-15µg BrdU (20µg/µl in H_2O with 0.01% Fast Green) were

injected into a vein of the chicken embryo developing on top of the yolk (Striedter and Keefer, 2000). Usually embryos with the age of 4-6 days (HH23 -29) were pulse labeled. 30 minutes to 6 days after injection the embryos were sacrificed.

6.9 *In situ* hybridization

6.9.1 Plasmid linearization

20 μg of plasmid-DNA were linerized with the appropriate enzyme (40 units) in a total volume of 50-60μl for 2.5 hours at 37°C. For purification of the linerized plasmid a phenol extraction was performed. Water was added up to 200μl, mixed with 200μl of Phenol/Chloroform/Isoamyalkohol (50:49:1) and strongly mixed for one minute. After centrifugation for five minutes in an Eppendorf centrifuge at maximum speed ($13.1x10^3$rpm), the water phase, which is the upper phase, had to be recovered. 1/10 vol. Sodium Acetat (3M) and 0.7 vol. Isopropanol had to be added and allowed to precipitate for 10 minutes at room temperature. After a centrifugation step of 15 minutes at maximum speed the DNA pellet was shortly washed with 70% Ethanol and subsequently resuspended in 20μl H_2O_{bidest}.

6.9.2 *In vitro* transcription

For *in vitro* transcription, the transcription mix (total 20μl), containing 1μg DNA, 2μl NTP mix (digoxygenin labeled UTP; DIG-UTP), 4μl 5x transcription buffer, 1μl RNAse inhibitor, 1μl T3,T7 or SP6 RNA-polymerase and RNAse-free water was incubated at 37°C for 2 hours. The reaction was stopped with 2μl 0.2M EDTA and the RNA was precipitated with 2.5μl 4M LiCl and 75μl pure Ethanol at -20°C over night or at –80°C for two hours. After centrifugation at 4°C for seven minutes the pellet was dissolved in 20μl RNAse-free water and 200μl hybridization buffer. The final probe should exhibit a concentration of around 100ng/μl.

Table of prepared *in situ* plasmids and antisense cRNA-probes

Plasmid	Vector	Insert	Digestion/ Transcription	Reference	Provider
Bmp7	pSK	0.7kb	XhoI/T7		A.Wizenmann
Cash1	pSK-	1.9kb (EcoRI)	XhoI/T3	UO1339	T.Reh
Dlx1	pBIISK-	960bp (XhoI+EcoRI)	EcoRI/T7		J.Rubenstein/ Debbie
Emx1	pSK	300bp	EcoRI/T7		E.Bell
Emx2	pKS		PvuII/T7		A.Lumsden/E.Bell
Fgf8 (S)	pBSK		PstI/T7		T.Edlund
Gli3	pBS SK	1.5kb (EcoRI/EcoRI)	EcoRV/T3		A.Wizenmann
Lhx2a			XhoI/T3		S.Richter
Msx2	pBSSK		HindIII/T3	(Graham et al., 1993)	A.Wizenmann/ A.Graham
Ngn1	pBSKS	1.3kb	SacI/T7	AF123883	S.Penez/ D.J.Anderson
Ngn2	pBSKS	0.8kb	SacI/T7	AF123884	S.Penez/ D.J.Anderson
Otx2			BamHI/T7		M. Wassef
Pax6	pBKS+		EcoRI/T7	M.Goulding	F.Schubert
Sfrp1	pBSKII	224bp	EcoRI/T7		L.W.Burrus
Ttr	PCRscript (Stratagene)		NcoI/T7	(Duan et al., 1991) X60471	M.Wassef
Wnt7b	pGem3zf	380bp	HindIII/T7		J.McMahon

6.9.3 *In situ* hybridization – non-radioactive

0.5-1µg of RNA anti-sense probe were diluted in 150µl hybridization buffer and heated at 70°C for 5 minutes to denature the RNA. The solution was applied on each slide and covered with a clean coverslip to prevent the sections from drying. Sections were incubated at 65°C over night in a box containing 1x SSC in 50% Formamide on whatman paper. The sections were washed 3-4 times with washing solution at 65°C, the first step lasting 10 minutes and the following steps each 30 minutes. These were followed by washing the sections in 1x MABT for 2 times lasting 30 minutes at RT. The blocking solution was applied for at least 1 hour at RT. Then, Anti-Digoxigenin Fab fragments coupled to Alkaline-Phosphatase, diluted in blocking solution (1:2500) were applied onto each slide (500µl). The sections were covered with a piece of parafilm and incubated in a humid chamber over

night at RT. After 4-5 washes in 1x MABT, each lasting 20 minutes, Alkaline-Phosphate staining solution was applied for 10 minutes at RT. NBT and BCIP were added to the staining solution (1ml of staining solution + 3.5µl NBT + 3.5µl BCIP) and 150µl were applied onto each slide, covered with a piece of parafilm. The incubation period depended on the quality of the probe and therefore varied between 2 to 24 hours. When the reaction was strong enough it was stopped by rinsing in staining solution and shortly in water. The slides had to be completely dry before mounting them with AquaPoly/Mount.

6.9.4 Whole-mount *in situ* hybridization

Young chicken embryos (HH9-21) were preferentially *in situ* hybridized as whole-mounts. After dissecting the embryos in PBS they were fixed in 4% PFA over night at 4°C. Two washing steps in PBT, each lasting 5 minutes, were performed at RT. It is important to puncture the head to avoid trapping of the reagents in the lumen. Embryos were dehydrated by taking them through a Methanol-series (25%, 50%, 75%, 100%), each step lasting 5 minutes (5'). An additional 100% Methanol step for one hour or over night was followed by taking them reversely through the Methanol-gradient (75%, 50%, 25%) for rehydration. After two washing steps in PBT (2 x 5'), 6% Hydrogen Peroxide in PBT was applied for 60 minutes, followed by three washing steps (3 x 5'). After the administration of detergent mix (3 x 20') the embryos were fixed again in 4% PFA, containing 0.2% Glutaraldehyde for 20 minutes at RT. Washing was performed (3 x 5') and pre-hybridization mix was applied for 60 minutes or over night at 70°C. This mix was replaced with preheated hybridization mix, containing 0.5 to 1µg RNA probe and incubated overnight at 70°C. For washing, preheated Solution X was administered for 15 minutes and four additional times for 30 minutes at 70°C. Three washing steps in 1x MABT (3 x 5') at RT were followed by a blocking step using 20% GS and 2% blocking solution in 1x MABT for 1-2 hours at RT. The antibody was added (1:2000) in blocking solution and the embryos were incubated over night at 4°C. Washing was performed in 1x MABT for 8 times, each step lasting 60 minutes and additional washing was performed over night at 4°C. After 3 washes in NTMT, embryos were incubated in NTMT with 3.5µl NBT and 3.5µl BCIP per 2-3ml at RT as long as the color reaction took place. The staining solution was replaced with PBT until it appeared clear and the Alkaline-Phosphatase reaction could be stopped by application of PFA over night at 4°C.

6.10 Immunocytochemistry

Cryosections were defrosted for 10 minutes and then rehydrated with PBS for 10 minutes at RT. As primary antibodies I used antibodies against transcription factors, proliferation-markers, differentiation-markers and cell subtype specific markers:

For the detection of transcription factors I used the polyclonal antibody (pAb) against Dlx (rbt, 1:75, 0.5% Triton-X100 (T), 10% NGS in PBS for 2 days), the pAb against Emx1 (rbt, 1:1000, 0.5% T, 10% NGS), the pAb against Emx2 (rbt, 1:4000, 0.2% tween TBS, 10% NGS), the pAb against Gsh2 (rbt, 1: 1000, 0.5% T, 10% NGS), the pAb against Pax6 (rbt, 1:300, 0.5% T, 10% NGS) and the pAb against Tbr (rbt, 1:200, 0.5% T, 10% NGS).

For the detection of proliferating cells, I used the monoclonal antibody (mAb) against BrdU (mouse IgG1; 1:10) to label cells that undergo DNA-synthesis and the pAb against the phosphorylated histone H3 (PH3; rbt; 1:200, 0.5% T, 10% NGS) to analyze cells in mitosis.

To label postmitotic neurons, markers like the pAb Map2 (mouse IgG1; 1:500, 10% NGS) and the pAb against NeuN (mouse IgG1; 1:50, 0.5% T, 10% NGS) were used.

To detect the electroporated cells I used the mAb and pAb against EGFP (mouse, IgG1, 1:300; rbt, 1:500 in 0.5% T, 10% NGS).

Certain subtypes of cells were labeled with the pAb against Blbp (rbt, 1:1500, 0.5% T, 10% NGS), the pAb against Calbindin (rbt, 1:500, 0.5% T, 10% NGS) and the mAb 142 against Reelin (mouse, IgG1, 1:500, 0.5 T, 10% NGS).

Usually the antibody mix was applied and incubated overnight at 4°C in a humid chamber. For some antibodies special pretreatments were necessary: All of the transcription factors and EGFP I pretreated for 15 minutes with 0.5% T and 10% NGS and NeuN even for 30 minutes.

Map2 had to be incubated with Ethanol-glacial acetic acid for 15 min at -20°C.

The staining signal for PH3 and Dlx was enhanced by boiling the sections in 0.01M Citrate buffer for 8 minutes.

To detect BrdU a series of pretreatments was necessary. Sections were treated with 0.5% T, 10% NGS for one hour, which permeables the membrane. This was followed by a denaturation step of the double-stranded DNA with 2N HCl for 30 minutes. To neutralize the acid, two washing steps of 15 minutes with 0.1M Sodium Tetraborat (pH 8.5) were necessary. The pretreatment has to be followed by three washing steps in PBS for 10 minutes before the staining could be performed.

The visualization of these antibodies was carried out by using secondary subclass specific antibodies coupled to Fitc, Tritc or biotinylated, which were applied onto the sections for 1h at RT. The monoclonal mouse antibodies were visualized by using anti mouse IgG1-Fitc (1:50)/ -Tritc (1:50)/ -biotinylated (1:250) and the polyclonal rabbit antibodies were detected by anti rabbit Ig-Fitc (1:50)/ -Tritc (1:50)/ -biotinylated (1:250). For the visualization of the biotinylated antibodies a third step, using streptavidin-AMCA (1:50)/ Fitc (1:100) was necessary.

Negative controls were performed to confirm a specific binding of the secondary antibody. This was controlled by using the secondary antibody only.

Primary antibodies (alphabetical order)

Name	Host-animal/ working dilution	Pretreatment	Marker	Supplier	Reference
Anti-BLBP	Rabbit (1:1500, 0.5% T, 10% NGS)		Brain Lipid Binding Protein, precursor cell subtypes	Nathaniel Heintz, Howard Hughes Medical Institute, Rockefeller University, New York, USA	(Feng et al., 1994) ; (Kurtz et al., 1994)
Anti-BrdU	Mouse IgG1 (1:10)	1h 0.5% T, 30' 2N HCl, 2x15' Borate buffer pH8.0	S-Phase marker	Bio-Science Products	
Anti-Dlx	Rabbit (1:75, 0.5% T, 10% NGS for 2 days)	Boiling in 0.01M Sodium-Citrate buffer, pH6.0 for 8' at max in the microwave enhances signal	TF expressed in precursor and postmitotic cells in MGE and LGE; tangentially migrating cells	Robert Hevner, Dep. Of Pathology, Univ. Of Washington School of Medicine, Harborview Medical Center, Seattle, WA, USA	
Anti-Emx1	Rabbit (1:1000, 0.5% T, 10% NGS, 2.Ab biot.)		Dorsal TF expressed in precursor cells and pyramidal neurons	Giorgio Corte, Department of Oncology, Biology and Genetics, University of Genova Medical School, Genova, Italy	

Anti-Emx2	Rabbit (1:4000, 0.2% Tween TBS, 10% NGS)		Dorsal TF expressed in precursor cells and Cajal-Retzius cells	Osamu Hatano, Department of Anatomy, Nara Medical University, 840 Saijo-machi, Kashihara, Nara-634-8521, Japan	
Anti-EGFP	Rabbit (1:500, 0.5% T, 10% NGS)	15' in 0.5%T/ 10%NGS	Cells containing the EGFP-gene	RDI	
Anti-EGFP	Mouse IgG1 (1:300, 0.5% T, 10% NGS)	15' in 0.5%T/ 10%NGS	Cells containing the EGFP-gene	Chemicon	
Anti-Gsh2	Rabbit (1:1000, 0.5% T, 10% NGS)	15' in 0.5% T/ 10% NGS	TF expressed in precursor cells of subpallium	Kenneth Campbell, Division of Developmental Biology, Cincinnati Children's Hospital Medical Center, Cincinnati, USA	
Anti-Map2	Mouse IgG1 (1:500, 10% NGS)	15': -20°C Acid-EthOH	Neuronal marker	Sigma	
Anti-NeuN	Mouse IgG1 (1:50, 0.5% T, 10% NGS)	30' 0.5% T, 10% NGS	Neuronal marker	Chemicon	(Mullen et al., 1992)
Anti-Pax6	Rabbit (1:300, 0.5% T, 10% NGS)	15' in 0.5% T/ 10% NGS	Dorsal TF	Babco	
Anti-PH3	Rabbit (1:200, 0.5% T, 10% NGS)	Boiling in 0.01M Sodium-Citrate buffer, pH6.0 for 8' at max in the microwave	M-Phase marker	Upstate Biotech	(Hendzel et al., 1997)
Anti-Reelin (142)	Mouse IgG1 (1:500, 0.5% T)		Cajal-Retzius cells in the cerebral cortex	André Goffinet, University of Louvain, Medical School, Brussels, Belgium	(de Bergeyck et al., 1998)

| Anti-Tbr | Rabbit (1:200, 0.5% T, 10% NGS) | 15' in 0.5% T/ 10% NGS | TF expressed in postmitotic cells in the cortex | Marta Nieto, Beth Israel Deaconess Medical Center, Howard Huges Medical Institute, Harvard Medical School, Boston, USA | |

Table 4.3 Secondary antibodies (alphabetical order)

Name	Supplier
Anti-rabbit Ig FITC / TRIC	Jackson ImmunoResearch / Dianova
Anti-rabbit Ig biotinylated Streptavidin AMCA Streptavidin Fitc	Vector Laboratories
Anti-mouse IgG1 FITC / TRIC / biotinylated	Southern Biotechnology Associates

6.11 Nuclear stain

To be able to count the number of cells I used DAPI (4', 6-diamidino-2-phenylindole) as a nuclear stain. DAPI forms strongly fluorescent DAPI-DNA complexes by attaching in the minor grove of A-T rich sequences of DNA. This can be visualized at a wavelength of ~460nm. The application of DAPI is usually the last step of the staining procedure. A solution of 1µg/ml DAPI in PBS is dropped onto the sections and incubated for 5-10 minutes at RT.

6.12 Data analysis

6.12.1 Confocal microscope

To analyze the cryostat sections of electroporated brains carefully a two-channel confocal laser scanning microscope (Leica-NT) was used. Pictures were taken with 10x, 20x or 40x oil immersions objectives. In this way I obtained images of single optical sections with a thickness between 1 and 4µm or maximum intensity images of 10-20µm.

6.12.2 Fluorescence microscope with camera

To analyze double or triple antibody stainings or take pictures of *in situ* hybridized sections I used the Zeiss Axiophot fluorescence microscope connected to an Axiocam Camera.

31

6.12.3 Statistics

For the evaluation of the proliferation in the transduced brain regions, statistical analyses were carried out. Proliferating cells (PH3+) were counted as proportion of all transduced cells (EGFP+) and values like arithmetic average, standard deviation and standard error of the mean were calculated.

The standard deviation is a statistic that tells you how tightly all the various examples are clustered around the mean in a set of data and the standard error of the mean is the standard deviation of the sampling distribution of the mean.

Arithmetic average $\bar{x} = \dfrac{1}{n}\sum\limits_{i=1}^{n} x_i$

Standard deviation $s = \sqrt{\dfrac{\sum\limits_{i=1}^{n}(x_i - \bar{x})^2}{n-1}}$

Standard error of the mean $SEM = \dfrac{s}{\sqrt{n}}$.

The error bars in the diagrams resemble the SEM. To test the data for significance I used the Student's t-test. The result (*p*) of this test tells us the probability of our conclusion being correct. There is a 95% chance of the means being **significantly** different if *p*=0.05, a 99% chance of the means being **highly significantly** different for *p* = 0.01 and a 99.9% chance of the means being **very highly significantly** different for *p*=0.001.

The calculations and construction of the diagrams were carried out with Microsoft Exel and the Student t-test was performed with the statistical program: STATS.EXE

6.13 Material

6.13.1 Microscope

Fluorescent microscope	
AxioPhot microscope	Zeiss
HBO 100W fluorescent lamp	Zeiss
AxioCam HRc camera	Zeiss
AxioVision 3.1.1.1 program	Zeiss
Objective Plan Neofluar 5x/0,15 (Phase 1)	Zeiss
Objective Plan Neofluar 10x/0,30 (Phase 1)	Zeiss
Objective Plan Neofluar 20x/0,50 (Phase 2)	Zeiss
Objective Plan Neofluar 40x/0,75 (Phase 2)	Zeiss
Objektive Plan-Apochromat 40x/1,30 Oil	Zeiss
Objektive Plan-Apochromat 63x/1,40 Oil (Phase 3)	Zeiss

Fluorescent stereomicroscope	
SZX 12 microscope	Olympus
U-RFL-T fluorescent lamp	Olympus
U-CMAD3 incl. U-TV1 X camera	Olympus
AnalySIS 3.1 program	Soft Imaging Systems

Confocal microscope	
Leica DM RBE microscope	Leica
Leica TCS NT confocal	Leica
HBO 50W fluorescent lamp	Leica
TCS NT Vers.1.6.587 program	Leica
Objective HC PL APO 10x/0.40 IMM	Leica
Objective HC PL APO 20x/0.70 IMM CORR	Leica
Objective PL APO 40x/1.25 oil Ph3	Leica
Objective PL APO 63x/1.32 oil Ph3	Leica

6.13.2 Electroporation

Electroporation setup	
Compressor	Jun-Air, Denmark
Electrodes (Platin covered gold electrodes)	TR Teck, Japan: CUY 611
Puller for capillaries	Flaming, Brown Micropipette Puller, Sutter instruments Co., Model P-97

Pulse generator (pneumatic picopump PV 820)	WPI, Sarasota, Florida, USA
Stimulator (TSS 10)	Intracell

6.13.3 Solutions, buffer and media

6.13.3.1 Adenovirus-production

CsCl-solution	$1.45g/cm^3$: 43g CsCl in 60ml 10mM Tris pH 8.0
	$1.32g/cm^3$: 56g CsCl in 116ml 10mMTris pH 8.0
Tris/Glycerol	10mM Tris
	10% Glycerol
DMEM-FCS	DMEM
	5%FCS

6.13.3.2 BrdU-puls

BrdU-Solution for *in ovo* injections	20mg/ml (w/v) BrdU
	in H_2O
Fast Green	1% in H_2O_{bidest}

6.13.3.3 Cell culture

Cytochalasin D (2mg/ml stock solution in DMSO)	$2\mu g/\mu l$ – $8\mu g/\mu l$ in culture medium
FCS-PS-Medium	10% (v/v) FCS (heat inactivated 30 min. at 56°C)
	1% (v/v) Penicillin-Streptomycin
	in DMEM
HEPES-HBSS-Medium	10 mM HEPES
	in HBSS
PFA (4%)	4% (w/v) Paraformaldehyde in 1xPBS
Sucrose-PBS-solution (20%)	20% (w/v) Sucrose in PBS

6.13.3.4 Electroporation

Font-India Ink in PBS	Font India ink 1:6 in PBS
Fast Green	1% in H_2O_{bidest}

6.13.3.5 Immunohistochemistry

HCl (2.4 N)	2.4 N HCl (37 % (w/v)) in H_2O_{bidest}
PBS (Phosphate buffered salt solution, 1x) pH 7.4	137 mM NaCl 2.7 mM KCl 80.9 mM Na_2HPO_4 1.5 mM KH_2PO_4 in H_2O_{bidest}
Sodium-Citrate buffer	10x 0.1M Sodium-Citrate, pH 6.0 in H_2O_{bidest}
Tween-20 (0.1% / 0.5%)	0.1% / 0.5% (v/v) Tween-20 in 1x PBS

6.13.3.6 *In situ* hybridization

Alkaline-phosphatase staining buffer (AP-buffer)	100mM NaCl 50mM $MgCl_2$ 100mM Tris pH9.5 0.1% Tween-20 1mM Levamisole in H_2O_{bidest}
AP - NBT/BCIP	AP buffer 350μg/ml NBT 175μg/ml BCIP
Blocking-solution	MABT 2% blocking reagent 20% heat inactivated sheep serum
Hybridization buffer	1x salt solution 50% Formamide 10% Dextran Sulfate 1mg/ml wheat germ tRNA 1x Denhardt's solution H_2O_{bidest}
LiCl (4M)	4M LiCl H_2O_{bidest}
MABT (5x) pH 7.5	500mM Maleic Acid 750mM NaCl 0.1% Tween-20 H_2O_{bidest}

SSC (20x)	3M NaCl
	0.3M Sodium Citrate
	in H_2O_{bidest}
Tween-20 (0.1% / 0.5%)	0.1% / 0.5% (v/v) Tween-20
	in 1x PBS
Washing solution	1x SSC
	50% Formamide
	0.1% Tween-20

6.13.3.7 Whole-mount *in situ* hybridization

BCIP	50mg/ml in dimethylformamide
Blocking solution	MABT
	20% GS
	2% blocking reagent
Detergent solution	1% Nonidet P-40 (Igepal)
	1% SDS
	0.5% Deoxycholate
	50mM Tris-HCL (pH 8.0)
	1 mM EDTA (pH 8.0)
	150 mM NaCl
Hybridization solution	50% Formamide
	5 x SSC
	2% SDS
	50 µg/ml tRNA
	2% BBR
	50-100µg/ml Heparin
MABT (5x) pH 7.5	500mM Maleic Acid
	750mM NaCl
	0.1% Tween-20
	H_2O_{bidest}
NBT	100mg/ml in (70%) dimethylformamid
NTMT	100 mM NaCl
	100 mM TrisHCl (pH 9.5)
	50 mM $MgCl_2$
	0.01% Tween 20
PBT	DEPC-PBS
	0.01% Tween

Solution X	50% Formamide
	2x SSC
	1% SDS
SSC	20x, pH 4.5 in DEPC
Tween-20 (0.1% / 0.5%)	0.1% (v/v) Tween-20
	in 1x PBS

6.13.3.8 Molecular biology

LB-agar	LB-medium (LB Broth Base 20g/l)
	15g/l Agar
SOB-Medium	2% Bacto trypton
	0.5% Bacto yeast extract
	10mM NaCl
	2.5mM KCl
	in H_2O_{bidest}
TBE (10x)	450mM Tris Base
	440mM Boric Acid
	10mM EDTA
	in H_2O_{bidest}

6.13.4 Product list

Product	Company
Agarose (electrophorese)	Biozym
Ampicillin	Sigma
Anti-DIG-FAB-fragments alkaline phosphatase	Roche
Aqua Poly/Mount mounting medium	Polysciences
Bacto-Agar	DIFCO Laboratories
BCIP (5-bromo-4-chloro-3-indolyl-phosphate, 4-toluidine salt)	Roche
Blocking reagent	Roche
BrdU (5-Bromo-2-Deoxyuridin)	Sigma
BSA	Sigma
$CaCl_2$	Sigma
CsCl	Sigma
Cytochalasin D	Sigma
DAPI	Pierce
Dextran Sulfate	Sigma

DIG-RNA labelling mix (10x ; DIG-UTP)	Roche
Di-Sodiumhydrogenphosphate Na_2HPO_4	Merck
EDTA (Titriplex)	Merck
Ethanol absolute (EtOH)	Riedel-deHaën
Fast Green FCF	Sigma
Formamide	Merck
Gentamycin	Gibco
Glycerol (87%)	Merck
Hank's buffered salt solution (HBSS)	Gibco
HEPES-Buffer solution 1 M, pH 7,2 - 7,5	Gibco
Immersion oil 518N	Zeiss
Isopropanol	Merck
Kaliumchloride KCl	Merck
Kaliumdihydrogenphosphate KH_2PO_4	Merck
LB Broth Base	Invitrogen
Levamisole	Sigma
LiCl	Merck
Maleic Acid	Fluka
$MgCl_2$	Merck
MidiPrep-Kit	Qiagen
MidiTip 100 column	Qiagen
Molecular weight marker (1kb-ladder)	Gibco
NaCl	Merck
NaH_2PO_4	Merck
NaN_3 (pure)	Merck
NBT (Nitroblue Tetrazolium Chloride)	Roche
Normal goat serum (NGS)	Boehringer Ingelheim (Vector Laboratories)
NP40 – Igepal	Sigma
Paraformaldehyde (PFA)	Merck
Penicillin/Streptomycin-Solution 10 000 E Penicillin, 10 0000 µg/ml Streptomycin, as PenicillinG (Sodium salt) & Streptomycinsulfate	Gibco
Phenol-Chloroform-Isoamylalcohol (50:49:1)	Gibco
Poly-D-Lysine Hydrobromide (PDL)	Sigma
Polyoxyethylenesorbitanmonolaurate (Tween-20)	Biorad
Propidium-Iodide (PI)	Sigma
Proteinase K	Roche

Restriction enzymes	New England Biolabs
RNA polymerase 50U/µl (T3, T7, SP6)	Stratagene
RNase A	Qiagen
RNase inhibitor	Boehringer Mannheim
RNeasy Kit	Qiagen
Sodium Citrate	Merck
Sodium Acetate	Merck
Sucrose	Merck
Top10 cells	Invitrogen living Science
Transcription buffer (5x)	Stratagene
Tris Base	Merck
TrisHCl	Merck
Triton X-100	Roth

6.13.5 Consumables

Product	Company
Adhesive tape	Tesa
Capillaries (thin-wall single-barrel standard borosilicate glass tubing; OD:1.2; ID:0.90; length: 4in./ 102mm)	WPI
Column (NAP-25)	Pharmazia
Coverslips 24 x 50 mm	Marienfeld
Eggs	Hölzl/ Moosburg
Eppendorf tubes (0.5, 1.5, 2.0ml)	Eppendorf
Glass slides Superfrost®-Plus 76 x 26mm	Menzel Gläser
Parafilm	American National can
Pasteur pipettes, autoclaved	Volac
Permeable filtermembrane inserts Millicell-CM (0,4µm pore, 30mm diameter)	Millipore
Pipettes, sterile (5, 10, 25ml)	Falcon
Razor blades, extra thin, Rotbart	Gillette
Superglue	UHU
Syringe filters 0.45µm	Renner
Syringe needles (Neolus, 0.4mm)	Terumo
Syringe - fine dosage (1ml)	Braun
Syringes (10-50ml)	Becton Dickinson
Ultracentrifugation tube (Quick-Seal)	Beckmann
Whatman chromatography paper	Whatman

7 Results

7.1 Characterization of the telencephalic regions during development

7.1.1 Expression pattern of Emx1 and Emx2 in the chick forebrain during development

Emx1 and Emx2 are two homeobox transcription factors, which are expressed in the dorsal telencephalon from early developmental stages onwards. I analyzed their expression domains at several developmental stages for a full characterization as basis for functional manipulation. To compare the different developmental stages, *in situ* hybridization was performed at E2, E4 and E7 (Fig.11). At E2 (HH 9-14), shortly after the neural tube has closed, the expression domains of Emx1 and Emx2 became fixed in the anterior prosencephalon, whereas di- and mesencephalon exhibited Emx1- and Emx2-expression in the complete region. No expression could be observed in the prosencephalon at HH10, whereas at HH11/12 Emx1 and Emx2 showed weak expression dorso/medially (Fig.11A, E). At E3 (HH18-21) both genes were expressed in the di- and mesencephalon and in the dorsal telencephalon (Fig.11B'), where they described a low rostro/lateral to high caudo/medial gradient with exception of the most medial located region. The expression domain of Emx2 (Fig.11F) seemed to extend further medially than Emx1 (Fig.11B), indicated by the white arrowheads. At E4 (HH24/25) Emx1 and Emx2 were strongly expressed in the dorso/medial region of the telencephalic vesicle, but excluded from the thinner medial tissue, the choroidal anlage (ChA; Fig.11C, G). Emx2-expression still extended slightly further medially than Emx1 (see empty arrowheads). The expression of both TFs decreased gradually towards the lateral region with Emx2 being expressed further laterally (Fig.11C, G; see black arrowheads). At E7 (HH30/31) both TFs were strongly expressed in the hippocampus and the medial pallium. Emx2-expression was also observed in the cortical hem but at lower levels, whereas Emx1 was only expressed in the dorsal-most region of the hem (Fig.11I, J; black arrowheads). Emx1 and Emx2 were not expressed in the choroid plexus (ChP), which was located medial to the region of the hem (Fig.11D, H, I, J). In the ventricular zone (VZ) of the pallium (PA) the expression of both, Emx1 and Emx2, decreased in a medial to lateral gradient, finally terminating in the DVR (see empty arrowheads). Weak expression of Emx2 extended further into the region of the DVR than Emx1 (Fig.11D, H), even though no clear border of expression could be detected in this region. Emx2-expression was observed in very low levels throughout the subpallial VZ (Fig.11H) and Emx1 was additionally detected in pallial postmitotic pyramidal neurons (see asterisk in Fig.11D).

Taken together, the expression of Emx1 and Emx2 began around HH11/12 in the dorso/medial prosencephalon and by HH18 exhibited a more restricted pattern in the telencephalon with strongest expression in the caudo/medial region. Both genes largely colocalized but Emx2-expression extended further medial into the cortical hem as well as further lateral into the region of the DVR.

7.1.2 Analysis of different markers in the developing chick forebrain

7.1.2.1 Characterization of forebrain regions at E4

At this developmental stage the forebrain still appeared as a small telencephalic vesicle, mainly consisting of neuroepithelium (NE). The different forebrain regions did not show specialized morphological characteristics yet. Analysis of specific transcription factors and secreted signals like Fgf8, Bmps and Wnts exhibited some interesting expression domains in the forebrain. The dorsal Emx1/2- positive region was also characterized by the homeodomain TF Pax6 (Fig.12E), which also abutted the ChA. In the dorso/lateral telencephalon the Pax6-signal weakened and stopped around the Emx1-expression border. The ChA strongly expressed signaling-molecules like Fgf8 rostrally (Fig.12A) and Bmp7 throughout the entire rostro/caudal extension (Fig.12C). The expression domain of the TF Otx2 (Fig.12B) also labeled this region but extended slightly further laterally. Fgf8- and Bmp7-expression bordered the expression of Emx1 and Emx2, whereby Emx1 delineated a small gap to the Bmp7-expression domain (compare Figs.12C and 11C, G). Wnt7b (Fig.12D) was absent from the ChA but bordered the Bmp7-expression and thus overlapped with the weakly lateral expression of Otx2 and the medial expression of Emx1 and Emx2.

As development proceeds, the midline-structure, pallial and subpallial regions become morphologically discernible. The medio/dorsal region fully invaginates and formes the midline-region. The DVR and the subpallium strongly increase in radial size and the DVR appears as predominant structure of the avian forebrain.

7.1.2.2 Characterization of forebrain regions at E6

The exact location of distinct areas of the midline region was studied by the distribution of midline markers, like Bmp7, Wnt7b and Otx2. The cortical hem expressed Wnt7b (Fig.13A) and very weakly Otx2 and Bmp7 (see arrowheads in Fig.13B, C). In the dorsal region of the hem, Wnt7b overlapped with Emx1 and to an even greater extend with Emx2.

Interestingly, the region located medially to the hem region, the ChP was completely devoid of Emx-expression. ChP-tissue could nicely be detected by coexpression of Otx2 and Bmp7 (Fig.13B,

C), even though the Bmp7-signal was not restricted exclusively to the region of the ChP. Its expression decreased dorsally, but the cortical hem interrupted the gradient and only showed very weak expression of the Bmp7-signal. Lhx2a and Gli3 labeled the VZ of the forebrain, with Lhx2a excluding ChP and hem and Gli3 only excluding the ChP (Fig.13D, E). Around E6/7 the tissue of the ChP matured and started to express Ttr (Fig.13F).

Emx1/2, Pax6 and Ngn1/2 were expressed in opposing gradients in the dorsal telencephalon, including the DVR (Figs.11D, H; 14A, B, C). Emx1/2 showed a decreasing medial to lateral expression with high expression in the midline-region and lower levels of expression in the DVR, while Ngn1/2 and Pax6 exhibited opposing gradients and formed a sharp expression boundary to the subpallium (Fig.14A, B, C, F, G, H). Although Pax6 was weakly expressed in the midline-region it extended furthest medial and even showed expression in the ChP (Fig.25D'), while neither Ngn1/2 nor Emx1/2 were detected in this region (Figs.11D, H; 14A, B). Interestingly, the dorsal region of the hem, the hippocampus and the choroidal roof expressed much lower levels of Pax6 protein than the ChP (Fig.25D'). The domain of high Pax6-expression in VZ-cells of the pallium and DVR stopped at the sulcus between the DVR and subpallium (Fig. 14C, H), where a band of Pax6-containing cells extended into the differentiated parts of the subpallium (see asterisks in Fig.14C, 15A). Low levels of Ngn1/2 were expressed in the region of the hem, whereby Ngn2-expression was slightly stronger in the hem-region than Ngn1 (see arrowheads in insets in Fig.14A''', B'''). While most cells in the VZ of the DVR expressed Ngn1 or Ngn2 (see insets in Fig.14A'', B''), only subpopulations of cells expressed these genes in the in the VZ of the dorsal pallium (see insets in Fig.14A', B'). As described earlier, Emx1-expression stopped dorsal of Pax6- and Ngn2-expression domains leaving a gap to the ventrally expressed Dlx1-gene (Fig.11D; 14B, C, D; Bell et al., 2001; Fernandez et al., 1998).

Specific markers for the subpallium are Dlx1, Cash1 and Gsh2 (Figs.14, 15). Neither Emx1/2, Ngn1/2 nor Pax6 were found in the subpallium. However, Pax6 was expressed in postmitotic cells in the dorsal part of the Dlx1-expression domain, but were absent from the ventral part (arrowheads in Fig. 14C). Cash1 and Gsh2 were expressed in the subpallium but seemed to extend slightly deeper into the DVR than Dlx1 (Figs. 14D, E, J, 15B). Cash1-expression continued at a low level through the DVR into the dorsal pallium (see arrow in Fig. 14E). Few Cash1-positive cells were observed in the cortical hem, whereas the choroid plexus completely lacked Cash1-expression (Fig.14E'). We also observed a small gap in Gsh2-immunoreactivity in the subpallium (see asterisk in Fig. 15B) comparable to the gap between the LGE and MGE in the mouse (Toresson et al.,

2000). Gsh2-expression was strongest in the subpallial VZ and only few cells in the SVZ were Gsh2-positive (Fig.15C; Yun et al., 2001), whereas Cash1 was expressed from early precursors in the VZ and SVZ at the transition from VZ to SVZ (Fig.14E, J; Yun et al., 2002) and Dlx1 could be detected predominantly in the SVZ (Fig.14D, I).

To directly examine the overlap of pallial and subpallial markers, we performed Pax6- and Gsh2-double immunostainings and observed a small zone of Pax6/Gsh2 double-positive cells at all rostro/caudal levels coinciding with the origin of the band of Pax6-positive cells described above (Fig.15A, B, C). Since the soluble frizzled receptor2 (Sfrp2) was detected in the dorso/ventral boundary in mouse (Kim et al., 2001), we examined expression of the chick homologues (Terry et al., 2000) in the developing telencephalon. While no expression of Sfrp2 could be detected in the telencephalon, Sfrp1-expression was restricted to a small region between the DVR and subpallium, where Gsh2 and Pax6 were coexpressed (Fig.16; Frowein et al., 2002). The Sfrp1-positive territory, however, appeared broader than the Pax6/Gsh2-overlap and extended equally into pallial and subpallial regions (compare Figs.15 and 16).

7.1.2.3   Characterization of forebrain regions at E10

At E10 (HH36) the different regions had accomplished characteristic features. The region of the avian wulst occupied a very small area whereas the DVR appeared as predominant structure, characterized by the formation of clusters of neurons (Fig.17C). The cells of the DVR that form its nuclei are born at E6, migrate to their final destination and form cell clusters around E10 (Striedter and Keefer, 2000). These clusters could be identified by birthdating experiments (Striedter and Keefer, 2000). BrdU was injected at E6 and embryos were analyzed at E10. Typically, BrdU-positive cell clusters in the DVR consisted of 10-50 cells in diameter and a thickness of 50-75 μm (Fig.17C, C'). The large region of the DVR was labeled with Tbr (Fig.17A), a marker for precursors and neurons in the pallial region and the DVR. Blbp characterized the dorso/ventral boundary region, which seemed to occupy a rather large region (Fig.17B). The choroid plexus has differentiated and strongly expressed Ttr (Fig.17D). Emx2 (Fig.17E) and Pax6 (Fig.17F) were still expressed in opposing gradients in the VZ of pallium and DVR.

Taken together, this expression analysis further show that the DVR is characterized by pallial gene expression (Puelles et al., 2000) and does not correspond to the dorso/ventral boundary in the

telencephalon of mammals (Fernandez et al., 1998). It rather appears that the pallial/subpallial border was shifted below the DVR in the chick telencephalon (see schematic summary, Fig.18).

7.1.3 Analysis of proliferation and differentiation at different stages

The expression pattern of Emx1 and Emx2 coincided with morphologically different regions that showed differences in proliferation and differentiation.

7.1.3.1 Analysis at E4

The thickness of the pallium and subpallium varied slightly and no clear border could be distinguished between these regions. The pallium was 7-12 cells thick (9.1±0.4; n=14; Fig.19B) and the subpallium contained 9-14 cells (10.8± 0.4; n=12; Fig.19C). The choroidal anlage formed a small, thin band that consisted of 2-4 cells in thickness (2.8±0.2; n=12; Fig.19A).

Proliferation was analyzed by staining for Phospho-histon H3, a marker for mitosis. By electroporating a GFP-plasmid, I labeled a certain amount of neuroepithelial cells. For quantification, GFP/PH3 double-positive cells were counted as proportion of all transduced cells. The pallial tissue contained around 5% mitotically active cells (n=3; Fig.19E), whereas the subpallium exhibited 8% PH3-positive cells (Fig.19F; n=2). The region of the ChA only exhibited very few proliferating cells (Fig.19D). In the subpallium, in contrast to the pallium, mitotically active cells seemed to be less restricted to the ventricular surface. This could be an early indication for the formation of the SVZ in the subpallium that will later occupy a large territory (see arrowheads in Fig.19F). PH3-positive cells lining the pial surface of the pallium belonged to blood vessels of the pia mater and not to the pallium (see arrows in Fig. 19E).

Differentiation was monitored by staining for Map2, a microtubule-associated protein which is expressed in postmitotic neurons. Map2-positive neurons were rarely observed in the pallial region (Fig.19H), but some postmitotic neurons were detected in the subpallium (Fig.19I), forming a thin band above the neuroepithelium. Also in the ChA no differentiated neurons were found (Fig.19G).

7.1.3.2 Analysis at E6

At E6 the regions of the dorsal telencephalon could be distinguished by their thickness, cell proliferation and neuronal differentiation. The thickness increased from the ChP to the pallium and DVR. The ChP consisted of 2-4 cells (2.4±0.2; n=12; Fig.20B, B'', E), the hem of 2-6 cells (4±0.3; n=16; Fig.20B, B', E) and the adjacent hippocampal area contained about 11 cells (11.1±0.4; n=9,

E). Interestingly, in a rostral to caudal direction the tissue of the cortical hem became thinner and more elongated. The pallium exhibited a thickness of 15-28 cells (20.6±1.4; n=10; Fig 20A', E). Proliferation was studied by the expression of PH3, which also strongly increased from the region of the ChP to the pallium. The rate of proliferation in the ChP was rather low (2.4±0.4; n=13; quantified as PH3-positive cells per area; Fig.20B, E). The rate of proliferation in the hem-region (5.4±1.6; n=5, E) was higher than in the choroid plexus, but still lower than in the pallium (18.3±1.1; n=3; Fig.20A, E). In the pallium, also cells in a region above the VZ underwent mitosis. This thin 1-cell layer of mitotic cells lining the VZ resembles the subventricular zone (SVZ) in analogy to the mammalian SVZ (Smart, 1976), which is composed of few cells in thickness. The DVR showed a similar rate of proliferation compared to the pallium (19.5±1.1; n=2; Fig.20C, E) but the size of the SVZ was greatly enlarged compared to the pallium.

Neuronal differentiation was not observed in the ChP (Fig.20B) but in the hem-region (Fig.20B), in the pallium (Fig.20A) and in the DVR (Fig.20C). In the pallium and in the DVR postmitotic neurons formed a strong Map2-positive band, whereby the territory in the DVR was much larger. Interestingly, the cortical hem exhibited Map2-positive neurons, that used their processes to reach the inner ventricular surface or cells resided in the VZ-tissue, a characteristic feature only observed in the tissue of the hem (see high power inset in Fig.20B). In the region of the DVR, postmitotic neurons formed a very thick layer (Fig.20C).

The size of the subpallium had strongly increased by E6. A high rate of proliferation was observed in the VZ (24.5±1.6; n=6) and in the SVZ (Fig.20D, E). The SVZ in the subpallium appeared similar to the SVZ in the DVR, but contained a larger number of proliferating cells. Many differentiated neurons were present in a prominent band, indicative of pronounced neuronal differentiation (Fig.20D).

This cell biological analysis demonstrated that the DVR rather resembled the structure of the subpallium. This is obvious in regard to the thickness of the tissue, the pronounced neuronal differentiation, the presence of a broad SVZ and the formation of nuclear cell clusters, while the rate of proliferation was rather comparable to the rate observed in the pallium. These observations are juxtaposed to the pallial pattern of transcription factors that characterize the region of the DVR. These opposing observations raise the question where the pallial/subpallial boundary is located.

7.1.4   Location of the pallial/subpallial boundary by migration analysis

To analyze the exact position of the pallial/subpallial boundary, I studied the migration of neurons using slice cultures transfected with EGFP-adenovirus at different regions. Pictures of the migrating cells were taken at different time-points after infection.

Cells infected in the avian pallium predominantly elongated radially (n=3/3; Fig.21A). Infected cells in the DVR, showed a migration into the pallium, using different routes. DVR-cells migrated through the marginal zone, the intermediate mantel zone and the proliferative SVZ (n=8/15; Fig.21B, D). However, about half of the slices with cells infected in the DVR did not show any migration (n=7/15; Fig.21B, D). Infections of the subpallium, also exhibited migration through marginal, mantel and SVZ to reach the pallium (n=7/12; Fig.21C, D). Similar results were obtained *in vivo* using quail-chick grafts (Cobos et al., 2001a). In few cases I observed that cells infected in the DVR migrated ventrally into the subpallium by crossing the pallial/subpallial boundary (n=1/15; Fig.21B, D). Cells that were infected in the region of the boundary acquired a radial morphology (n=3/5; Figs.21D; 22A), reminiscent of the mammalian boundary in this area, which is characterized by a bundle of radial glia cells. This boundary-region was also labeled for Blbp (Fig.22B), an antibody that marks mammalian radial glia cells in the boundary-region (Hartfuss et al., 2001; Li et al., 2004). The migration analysis demonstrated a shift of the pallial/subpallial boundary below the region of the DVR. This boundary coincided with the Pax6-positive stream of cells, the Sfrp1-positive region, the radially oriented morphology of cells, the migratory boundary and the dorsal and ventral expression of characteristic transcription factors.

7.2   Analysis of telencephalic development upon misexpression of Emx1/2

To elucidate the role of Emx1 and Emx2 on regionalization, proliferation and differentiation of the different forebrain regions, I overexpressed these genes in the pallium, subpallium and midline-region by *in ovo* electroporation.

7.2.1   Electroporation and conformation of plasmid transduction

Electroporation yielded the highest efficiency, when it was carried out at embryonic day 2 (E2; HH9-13). One day after electroporation, at E3, in about 90% of the electroporated brains the entire neuroepithelium was GFP-positive (Fig.23A). As development proceeded, cells of the VZ started to loose GFP-immunoreactivity; supposedly they diluted the plasmid during proliferation. This effect was observed most strongly in high proliferative regions, like the DVR and subpallium. Thus, by E6, few cells in the VZ were still positive for the control plasmid (Fig.23B) and by E7 even less

cells in the VZ were GFP-positive. These remaining few GFP-positive cells were organized in a column like manner, which could be an indication for slowly dividing stem cells (Fig.23C).

To misexpress Emx1 and Emx2 I cloned the mouse fulllength cDNA into the expression plasmid Pmes, which contained an IRES-EGFP sequence after the multiple cloning site (kind gift of Cathrin Krull; Swartz et al., 2001b). The IRES-EGFP sequence has been demonstrated to mediate reliable coexpression by the generation of a bicistronic mRNA and internal translation (Fig.24; Ghattas et al., 1991; Heins et al., 2001; Heins et al., 2002). To test ectopic Emx-expression, the constructs were electroporated into the subpallial region of the forebrain at E2, sacrificed at E4, and analyzed for the coexpression of Emx and GFP by immunohistochemistry. This showed that the GFP-signal nicely colocalized with Emx1 or Emx2 (Fig.24A, B; see arrows). Some cells in the VZ as well as in the MZ seemed not to show coexpression of Emx1 and GFP (see arrowheads in Fig.24A, B). The lack of red stained Emx-positive cells in the VZ might be due to the strong GFP-signal outshining the red staining, whereas in the MZ, non-pyramidal postmitotical cells might have downregulated Emx-protein posttranslationally. Electroporation was performed either with one of the plasmids or with a mixture of both at equal proportion, aiming for the strongest effect. By coelectroporation approximately 90% of all transfected cells expressed both constructs (Swartz et al., 2001a). This confirmation of coexpression of Emx and GFP allowed the assumption of Emx being expressed in the green GFP-transduced tissue.

7.2.2 Ectopic expression of Emx1/2 promoted defects in the midline-region at E6

At E6 GFP-electroporated control brains exhibited a normal midline-region folded to the inside, bifurcating the forebrain into two hemispheres with a thin ChP at the most ventral part (Fig. 25A, B, C, D; n=3). In contrast, high levels of Emx1/2-misexpression in a large region did not allow the development of an apparent midline-structure (Fig. 25E, F, G, H; n=4). In some cases the morphology rather resembled a holoprosencephalic brain (Fig.25E; n=2). Some manipulated forebrains also exhibited foldings of midline-structures to the outside (Fig.25I; n=2). These strong morphological deformations prompted me to look at the question of the regional identities of these abnormal structures.

7.2.2.1 Identity of the manipulated midline-region

In order to determine the identity of the Emx1/2-transduced GFP-positive area, I examined Pax6, which is normally expressed in the dorsal telencephalon, including the ChP but excluding the

choroidal roof, dorsal hem and hippocampus (Fig.25D, D'). In manipulated brains at E6, the Pax6-expression extended across the midline-region coinciding with the GFP-positive territory and did not exclude a region that could resemble the hem, hippocampus or the choroidal roof (Fig. 25H). Interestingly, strongly GFP/Emx1/2-positive cells seemed to lack the expression of Pax6, whereas weaker GFP-positive cells still expressed Pax6. This suggested a downregulation, direct or indirect, of Pax6 by Emx1/2.

Analysis of Otx2, which was expressed exclusively in the choroid plexus and which was normally absent from the Emx-territory (Fig. 25B) showed that upon Emx-transduction, Otx2 was consistently excluded from the Emx/GFP-territory (n=3; Fig. 25F, J). The Otx-positive region rather seemed to be shifted to an area, adjacent to the Emx/GFP-positive region. Bmp7 was shifted too, coinciding with the ectopic Otx2-positive region (Fig. 25G). To evaluate the location of the hem-region in the transfected embryos, I analyzed Wnt7b in the Emx/GFP-transfected regions. Wnt7b clearly marked the regions adjacent to the expression of Otx2 (Figs.26C, E; 13A, C), which indicated that the hem-region was unaltered (Fig.26A). Gli3 was ectopically upregulated in the Emx1/2-positive region (Fig.26D, F) compared to the control (Fig.26B). Sometimes it even overlapped with the Otx2-positive region, which indicated a misspecification of this region, since coexpression of Otx2 and Gli3 was never observed in control brains (Figs.25B; 26B). These deformations indicate a misspecification of the midline-region promoted by the overexpression of Emx1/2 in the territory normally devoid of Emx-expression. This gene expression analysis suggests that upon ectopic Emx-expression the pallial territory expands into the midline-region that normally acquires a non-neuronal (ChP-) phenotype.

7.2.2.2 Analysis of proliferation and differentiation

To further study differences induced by ectopic Emx in the dorsal telencephalon, I examined the cell biological characteristics of these regions. The cell biological features discriminating pallium and midline-region are the thickness of the epithelium, the cell proliferation and the formation of neurons (Fig.27). In the Emx-transduced region (see Fig.25E, I) a mean thickness of 9 cells was observed (brain #1: 11.8±0.8, n=9; #2:11±0.5, n=10; #3:4.3±0.3, n=11; Fig.27A, A2, B, B2, C), which closest resembled the thickness of the cortical hem in the control situation (4±0.3; Fig.20B, B'), a region with low levels of Emx-expression. Thus, the region normally giving rise to a thin ChP changed into an apparently neuroepithelial tissue.

Consistent with this observation, the manipulated Emx/GFP-positive region showed a higher rate of proliferation ($\varnothing$10.8 cells/area; brain #1: 7.3±0.3, n=3; brain #3: 14.3±1.1, n=4; Fig.27B2', C), than a normal cortical hem (5.4±1.6; n=5; Fig.20B) but a lower proliferation rate than normally found in the pallium (18.3±1.1, n=3; Fig.20A).

To analyze the formation of neuroepithelium in the manipulated area, I examined the presence of neurons (Fig.27B2''). A territory of strong Emx-misexpression displayed postmitotic neurons although they appeared to be fewer in number than in the control elctroporated pallium. This means that ectopic Emx induces the ectopic formation of neuroepithelium but also restricts the process of maturation.

The shifted Otx2-positive tissue exhibited a mean "hem-like" thickness of 6 cells ($\varnothing$=6.4 cells; brain #1: 5.8±0.7, #2: 5.8±0.3, #3: 7.6±0.3; Fig.27A, A1, B, B1, C), which indicated a slight enlargement of the thickness compared to the normal choroid plexus (Fig.20B''). The region of Otx2-expression also exhibited an increased "hem-like" rate of proliferation (8 cells/area; brain #1: 10±1.2, n=3; brain#3: 5.8±0.7, n=5; Fig.27B1', C) compared to tissue of the normal ChP (5.4±1.6; n=5; Fig.20B). This means, the misspecified region was able to proliferate stronger than the normal Otx2-positive tissue of the ChP normally allows. Comparing the Emx-transduced region to the Otx2-positive territory, 5x more PH3-positive cells were detected. In the Otx2-positive region no Map2-positive cells could be observed above the VZ, which would be an indication for shifted ChP-tissue (Fig.27B1'').

In some cases (n=3), when the transduction level of Emx1 or Emx2 was very high and when the manipulation affected a large region, strong folding of the transduced tissue was observed (Fig.28). Especially the pallium of the forebrain (E6), transduced with Pmes-Emx2 (Fig.28A) showed strong foldings and an enlargement of the dorsal tissue. Even in the subpallium eventually additional foldings appeared, when it was electroporated with Pmes-Emx1 (Fig.28B). This suggests an expansion of the tissue due to enhanced proliferation, which supports the role of Emx1/2 in upregulating cell proliferation.

Thus, these results show that ectopic Emx suppresses the formation of a proper midline-region and that shifted midline-structures cannot differentiate properly. Emx-transduction into regions that are normally devoid of Emx, like the ChP, suppresses the development indicated by downregulation of markers like Otx2, Bmp7 and Pax6 (for summary see Fig.29).

7.2.3   Influence of Emx1/2-misexpression on the development at E4

7.2.3.1   Early regulation of midline-markers

In order to determine the mechanisms of how Emx-genes mediate the suppression of midline-formation, earlier developmental stages were analyzed. Chick embryos were electroporated at E2 (HH9-14) and sacrificed at E4, at which stage the midline just begins to be detectable, but has not yet morphologically differentiated and invaginated.

The control embryos (Fig.30A, B, C, D; n = 3), transfected with a GFP-construct showed a clear overlap of the GFP-region with Otx2, Wnt7b and Bmp7 in the region of the presumptive midline. In contrast, Otx2 was suppressed in the region of misexpression (Fig.30E, F; n = 4). It is clearly visible that Emx1/2 suppressed the expression of Otx2 at different levels of the rostro/caudal axis. Two different levels are depicted, the caudal region (Fig.30E) and the rostral region (Fig.30F). Interestingly, Wnt7b-expression was reduced in the Emx1/2-positive region in the rostral region (Fig30.G). In the caudal region Wnt7b was not expressed dorsally at this stage and therefore, no regulation could be observed. This downregulation of Wnt7b is not detected in older embryos (Fig.26C, E), as mentioned earlier. Emx1/2-overexpression did also not affect Bmp7-expression (Fig.30H) at this developmental stage. Notably, Pax6-immunoreactivity was strongly reduced upon overexpression of Emx1/2. In control electroporated brains 66% of the GFP-labeled cells coexpressed Pax6, whereas only 7% of the Emx1/2-transduced cells also expressed Pax6. This indicated a downregulation of Pax6 by 89%, mediated through Emx1/2.

Taken together, Emx-misexpression already induces alterations at E4, evident in the reduction of Otx2, Wnt7b- and Pax6-expression, while Bmp7-expression seems unchanged.

7.2.3.2   Analysis of proliferation and differentiation

To analyze proliferation, tissue electroporated with the control plasmid was compared to the Emx1/2-transduced tissue. The proliferation was quantified by the amount of cells undergoing mitosis as proportion of all transfected cells. When the dorsal pallium was transduced with the control plasmid, I observed an average of 5.3% PH3-positive cells (control: 2 brains, 1499 cells; Fig.31A, A', A'', A''', B). Emx1- and Emx2-coelectroporation resulted in an increase of proliferation to 7.8% PH3-positive cells (911 cells, 2 brains). Interestingly, the presence of Emx1 alone led to 10% proliferation, which is a 2-fold increase compared to the control (1508 cells, 3 brains; Fig.31B). This increase could well explain the additional foldings of the dorsal pallium observed at E6 (Fig.28). Emx2-transduction into the dorsal pallium of the chick embryo resulted in

an upregulation to 8.5% (210 cells, 2 brains; Fig.31B). Proliferation analysis of the choroidal anlage could not be performed because this region could either not be located properly or the electroporation did not affect this region.

Electroporation of the control plasmid into the ventral telencephalon resulted in 8% PH3-positive cells, a region with a significantly higher rate of proliferation than the pallium (control: 278 cells, 2 brains; Fig.31B), whereas overexpression of Emx1/2 showed even a decrease to 5.7% (279 cells, 1 brain; Fig.31B). Emx1-overexpression in the subpallium showed that brains 7% of the GFP-expressing cells were PH3-positive (439 cells, 1 brain; Fig.31B), which also did not indicate any increase in proliferation.

To analyze the differentiation of the Emx-transduced region, a staining for Map2 was performed (Fig.32). The control showed few Map2-positive cells in the transduced side (Fig.32A). Electroporation of Emx1 revealed a decrease of Map2-positive differentiated neurons at the pial surface (Fig.32B, B'; n=2) at two different rostro-caudal levels. These results suggest that Emx1 keeps the cells in a proliferative mode not allowing them to differentiate, an effect not observed by overexpression of Emx2 (n=2).

In summary, Emx1 and Emx2 are able to enhance proliferation in the pallium *in* vivo, whereby Emx1 exhibits a stronger effect. In Emx1-transduced brains the differentiation seems blocked by maintaining the cells in precursor state. Both genes, Emx1 and Emx2, are able to induce additional folding of the tissue, an indication for enhanced cell divisions.

7.2.4 Stage dependence and dosage effect of gene regulation

Occasionally (n=2), Emx1/2-transduction did not result in a downregulation of Otx2 in E6 as well as in E4 embryos (Fig.33). I examined whether the dosage of Emx1/2 or the stage of electroporation may cause this variability. All manipulated embryos that showed the Otx2-downregulation effect were electroporated between stages HH9 and HH12 (n=4). Electroporation after HH12, at HH13 or HH14 (n=2), never resulted in a downregulation of Otx2 in the region of Emx1/2-misexpression. The brain depicted in Fig.33A developed a normal thin (1.8±0.2; n=9; Fig.33B'), Otx2-positive region despite Emx1/2-transduction of this tissue, with a low rate of proliferation (2.5±0.3; n=4; Fig.33B'). However, the midline-region did not invaginate although Otx2-expression was not altered. Emx1/2-transduced embryos, analyzed at E4, occasionally also showed normal Otx2-

expression, but only when manipulated at HH14 (Fig.33C, D). Wnt7b could still be downregulated (Fig.33E), when the manipulation was performed at these later stages, whereas Bmp7 seemed also not affected by manipulations after HH12 (Fig.33F). This indicates that around HH13 the region of Otx2-expression becomes irreversibly specified to develop into a thin non-neuronal tissue.

8 Discussion

Gene expression analysis of various transcription factors demonstrated that the dorso-ventricular ridge (DVR), expresses mostly transcription factors characteristic for the dorsal telencephalon, the pallium. I could further show that the typical migrational restriction boundary between pallial and subpallial regions is located between the DVR and the subpallium.

To investigate the influence of Emx1 and Emx2 on the development of forebrain regions, where they show a distinct partially overlapping expression pattern, I used over- and misexpression experiments to determine their function: When either Emx1 or Emx2 were overexpressed in the pallium, proliferation of precursor cells was drastically enhanced. This effect could not be observed in the subpallium. On the other hand, neurogenesis was reduced upon Emx-overexpression, further supported by the downregulation of Pax6, a neurogenic homeobox transcription factor.

Finally, when either Emx1 or Emx2 were misexpressed in the midline-region of the forebrain, the choroid plexus failed to form and acquired instead a neural identity. This effect was mediated by Otx2 in a stage dependent manner.

8.1 Expression domains of Emx1 and Emx2 in the avian compared to the mammalian forebrain

Emx1 and Emx2 are two dorsally expressed homeobox transcription factors that showed largely overlapping expression domains from early developmental stages onwards. Around E2 (HH11/12) their domains became restricted to the dorsal prosencephalon and by E3 (HH18) the low rostro/lateral to high caudo/medial gradients were detectable. At all stages analyzed, Emx2 extended further medially into the region of the hem than Emx1, as well as further ventrally into the region of the DVR (Fig.34). In the region of the midline, Emx1- and Emx2-expression was strong in the hippocampus but only Emx2 was detectable throughout the cortical hem. Similarly, the Emx2-expression domain extended further ventrally throughout the DVR, while Emx1 was only expressed in its most dorsal part. This observation corresponds to the expression pattern of Emx1 and Emx2 in the mammalian brain, where Emx2 also extends further into the hem-region than Emx1 (Tole et al., 2000; Yoshida et al., 1997). Ventrally, Emx2 extends weakly around the pallial/subpallial boundary (Cecchi, 2002), while Emx1-expression terminates further dorsally, leaving a small gap to the boundary-region (Muzio et al., 2002). This means that medially in the hem as well as laterally in the region directly above the pallial/subpallial boundary (mouse: ventral pallium; chick: ventral DVR) the situation in mammalian and avian forebrains is very similar. Thus,

the lack of Emx1 in the hem-region in chick and mouse gives rise to very similar regions in mouse and chick medially, while the expression gap of Emx1, detected in mouse and chick laterally, gives rise to the structure of the DVR in the avian telencephalon and has been suggested to give rise to the amygdala in mammals (Fernandez et al., 1998).

However, Emx-expression does not strictly respect borders to the neighboring structures. Hem and DVR share the identity of border areas where two different regions meet. The hem-region separates the pallial region from the ChP and the DVR separates pallium from subpallium, which somehow attributes an intermediate character to them. Hem and DVR share the expression of factors from the adjacent domains at low levels. The hem-region displays medial and dorsal characteristics, such as low levels of Otx2 and Bmp7 (ChP-markers) as well as low levels of Emx1 and Emx2 (pallial markers). The DVR also shows some dorsal and ventral characteristics, such as high levels of Cash1-expression ventrally and low levels dorsally but also dorsal markers like Emx1/2. A similar distribution of TFs that pattern dorsal and ventral regions lead to a general mode of development of dorsal and ventral telencephalic regions. However, not all TFs are distributed in a similar way in the avian and mammalian forebrain, which might lead to the distinct morphology in these vertebrate classes and will be described in more detail below.

Since it has been proposed that the region between the expression domains of Emx1 and Dlx1 might give rise to the DVR (Fernandez et al., 1998), it would be interesting to test this model by overexpressing Emx1 in this region to possibly block the process of cell cluster formation in the DVR. Therefore, I introduced Emx1 by electroporation at E2 into the early region of the DVR to possibly manipulate the development of the nuclear cell clusters that become detectable by E10. To label these cells, I injected BrdU into a vein of the embryo at E6, the day when the cells, forming the clusters, are born. It was not possible to study the question in this way, because at E6 the Emx1-GFP construct has almost disappeared from VZ-cells because of strong proliferation in the DVR. The electroporated DNA plasmids do not integrate into the genome and therefore in each round of cell division the number of copies of the plasmid may decrease by dilution between the daughter cells. To study the influence of Emx1 on the development of the nuclear structure of the DVR, I would suggest using a replication competent retrovirus (Greenhouse et al., 1988; Hughes and Kosik, 1984; Hughes et al., 1987), to label higher amounts of proliferating cells without loosing the construct.

8.2 SVZ in the avian brain

A characteristic of the subpallium in mammals (Smart, 1976; Smart et al., 2002) is the establishment of a second proliferative layer, the SVZ (Smart, 1985). In chick, the band of proliferating precursors superficial to the VZ was also most pronounced in the subpallium, as described from Striedter and Keefer (2000). The SVZ in this region was about 50µm thick. Interestingly, the region of the DVR also exhibited an SVZ, comparable to the SVZ in the subpallium in regard to its thickness, but containing fewer proliferating cells. The pallium also showed cells undergoing mitosis in the SVZ, but only few as is the case in the developing mouse pallium (Ishii et al., 2000; Valverde et al., 1995). Here, the cells formed a thin band, which was not described previously by Striedter and Keefer (2000). The fact that the DVR exhibits such a large SVZ-region, comparable to the subpallial SVZ, attributes a ventral characteristic to the DVR.

8.3 DVR: a debate of homology

Homologizing the DVR to a mammalian structure has been a matter for debate for a long period of time (Aboitiz, 1999; Aboitiz et al., 2003; Striedter, 1997). Once the DVR was believed to be homologous to the mammalian striatum (subpallium) because of its organization into distinct nuclei (Ariëns Kappers, 1936). But when modern anatomical studies revealed that the DVR receives major ascending input from the dorsal thalamus, the DVR began to be homologized with the mammalian neocortex (Karten, 1969; Lohman, 1990). Still another theory hypothesized to homologize the DVR to an enlarged pallial/subpallial boundary-region, which would be characterized by the expression gap between Emx1 and Dlx (Fernandez et al., 1998). By comparing the expression pattern of several pallial (Ngn1, Ngn2, Pax6, Emx1, Emx2), boundary (Sfrp1, Pax6/Gsh2 double-positive cells) and subpallial markers (Dlx1, Cash1) and by migration studies I demonstrated that the DVR resembles a pallial structure and that the pallial/subpallial boundary is shifted below this region. These observations support the suggestion from Puelles et al. (2000) and contradict the theory of the enlarged boundary proposed by Fernandez et al. (1998). But the question remains, why the DVR is able to generate a nuclear organization of neurons, while the expression of several markers resembles the pattern in the mammalian cortex, where neurons are organized in layers (McConnell, 1988; McConnell and Kaznowski, 1991). Interestingly, the molecule Reelin was found to be expressed differently in mouse and chick in this region (Fig.35A, B; Bar et al., 2000; Bernier et al., 2000; Tissir et al., 2002). In the mammalian forebrain, Reelin is secreted by Cajal-Retzius cells located in the marginal zone (MZ) lining the pial surface (Hevner et al., 2003). In the avian brain it

was also detected in the MZ of pallium and subpallium, but in the DVR no Reelin was detected in the MZ. But surprisingly the cells of the VZ strongly expressed Reelin and it was also detected throughout the mantel zone of this region (Fig.35A, B; Bar et al., 2000; Bernier et al., 2000; Tissir et al., 2002). Since Reelin is known to regulate neuronal migration (Lambert de Rouvroit and Goffinet, 1998) and influence radial glial cells (Hartfuss et al., 2003) it may be a candidate to influence the specific migration in the DVR. For investigating this hypothesis, cells from a cell line that expresses Reelin (293) were injected into the telencephalic forebrain vesicle at E5 and analysis was performed at E10. It was tested if this alteration could induce the formation of ectopic cell clusters also in regions like the pallium, which normally lack Reelin-expression in the VZ. Indeed, a 10-fold enhancement in the formation of small clusters, containing approximately 16 cells, could be observed in a first experiment. This could be a first hint for this molecule being involved in the organization of patch (cell clusters) and matrix (grey matter surrounding) in the DVR. Electroporation of Reelin might even be a better attempt to investigate its function because Reelin is a large protein, which might not easily diffuse within the tissue.

Cadherins have also been suggested to play a role in the formation of these clusters since they express cadherin7 (Cad7), whereas the matrix is R-Cadherin-positive (Heyers et al., 2003). Since cadherins bind mostly homotypically, cells that express the same cadherin subtype would segregate and thereby patch and matrix cells may sort into distinct compartments (Redies, 2000). Similar mechanisms have been suggested to be involved in the generation of the mammalian striatum (Redies, 2000; Redies et al., 2002; Takeichi, 1995). Also ephrins and their receptors might contribute to this segregation effect (Janis et al., 1999; Mellitzer et al., 1999). It will be interesting to compare the molecular mechanisms that mediate the arrangement of neurons into nuclei in the avian DVR compared to the mammalian striatum.

8.4 Differences in gene expression patterns in the mammalian and avian forebrain during development

During the course of this work, many similarities, but also some differences in gene expression were observed between mouse and chick. One of these was Reelin as described above (Fig.35). In addition, Cash1, an avian homologue of Mash1, was strongly expressed in the subpallium, extended slightly into the region of the DVR and continued to be weakly expressed in the VZ of the pallium, hippocampus and hem. Only the ChP was devoid of Cash1-expression (Fig.36A). While the mammalian Mash1 homologue also showed strong expression in the subpallium, there was a clear

medial high and lateral low gradient in the pallium and a specifically strong expression in the hem (Fig.36B; Fode et al., 2000). Thus Mash1 is only expressed in the hem-region of the mouse, but not the chick at comparable stages of development.

The most diverse patterns of expression were observed for Wnt7a and Wnt7b. Chicken Wnt7a marked the region of the pallial/subpallial boundary (M; Fig.36C), whereas mouse Wnt7a was expressed throughout the VZ of the forebrain excluding the region of the hem (Fig.36D) and ChP. Wnt7b was expressed in the chick exclusively in the region of the hem, while in the mouse it was detected in addition to the VZ of hem and subpallium also throughout the pallium in neurons (Fig.36E, F).

Since the expression pattern of most avian and mammalian forebrain genes was equivalent during development, the different expression of these few genes could play some role in the different development of some forebrain regions in these distinct vertebrate classes.

8.5 Emx1 and Emx2 induce proliferation

Transduction of Emx1 and Emx2 strongly enhanced the proliferation in the dorsal and medial region of the avian forebrain. The effects of Emx1 appeared even stronger in comparison to Emx2. This observation contradicted the results from Heins et al. (2001), who showed that *in vitro* only Emx2 was able to drive cells to proliferate more often and generate larger clones. For Emx1 he proposed a cell autonomous role in keeping the cortical precursor cells in an undifferentiated state, but he did not observe an influence on proliferation (Heins, 2004). His results are consistent with the observation in Emx1- and Emx2-single mutant mice. Emx2-mutant mice show a reduced size of the cortical hemispheres and a shortened midline-region (Bishop et al., 2000; Mallamaci et al., 2000b; Tole et al., 2000), which could be explained by a lack of proliferating precursors, whereas the Emx1-mutant do not exhibit proliferation defects (Guo et al., 2000), which might be due to a compensation effect of Emx2. An explanation for Emx1 not being able to enhance proliferation *in vitro* could be due to a species difference in mouse and chick or to some artificial effects *in vitro*, e.g. that Emx1 needs cofactors for triggering proliferation, that are only present *in vivo*, but absent *in vitro*. Wnt-molecules could act as such a signal. Several studies have demonstrated that the loss of Wnt3a or Wnt8b induce a strong decrease in proliferation in the region of the hem (Lee et al., 2000; McLaughlin, 2000). Furthermore, Theil et al. (2002) have demonstrated that Emx2 is a direct transcriptional target of Wnt-signaling. All these observations hint to Wnt-genes being involved in

the promotion of proliferation by regulating Emx-genes, which in a feed-back loop increase the precursor pool of Wnt-expressing cells.

I observed additional foldings of the forebrain-tissue in Emx1 as well as Emx2-transduced brains, which hints to an enlargement of the ventricular surface due to increased symmetric instead of asymmetric cell divisions. It has been suggested that the increase in symmetric cell divisions together with a decrease in asymmetric cell division might influence the size of the pallial surface (Caviness et al., 1995; Rakic, 1995) and thus account for the enlarged cerebral cortex, containing gyri and sulci, which is characteristic for humans. An increase of symmetric cell divisions has also been predicted for the increase of precursor cells *in vitro*, observed upon Emx2 infection, whereas the asymmetric mode of cell division was enhanced in case of loss of Emx2 (Heins et al., 2001). This increase of pallial surface and additional folds by an expansion of the precursor pool were also observed in transgenic mice expressing the stabilized form of ß-catenin in neural precursor cells (Chenn and Walsh, 2002). ß-catenin is an important factor that interacts with proteins of the TCF/Lef (T-cell factor/lymphoid enhancer binding factor) family to transduce Wnt-signals (Peifer and Polakis, 2000). This is an additional hint for Wnt-molecules being involved in the regulation of proliferation which might be accomplished by the regulation of Emx-genes.

It could also be observed that the enhanced proliferation was accompanied by a reduction of neuronal differentiation. Upon Emx1-transduction, no continuous band of postmitotic neurons was lining the proliferative tissue in contrast to the control situation, which was consistent with the observation that Emx1-transduced cells strongly enlarged the precursor pool but did not differentiate. The normal program of pallial cells to undergo few cell divisions (Grove et al., 1993; Reid et al., 1995; Takahashi et al., 1999) was altered to a prolonged state of proliferation.

Interestingly, transduction of Emx1/2 into the ventral telencephalon had no effect on cell proliferation or neurogenesis, similar to the results obtained *in vitro* (Heins, 2004; Heins et al., 2001). The absence of an obvious effect of Emx1- or Emx2-misexpression in the ventral telencephalon in chick and mouse may be explained by the lack of potential cofactors or the inaccessibility of some crucial target genes.

8.6   Specification of the dorsal and medial pallium

8.6.1   Emx2 versus Pax6

A drastic downregulation of Pax6 protein could be observed upon overexpression of Emx1/2 in the pallial region. Pax6 and Emx2 are normally expressed in opposing gradients in the developing forebrain, with high expression of Pax6 rostro/laterally and Emx2 caudo/medially (Gulisano et al., 1996; Mallamaci et al., 1998; Walther and Gruss, 1991). Comparing Pax6- and Emx2-mutants revealed complementary phenotypes. The absence of Emx2 lead to reductions in the caudo/medial regions together with rostro/lateral enlargements (Bishop et al., 2000; Mallamaci et al., 2000a) and complementary alterations were observed in the Pax6-mutant (Sey/Sey; Bishop et al., 2000). Notably, there was a strong reduction of Wnt-expression in the Emx2-mutant hem, while certain Wnt-genes were expanded in the Pax6-mutant (Muzio et al., 2002). Analysis of these mutant mice showed that Emx2 and Pax6 proteins are necessary to establish their graded expression by negatively regulating the expression of each other (Muzio et al., 2002).

My observation that Pax6 is detected in fewer cells in the region of ectopic Emx1/2 could be explained by a suppression of neurogenesis by Emx-genes. Emx1/2 and Pax6 might be expressed sequentially. Emx1 and Emx2 are expressed by strongly proliferating cells of the VZ while Pax6 is expressed by cells that are specified to differentiate into neurons. Thus, Emx-positive proliferating precursor cells might downregulate Emx-expression in order to upregulate Pax6 for differentiation. The level of either Emx- or Pax6-expression in a cell might be responsible for its fate to either proliferate or differentiate. However, some populations of postmitotic neurons are located in the forebrain, which still express Emx1 or Emx2. In the mouse, all postmitotic pyramidal neurons in the pallium are Emx1-positive (Briata et al., 1996; Chan et al., 2001) and a subpopulation of Reelin-expressing Cajal–Retzius cells is Emx2-positive (Stoykova et al., 2003). Both cell types somehow lost their ability to proliferate despite their expression of Emx1 or Emx2. The Emx1-expressing Cajal-Retzius cells are proposed to be born early in the region of the cortical hem, which lacks the expression of Pax6, and tangentially migrate into the marginal zone (Takiguchi-Hayashi et al., 2004), whereas pyramidal neurons are born throughout corticogenesis and reach their position in the pallium by migrating along radial glia (Mione et al., 1997; Tan et al., 1998). For the differentiation of Emx1-positive pyramidal neurons as well as Emx2-positive Cajal-Retzius cells no downregulation of the Emx-genes occurs. Therefore, Pax6 might not be involved in the

differentiation process, since Emx-genes and Pax6 negatively regulate each other. Thus, Emx1/2 are also expressed in some populations of postmitotic neurons but play a different role here.

8.6.2 Generation of the midline-region

The analysis of several markers was used to better understand the specification of regions that will give rise to midline-structures, such as the ChP. Already at E4 (HH24/25) when the forebrain still consists of a small vesicle, the midline showed a specific pattern of gene expression. The choroidal anlage (ChA) strongly expressed Fgf8 rostrally, Bmp7 and Otx2 throughout the entire rostro-caudal extension of the forebrain. This region will probably give rise to the ChP and choroidal roof. Otx2 extended slightly more laterally where it overlapped with the domain of Wnt7b-expression. This region will most likely form the cortical hem. Emx2 was also expressed in the hem-region, but was absent from the ChA (see summary Fig.37).

8.6.3 Manipulation of the midline-region

When introducing Emx1 and Emx2 into the region of the presumptive midline-region at E2 (HH9-12), a suppression of Otx2 and Wnt7b was observed at E4 (HH24/25). This hints to a misspecification or suppression of ChA- and hem-tissue. A loss of Otx2 and Bmp7 in the region of Emx1/2-overexpression was apparent in the manipulated tissue at E6 (HH28/29). This indicates a persistent downregulation of Otx2, a transient downregulation of Wnt7b and maybe a secondary downregulation of Bmp7. The reduced expression of Wnt7b could not be observed anymore when the embryos developed until E6, which might be accomplished by the function of other regulatory genes or by the dilution of Emx1/2 plasmid after several rounds of cell division. The downregulation of Bmp7 has not occurred at E4 and could only be observed at E6, which would suggest that Bmp7 is not a direct target of Emx1 or Emx2.

In the normal situation, Otx2-expression can be detected much earlier in the in the developing forebrain neuroepithelium than Emx1/2, occupying a large domain (Bell et al., 2001; Crossley et al., 2001). By the time Emx1/2-expression is detectable (HH11/12), Otx2-expression has shifted to a small territory, the ChA of the telencephalic vesicle, which might be a first hint for Emx-genes being able to restrict Otx2-expression.

The misexpression of Emx1/2 induced a suppression of Otx2 and did not allow the development of a proper ChP (Fig.38B, 2). Further analyses of proliferation and neuronal differentiation suggested a

misspecification of the Emx1/2-positive tissue with a higher rate of proliferation, enhanced thickness of the tissue and the appearance of few neurons, which rather resembled the structure of the hem. This means that Emx-genes are sufficient to block the proper development of non-neuronal ChP-fate and instead induce neural fate in the ChP. In contrast, molecules normally restricted to the ChP were forced laterally into the previously neural region. This shifted Otx2/Bmp7-positive region (Fig.38B, 1) exhibited an increased thickness of the tissue and an enhanced rate of proliferation. This demonstrated a clear misspecification of the tissue, which besides the characteristic expression of ChP-markers (Otx2, Bmp7) exhibited a "hem-like" phenotype. This region could not acquire a ChP identity and thus Otx2 is not sufficient to specify ChP-tissue (for summary see Fig.38).

8.6.4 Comparison of the ChP-phenotype in Emx1/2 double-mutants and after Emx1/2-overexpression

The observation of Emx1/2-misexpression experiments in the region of the hem and ChP appear to contradict data obtained by analysis of Emx1/2 deficient mice, since both alterations induced the suppression of ChP-markers. Therefore, I will try to explain the similar phenotypes induced by either loss or overexpression of Emx1 and Emx2. Emx1/2 double-mutant mice lack the hippocampus, choroid plexus and cortical hem, but exhibit an enlarged choroidal roof (Shinozaki et al., 2004). Due to the lack of the hem-region, Wnt-signals are missing, which on the one side might be important to induce proliferation by instructing Emx1/2-positive cells to proliferate and on the other hand might be important to induce ChP-differentiation. Wnt-genes might also be important to induce Otx2-expression, which is lost in the double-mutant but is an essential factor for inducing ChP-differentiation. Without Wnt-signaling the anlage of the ChP lacks important signals and thus just achieves features of a choroidal roof (Shinozaki et al., 2004). In case of Emx1/2-transduction, I manipulated the tissue of the ChP and hem directly, which induced a misspecification of the electroporated cells. Emx1/2 suppressed the normal expression of Otx2, which consequently disabled the cells to differentiate properly into ependymal ChP cells but rather changed their fate into neuroepithelial cells with an enhanced rate of proliferation. Strong Emx1/2-overexpression in the region of the hem transiently downregulated Wnt-expression, observed at E4 while after some rounds of cell divisions the level of Emx1/2-expression may be strongly reduced and allowed the expression of Wnt7b again, like observed at E6.

8.6.5 Integration of phenotypes affecting the midline-region

The regulation mechanisms which establish the genetic pattern that enable the formation of the ChP-region are rather complicated to understand. Analysis of several mutant mice revealed some gene interactions being involved in the formation of this region. Signaling from the hem-region has been shown as crucial inducer of the ChP. Mutant mice lacking the region of the hem, usually also lack the ChP, which can be observed in Emx1/2- (Shinozaki et al., 2004), Gli3- (Grove et al., 1998) and Lhx5-mutants (Zhao et al., 1999). Mice with a reduced hem-region e.g. Emx2-mutants (Tole et al., 2000; Yoshida et al., 1997) and Wnt3a-mutants (Lee et al., 2000) also exhibit a reduced ChP-region. On the other hand, when a mutation leads to an enlarged hem, also the ChP seems to be significantly enlarged, which could be observed in the Lhx2-mutant (Bulchand et al., 2001).

A short description of these mutants will help to better understand the alterations in the gene expression (for comparison see Fig.39): Like mentioned above, Emx1/2 double-mutant mice lack the hippocampus, choroid plexus and cortical hem and exhibit an enlarged roof (Fig.39B; Shinozaki et al., 2004). Since these structures show great differences in their expression level of Emx1 and Emx2, the defects of the mutant forebrains cannot just be due to a loss of Emx1 and Emx2. The hippocampus strongly expresses Emx1 and Emx2, the hem-region expresses Emx2 but Emx1 only dorsally, whereas the choroid plexus and choroidal roof completely lack Emx1/2. Therefore, Emx1/2 do not directly influence the development of the ChP. The loss of the hem, which serves as a Wnt-signaling center, rather might account for the loss of the ChP. The decrease of midline-tissue, including the hem, might be due to an Emx-related decrease in proliferation and thus reduced expansion of this region, while in contrast, the Emx-negative territory expands.

Similar phenotypes are observed in the Lhx5 (Fig.39D) and Gli3-mutant. Lhx5 is normally expressed from the choroidal roof in close relation to the ChP, whereas Gli3 is expressed in the neuroepithelium of the forebrain except the ChP. Both mutations result in a loss of the hem-region and ChP. The tissue in both regions appears amorph (Grove et al., 1998; Zhao et al., 1999), which could also hint to a failure to differentiate. Interestingly, both genes are expressed in different regions, excluding the ChP, even though both mutations induce similar phenotypes regarding the ChP.

Lhx2 also seems to play a role in early patterning, which is leading to a patterned cortical neuroepithelium dividing it into cortex and hem (Bulchand et al., 2001). In Lhx2-mutant mice ChP and hem are massively enlarged and the pallium is strongly shortened. Therefore, Lhx2 seems to restrict the Bmp- and Wnt-territories (Fig.39C).

8.6.6 Choroid plexus development

Signaling from the hem-region seems to be necessary to establish the choroid plexus correctly. Early in the development of the ChP, cells of the head mesenchyme invade the ChP to form the second mesenchymal or stromal layer of the ChP (Birge, 1961; Sturrock, 1979). These invading cells have been suggested to be a force that pushes the ChP into the ventricle (Birge, 1961; Birge, 1962) and the interactions between mesenchyme and neuroepithelium appear to be required for ChP-differentiation (Birge, 1961; Birge, 1962; Cavallaro et al., 1993). Such epithelial/mesenchymal interactions have been observed in different developing regions, like kidney and tooth, areas closely associated to Bmp- and Msx-expression. Since the ChP is a region of strong Bmp- and Msx-expression these interactions could also occur in this region. Grove et al. (1998) suggested that Wnt-signaling might play a role in some aspects of ChP-differentiation, since she observed Wnt5a-positive cells invading the ChP mesenchym. This would attribute to the hem a strong inductive role for the generation of the ChP, a model consistent with the phenotypes of mouse-mutants exhibiting deficiencies in the hem-region and ChP-differentiation. Also the Insulin-like growth factorII (IgF-II), which is synthesized by mesenchymal cells might serve as an inducing principle for ChP epithelial differentiation (Cavallaro et al., 1993).

For the specification or differentiation of the ChP, genes like Bmps, Bmp-receptors, Otx and Msx are probably involved. Bmps seem to be important for the formation of the ChP, by enhancing apoptosis and cell differentiation (Panchision et al., 2001; Solloway and Robertson, 1999). A mutation in the Bmp-Receptor1 (BmpR1) leads to differentiation defects of the ChP. Cells do not start to express the ChP-marker Ttr and the tissue does not achieve its characteristic thin morphology because precursor cells remain proliferative (Hebert et al., 2002). It has been shown that Bmps promote apoptosis by inducing Msx1/2 (Furuta et al., 1997; Marazzi et al., 1997; Shimamura and Rubenstein, 1997; Song et al., 1998; Timmer et al., 2002).

I showed that certain gene regulations, like the downregulation of Otx2 could only be induced during a certain developmental period (HH9-12), whereas other markers like Wnt7b could still be regulated at later stages. This means that before HH13 the commitment of Otx2-positive cells is still capable of being reversed and at later stages the cells are determined to differentiate to their distinct fate, even in case of misexpression of Emx1/2. Wnt7b-expressing cells were not committed to a distinct cell fate at HH12 and therefore a downregulation was still possible to occur.

In conclusion, I propose a model for the interactions taking place for establishing a proper midline-region (Fig.40). Wnt-signaling plays a key role in this model. The region of the Wnt-rich hem is restricted by the pallial expression of Lhx2. Wnt-signals induce Emx-genes to proliferate, which in a feed-back loop enlarge the medial region and thus also the region of the Wnt-expressing hem. Wnt-expressing cells invade the stroma of the ChP and might induce the formation of the ChP. The action of Otx2, Bmp- and Msx-genes induces apoptosis and a correct differentiation. The absence of Emx1 and Emx2 from the ChP and the absence of high levels of these genes from the cortical hem are important for a proper ChP-differentiation. It appears as if the cortical hem must be present for the ChP-differentiation.

8.6.7 Malformation of the telencephalon induced by Emx1/2-transduction

Manipulation of the presumptive midline-region induced changes in the morphology of the forebrain. I observed holoprosencephalic brains with no midline-region and brains, where the midline-region was folded to the outside. These manipulated brains usually had small ventricles, potentially due to a misspecification of ChP-tissue that would obviously effect the composition and pressure of the CSF in the ventricle. This might explain the reduced expansion of the hemispheres. Ectopic expression of Bmps was demonstrated to cause holoprosencephaly in forebrains of chicken (Wallis and Muenke, 1999). Since I also observed ectopic expression of Bmp7, this could be another explanation for the brain deformations.

Thus, these data implicate a new role for Emx1 and Emx2: These genes mediate neural identity also in the midline-region, even in the non-neural tissue of the ChP. In contrast, the absence of Emx1/2 is essential to allow the development of the ChP.

9 Figures

Formation of the neural tube

(1a) **Shaping** — Neural plate, Neural crest, Epidermis

(1b) **Folding** — MHP, Notochord

(2) **Elevation**

(3) **Convergence** — DLHP

(4) **Closure** — Neural crest, Epidermis, Neural crest cells, Neural tube
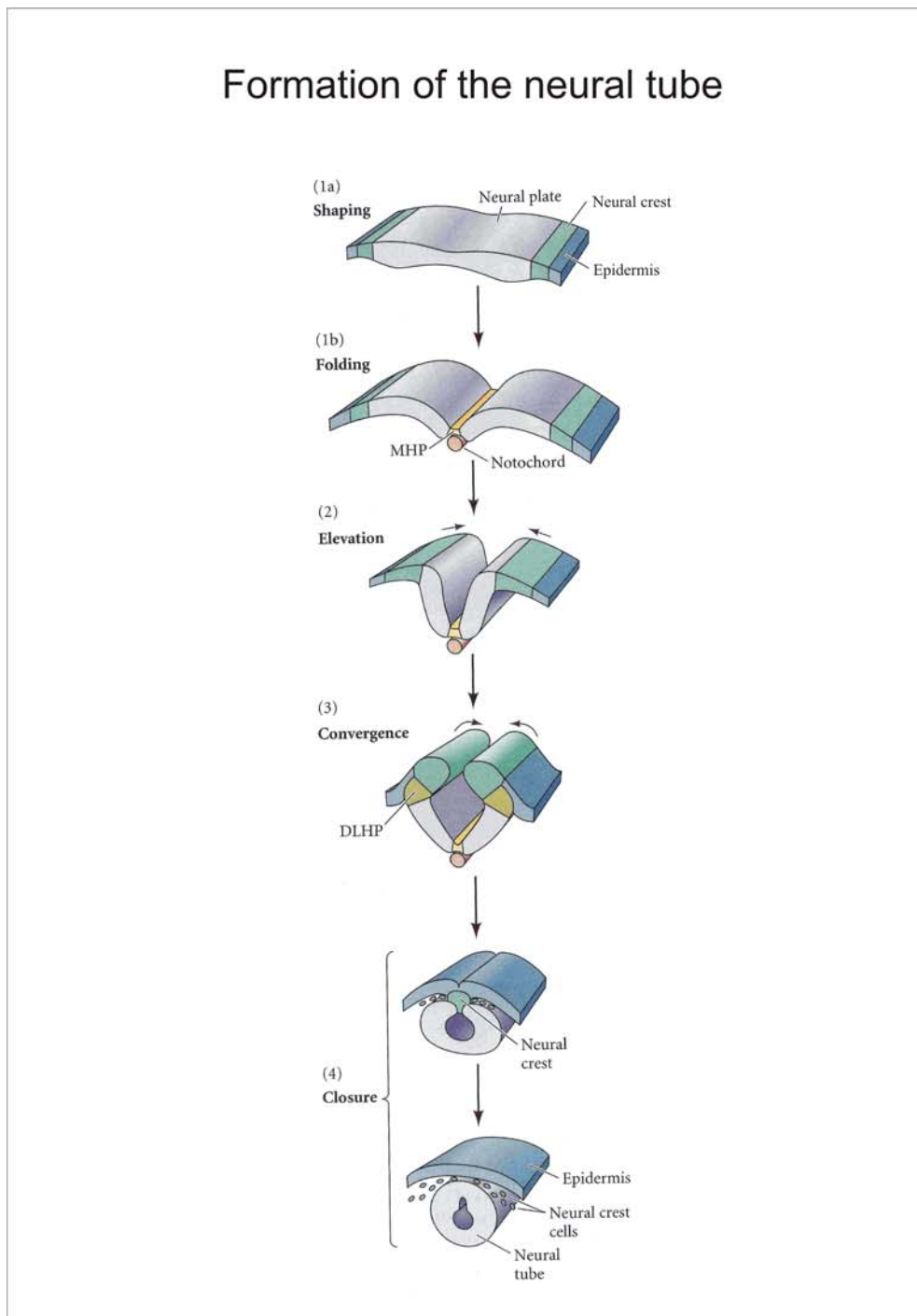
Fig.1 Formation of the neural tube in the chick embryo. Folding of the neural plate (1a) begins at the medial neural hinge point (MHP; 1b), where cells are anchored to the notochord. Epidermal cells move towards the dorsal midline (2), the neural folds converge at the dorso/lateral hinge point (DLHP; 3) and the neural tube closes (4). Neural crest cells link the neural tube with the epidermis (4). Neural crest cells migrate away. (Drawings after Smith and Schoenwolf, 1997; Scott F. Gilbert, Developmental Biology, Seventh edition)

Early brain development
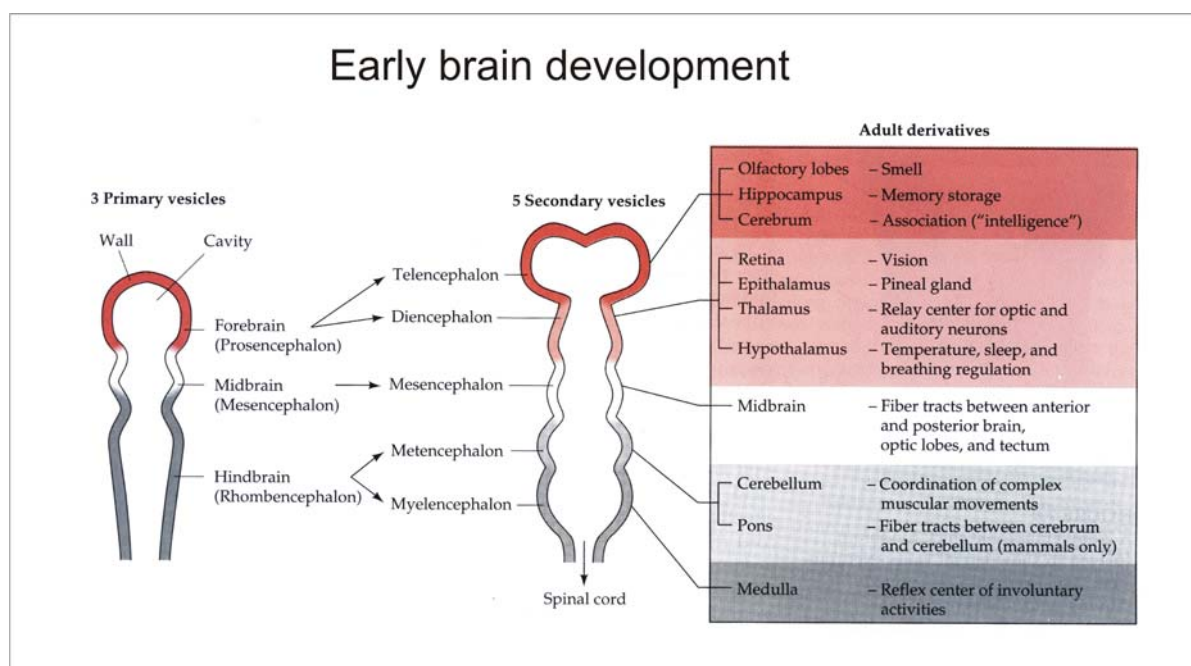
Fig.2 Development of the early human brain. Three primary vesicles are subdivided into five secondary vesicles as development proceeds. These secondary vesicles develop into regions with very different functions, depicted in the box (after Moore and Persaud, 1993; Scott F. Gilbert, Developmental Biology, Fourth Edition).
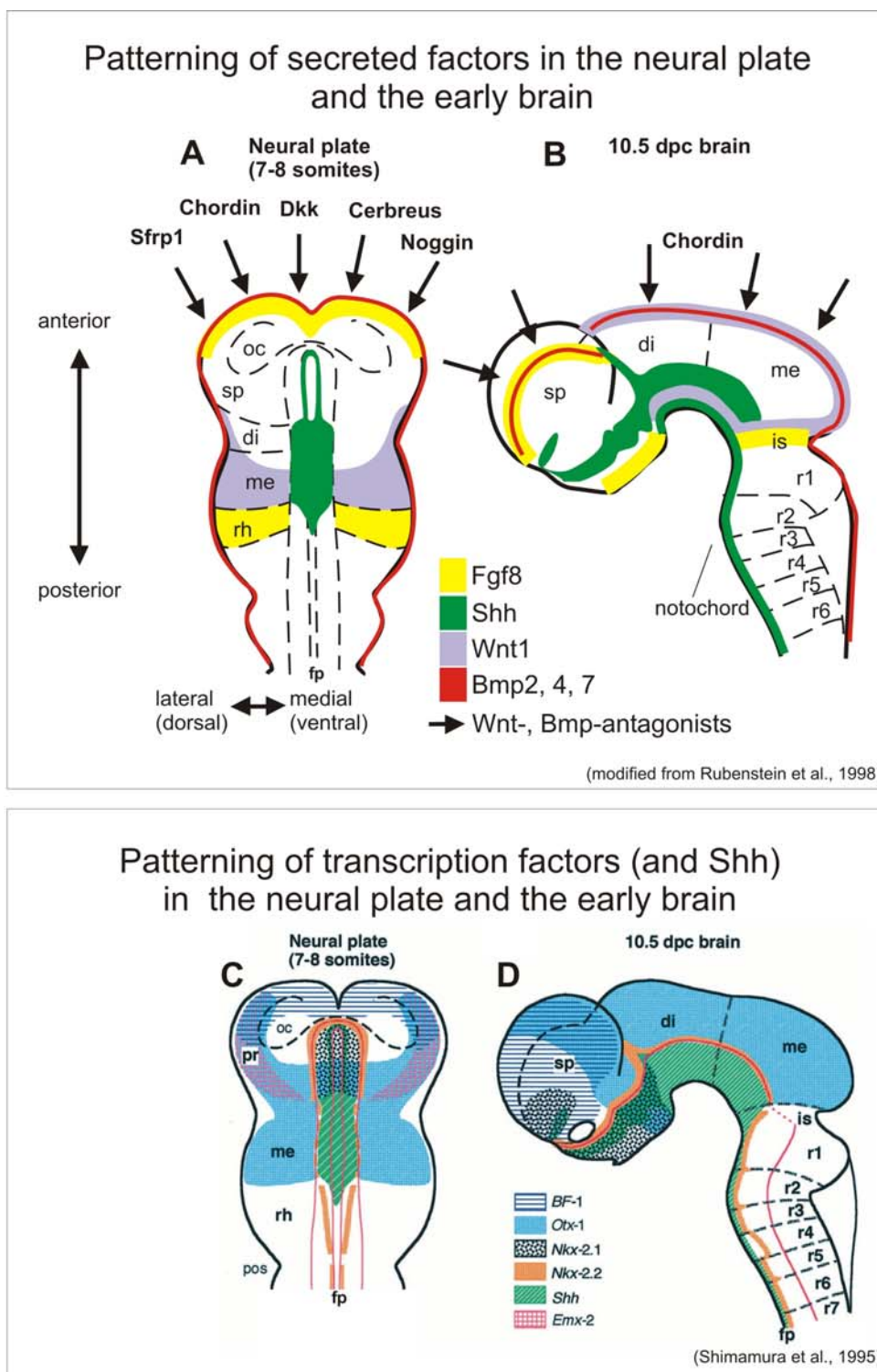
Fig.3 Schematic summary of patterning. The distribution of secreted factors (Fgf8, Shh, Wnt1, Bmps, Wnt- and Bmp-antagonists) is depicted in (A, B) and transcription factors (Bf1, Otx1, Nkx2.1, Nkx2.2 and Emx2) in (C, D) at neural plate stage (A, C) and in an early brain at E10.5 (B, D). A general medial (ventral) patterning signal is Shh, while general lateral (dorsal) signals are Bmps. Wnt- and Bmp-signaling is blocked rostrally by the action of several antagonists (Sfrp1, Chordin, Dkk, Cerberus, Noggin). A local rostral signal is e.g. Fgf8, while Wnt1 rather signals caudally. These patterning molecules regulate the development of specific forebrain structures by controlling the expression of distinct transcription factors. Fgf8 e.g. induces the expression of Bf1 and Shh induces Nkx2.1. The induction of Emx- and Otx-genes is important for the development of the telencepahlon. oc, optic cup; sp, secondary prosencephalon; di, diencephalon; me, mesencephalon; rh, rhombencephalon; Dkk, dickkopf; is, isthmus; r, rhombomere; pr, prosencephalon; fp, floor plate.

Comparison of the avian and mammalian forebrain

Chick telencephalon

Mouse telencephalon

MZ
CP
SP
SVZ
VZ

dorsal pallium
=avian wulst

dorsal pallium
= cortex

VZ

SVZ

ventral pallium
= DVR

pallial/subpallial
boundary

pallial/subpallial
boundary

subpallium
= striatum
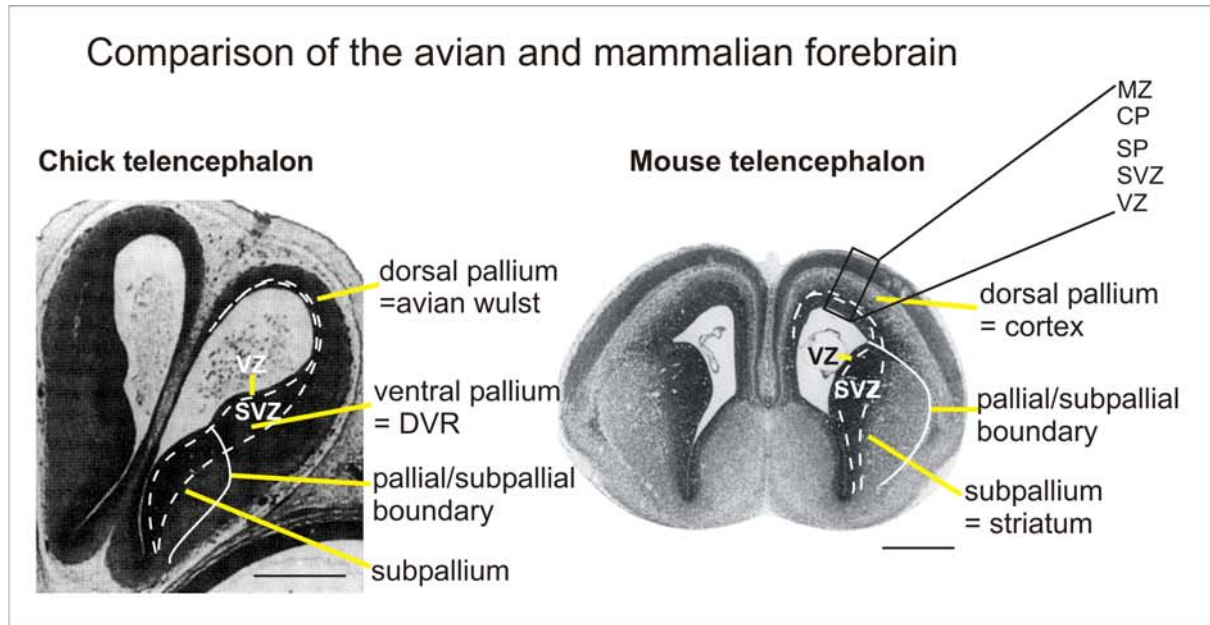
subpallium

Fig.4 Comparison of different regions of the chick and mouse forebrain. Frontal sections of a chick (~E6) and mouse (~E14) forebrain, consisting of pallial and subpallial structures. The avian telencephalon possesses an additional structure located between the dorsal pallium and the subpallium, called dorso-ventricular ridge (DVR) or ventral pallium. The boudary-region delineates pallium from subpallium. Ventricular zone (VZ) and subventricular zone (SVZ) are two proliferative layers in the forebrain. In the right corner the different cortical layers are indicated: marginal zone (MZ), cortical plate (CP), subplate (SP), SVZ and VZ. Scale bars: 500µm.

The midline-region

pallium

hippocampal anlage

DVR

cortical hem

choroid plexus

choroidal roof

subpallium
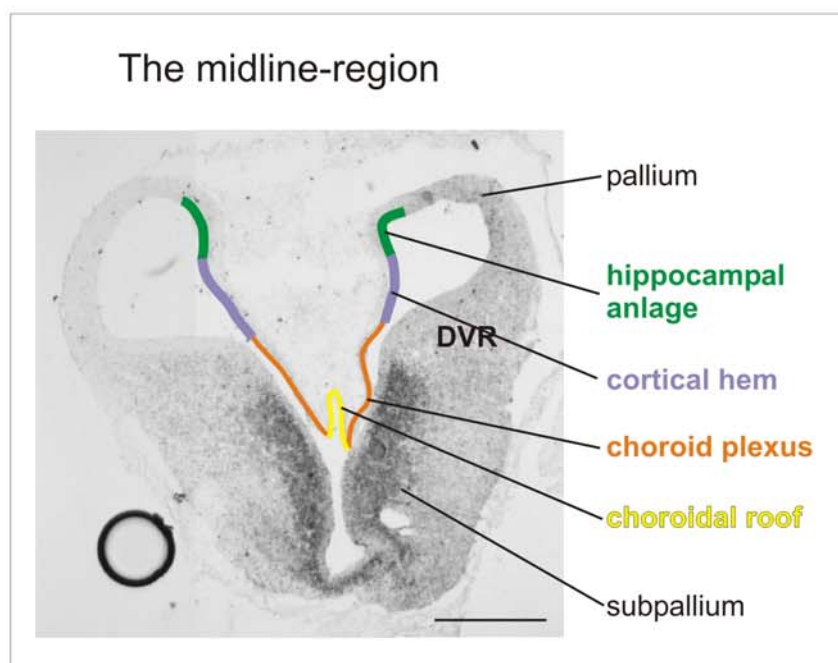
Fig.5 Schematic overview over a frontal section of a chick forebrain at E7. The midline-region is composed of hippocampal anlage, cortical hem, choroid plexus and choroidal roof. Their relative position is indicated in the picture. Scale bar: 500µm.

Tangential migration
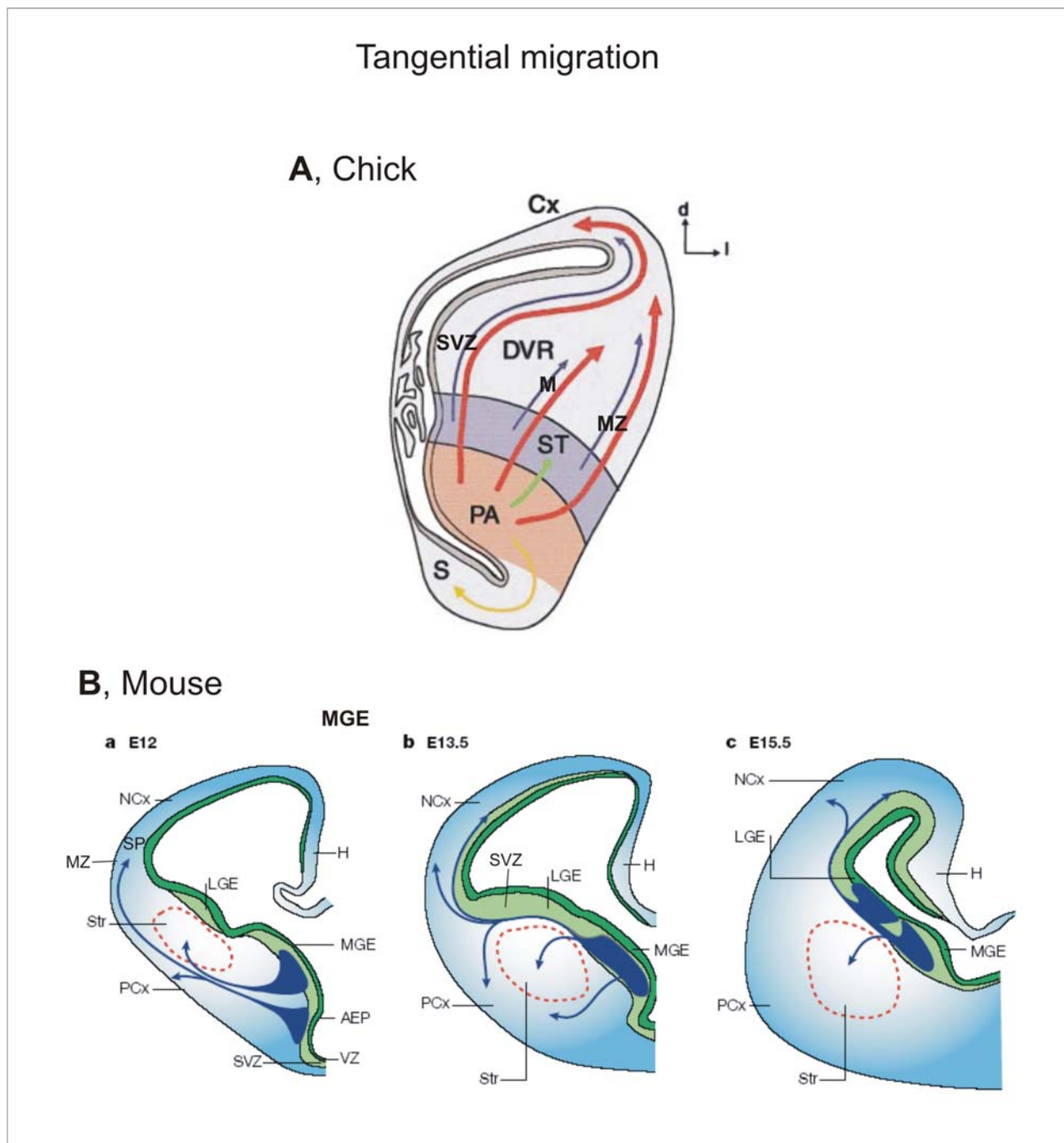
A, Chick

B, Mouse

Fig.6 Schematic illustration of tangential migration in the chick (A) and mouse (B) forebrain. Neurons, mostly originating from the pallidum (PA) in the chick and the medial ganglionic eminence (MGE) in the mouse migrate by taking three different routes into the pallium (Cx, NCx). In the chick forebrain, neurons migrate through the marginal zone (MZ), mantel zone (M) and subventricular zone (SVZ) and in the mouse they migrate through MZ, Subplate (SP) and SVZ. Pictures modified from Cobos et al., 2001 (A) and from Marin and Rubenstein, 2001(B).
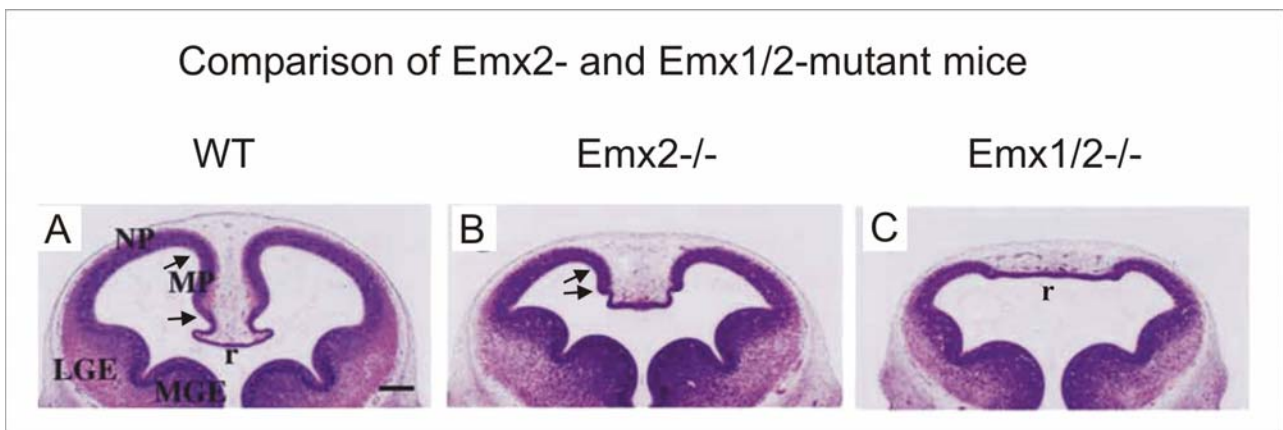
Fig.7 Morphological features of Emx2 single- and Emx1/2 double-mutant mice at E12. All sections are stained with Hematoxylin and Eosin. (A) shows a frontal section of a wildtype mouse with a normal neopallium (NP) and medial pallium (MP). Arrows indicate the region of the MP. (B) depicts the forebrain of an Emx2-mutant mouse with a shortened MP. Emx1/2 double-mutant mice (C) completely lack the MP and also exhibit a reduced NP, while the region of the choroidal roof (r) is enlarged. Scale bar: 200μm (Pictures from Shinozaki et al., 2004)
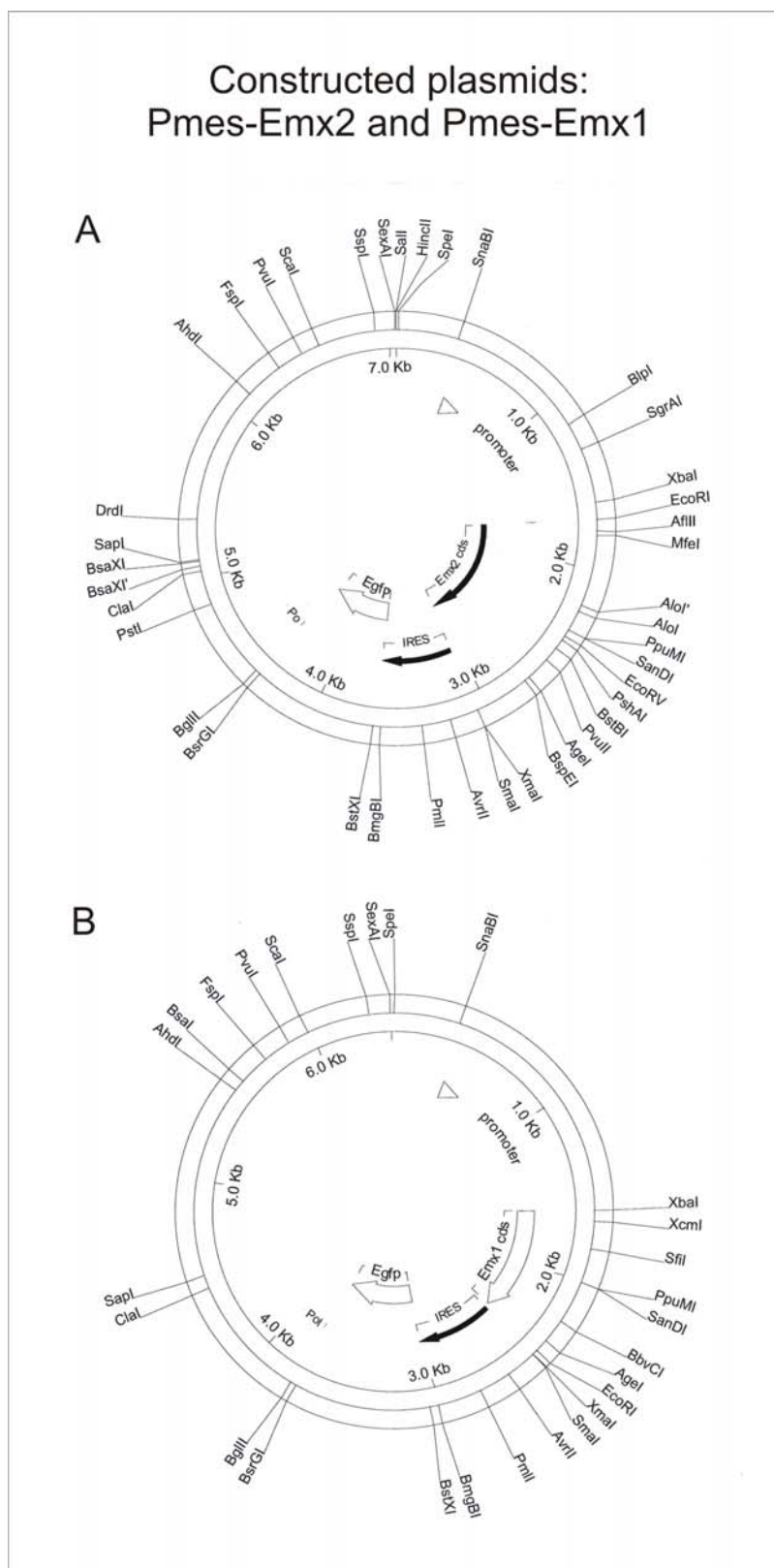
Fig.8 Pmes-Emx2 and Pmes-Emx1 plasmids. Constructed plasmids Pmes-Emx2 (A) and Pmes-Emx1 (B) containing a chicken ß-actin promotor, the gene of interest, an IRES-sequence and the EGFP-gene.
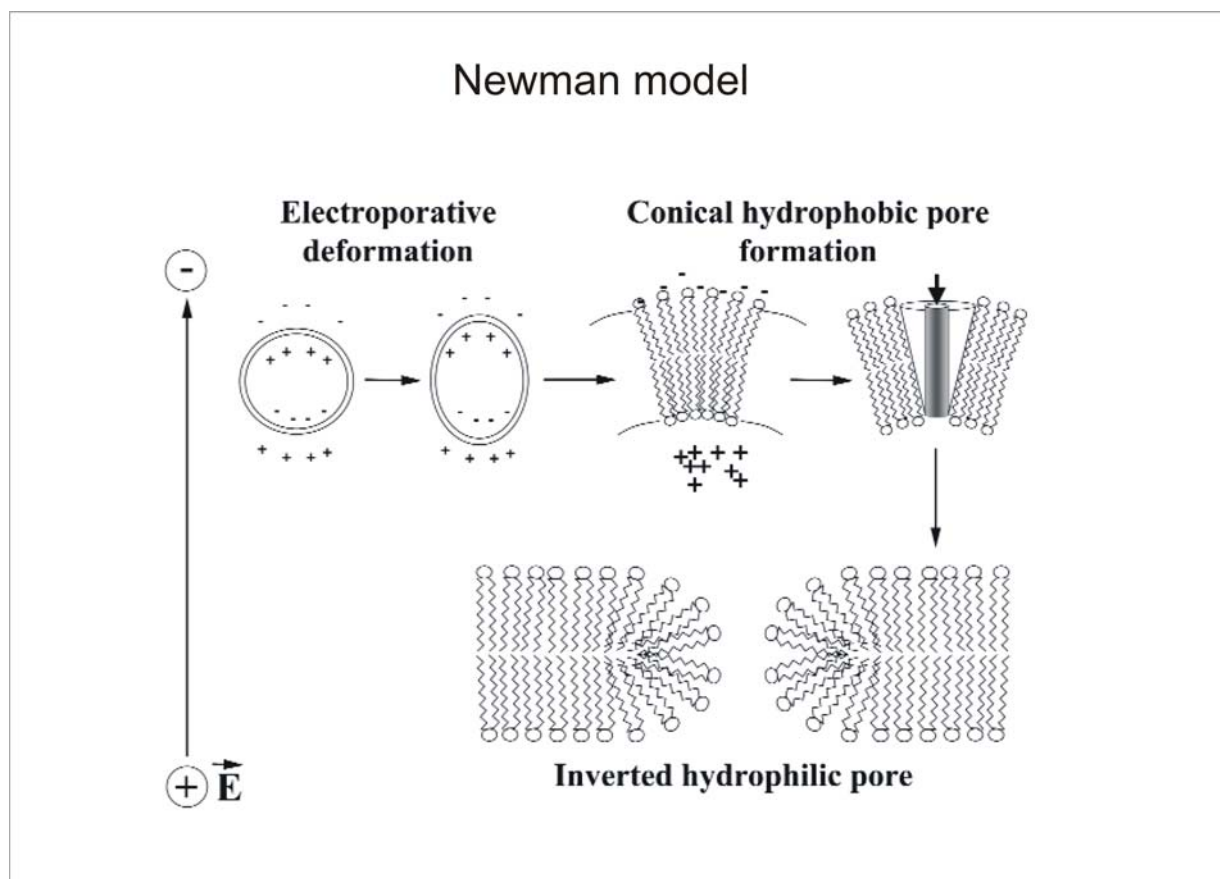
Fig.9 Newman model for the development of electroporative channels. The application of an electric field might lead to differences in the distribution of ions at the inner surface of the cell membrane, which results in membrane alterations and consequently to pore formation (figure after Neumann et al., 1999; Somiari et al., 2000).
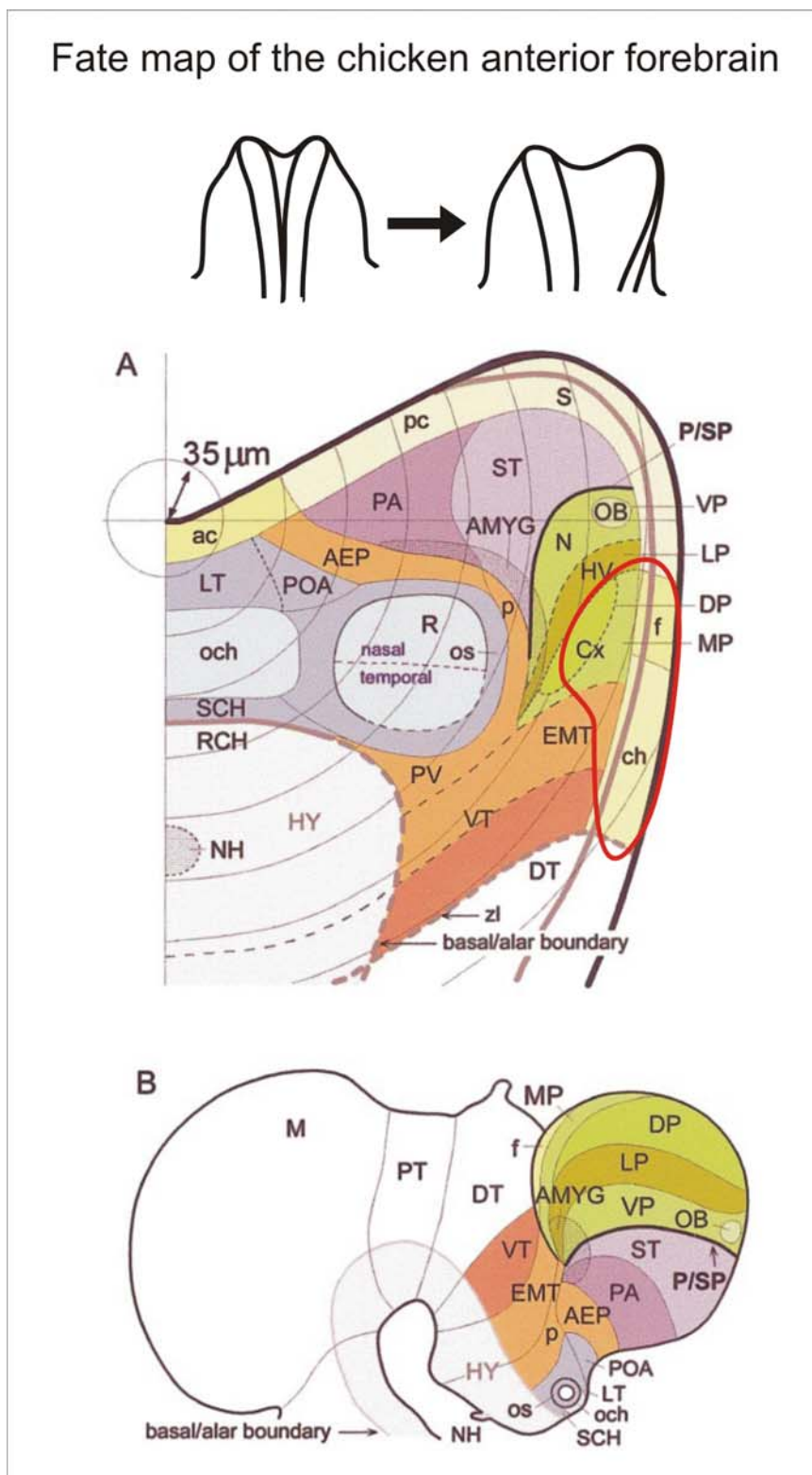
Fig.10 Fate map of the chicken anterior forebrain at stage HH8.
The schematic drawing shows the partially flattened anterior neural tube (A). The red circle indicates the region of preferential manipulation (ch, choroid plexus; cx, dorsal pallium; f, fimbria hippocampi). (B) Fate map of the forebrain-regions at around stage HH28. Picture modified from Cobos et al., 2001.
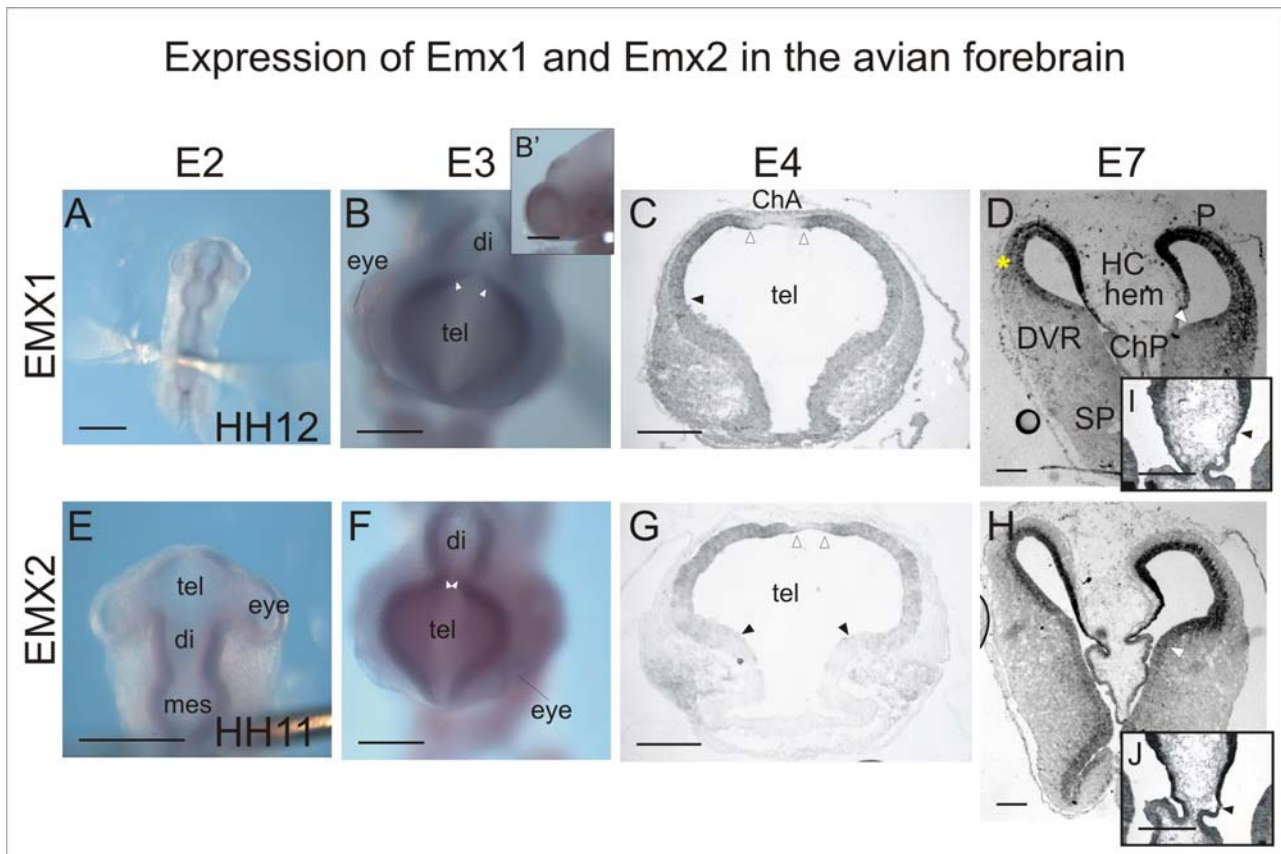
Fig.11 Emx1 and Emx2 in the avian forebrain. Expression pattern of Emx1 (A, B, B', C, D, I) and Emx2 (E, F, G, H, J) during early telencephalic development of the chick analyzed by *in situ* hybridization. At E2 (HH9-14) the expression of Emx1 and Emx2 starts to be restricted to the dorsal part of the telencephalon, but still labels the entire di- and mesencephalic neuroepithelium. By HH11/12 the expression is detectable in the anterior prosencephalon where Emx1/2 show weak expression medially. At E3 (HH18-21) these genes are expressed in the dorsal telencephalon (B') with exception of the most medial located region. Emx2 (F) seems to be expressed further medial than Emx1 (B). At E4 (HH24/25) Emx1 and Emx2 are expressed in the dorsal region of the forebrain vesicle, excluding the choroidal anlage (ChA). The expression is strongest in the region adjacent to the ChA. At E7 (HH30/31) both TFs are strongly expressed in the in the medial pallium, hippocampus and hem, excluding the choroid plexus. In the pallium (P) the expression decreases from the medial to the lateral region, finally terminating in the DVR. The expression of Emx2 extends further into the region of the DVR than Emx1 (see empty arrowheads in D, H) and also in the region of the cortical hem Emx2 extends further medially than Emx1 (see black arrowheads in I, J). The VZ of the subpallium seems to express Emx2 in very low levels. Emx1 is further detectable in postmitotic pyramidal neurons (see yellow asterisk in D). tel, telencephalon; di, diencephalon; mes, mesencephalon, HC, hippocampus; ChP, choroid plexus. Scale bars: 250μm.

Distribution of transcription factors and secreted signals in the neuroepithelium and the midline at E4
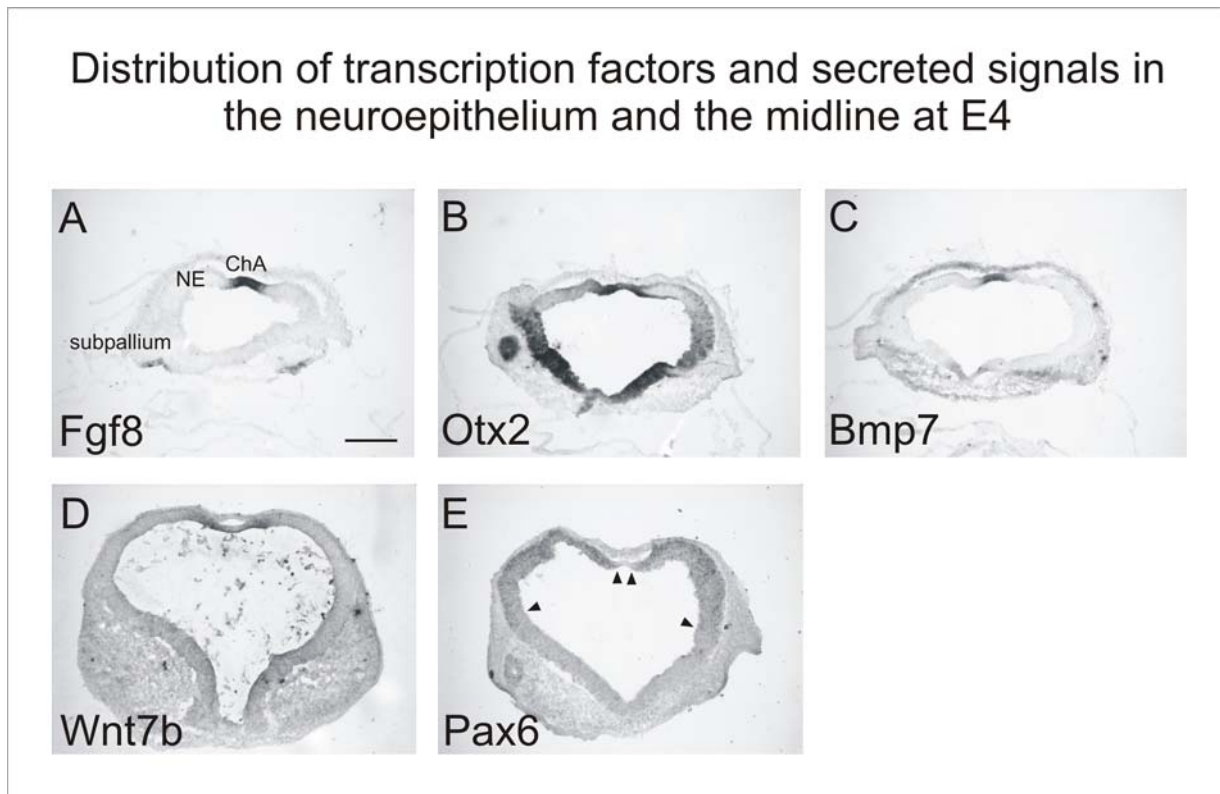
Fig.12 Analysis of transcription factors and signaling molecules at E4. *In situ* hybridization of different dorsal markers at E4. The thin ChA strongly expresses Fgf8 (A) and Bmb7 (C). The expression domain of Otx2 (B) also labels this region but extends slightly further lateral. Fgf8- and Bmp7-expression is bordered by the expression of Emx1 and Emx2, whereas Emx1 leaves a small gap. Wnt7b (D) is also absent from the ChA and is coexpressed with Emx1/2 in a small territory adjacent to the Bmp7-positive region. Pax6 (E) is dorsally expressed reminiscent of the Emx2 pattern, also avoiding the ChA (see arrowheads for expression domain). In the lateral region the Pax6-signal is very weak. NE, neuroepithelium. Scale bar: 250μm.
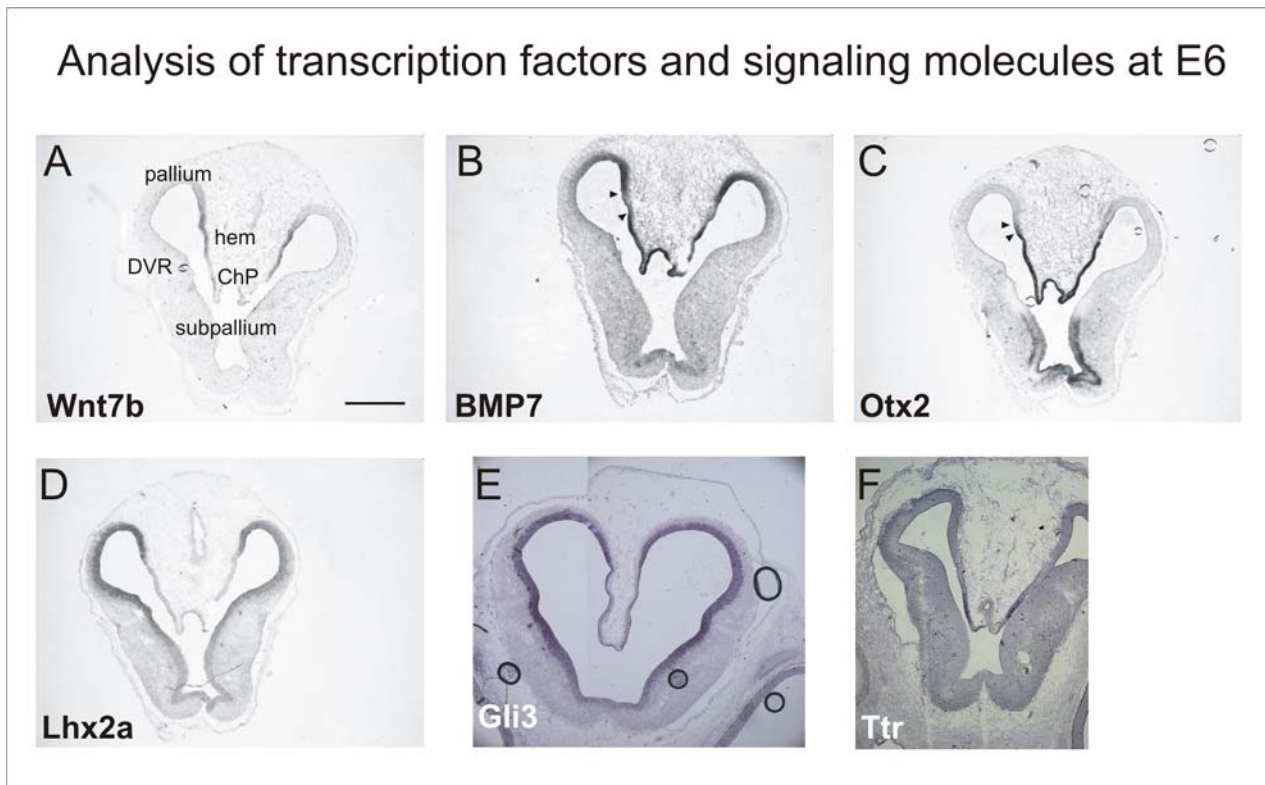
Fig.13 Analysis of different transcription factors and signaling molecules at E6. Wnt7b (A) marks the region of the cortical hem. Bmp7 (B) is strongly expressed in the region of the choroid plexus (ChP) and slowly decreases in the dorsal region. In the region of the hem, the Bmp7-signal decreases significantly (see arrowheads). Otx2 (C) strongly marks the ChP and very low levels are detectable in the hem (see arrowheads). Lhx2a (D) labels the telencephalic VZ except the ChP and hem with stronger expression dorsally. Gli3 (E) completely labels the VZ of the forebrain except the ChP. Ttr (F) expression weakly starts in the ChP around E6. Scale bar: 500µm.

Dorsal and ventral expression pattern
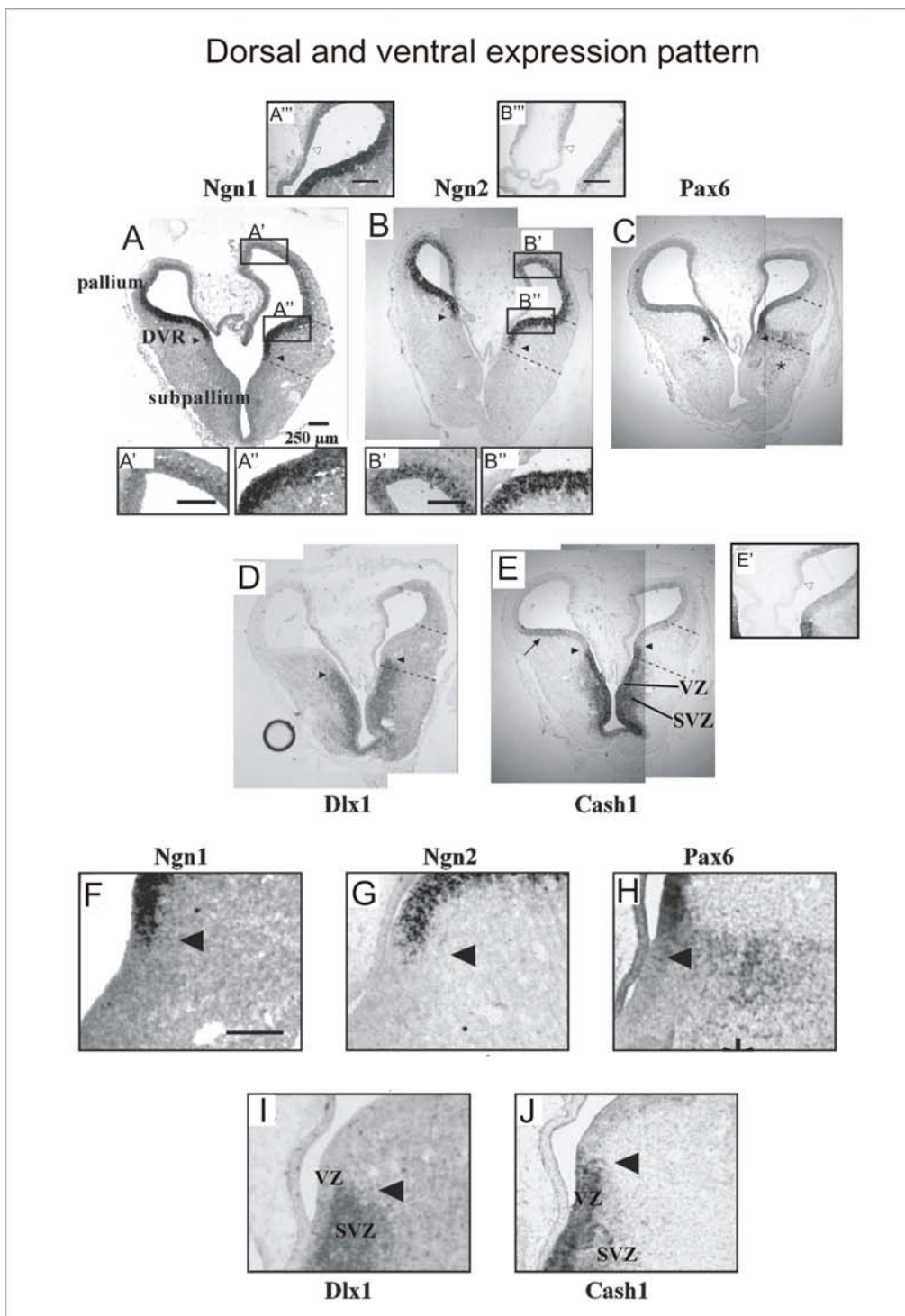
Fig.14 Transcription factor analysis in the forebrain. *In situ* hybridization of frontal sections of E7 chick telencephalon at comparable mid-rostro/caudal levels. The arrowheads mark the dorso/ventral expression-border and the dashed line delineates the region of the DVR. (A) and (B) show the expression of Ngn1 and Ngn2 in the dorsal pallium, DVR and cortical hem. (A', A'', A''') and (B', B'', B''') depict higher magnification insets of those regions. Pax6 also marks the dorsal pallium and the DVR. There is a stream of Pax6-expressing cells (*) which extends tangentially into the subpallium (C). (D) shows the ventral expression of Dlx1 stopping below the DVR, while the ventral marker Cash1 extends further dorsally into the DVR (E). The arrow indicates the dorsal expression of Cash1 at low levels. (E') depicts the distribution of Cash1 in the hem region. (F-J) depict higher magnifications of the expression border in the panels shown in A-E. Scale bars: 250µm.

Pax6 and Gsh2 double-positive cells in the pallial/subpallial boundary
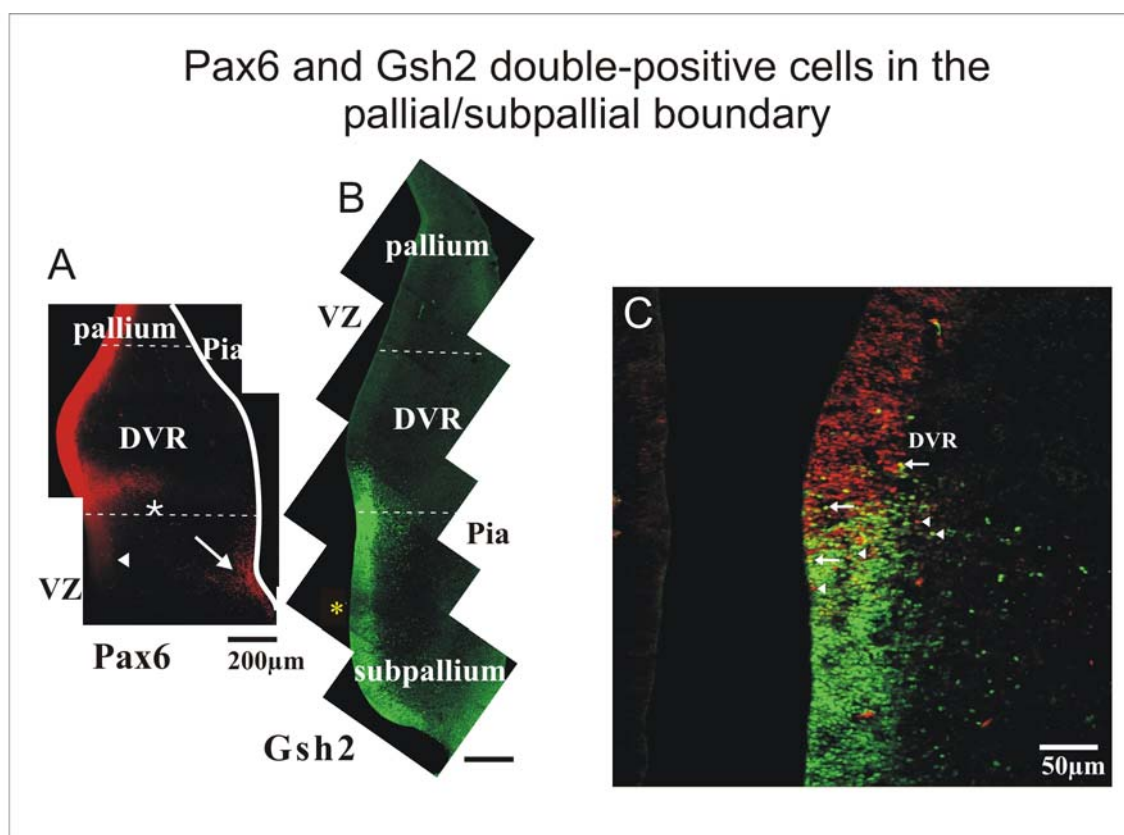
Fig.15 Pax6- and Gsh2-expression in the pallial/subpallial boundary-region. (A) and (B) show immunostainings of Pax6 (red) and Gsh2 (green) in frontal sections of chick telencephalon at E7. The asterisk in (A) indicates a band of Pax6-positive cells extending into differentiated regions of the subpallium (arrow). The arrowhead in (A) depicts a weak Pax6-immunoreactive band extending into the subpallium. The dashed lines indicate the region of the DVR. In (B), a staining for Gsh2 with a characteristic gap of expression (yellow asterisk) is shown. The overlapping region of Gsh2 (green) and Pax6 (red) is depicted in high power in (C). Arrows indicate the double-positive cells and arrowheads mark Gsh2- or Pax6- positive cells. Scale bars: 200µm (A, B); 50µm (C).

Expression of Sfrp1 in the boundary-region

A **B** **C**

Sfrp1

500μm

frontal   medial   caudal

D **E** **F**
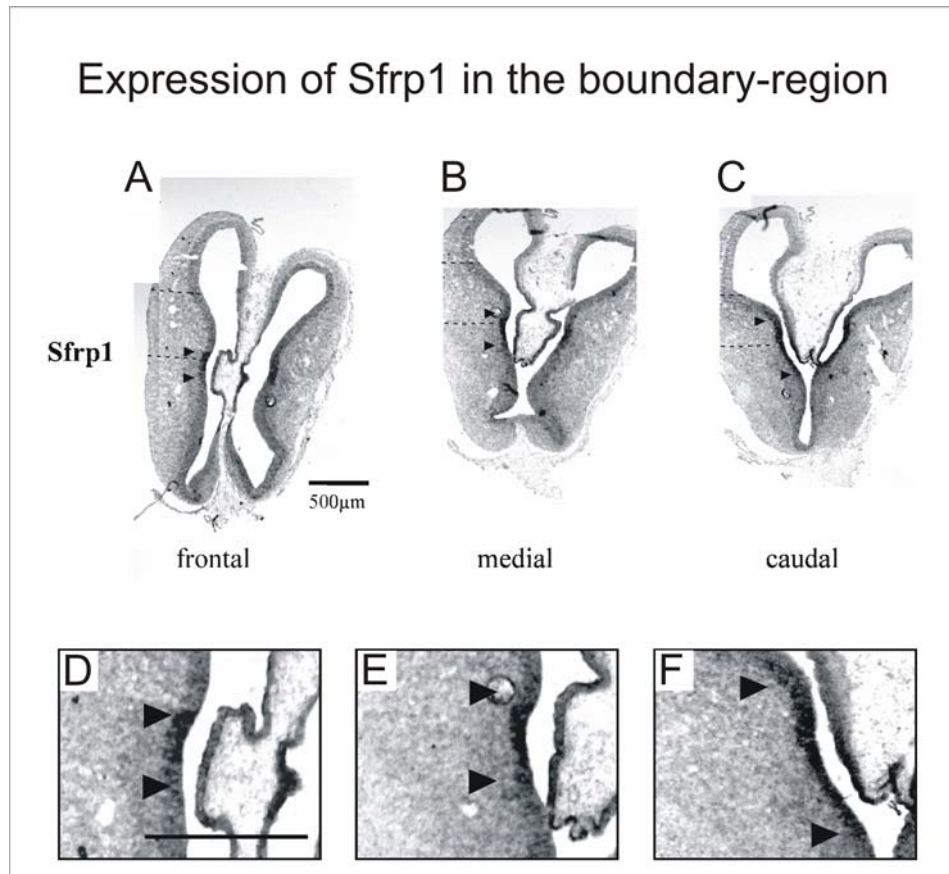
Fig.16 Sfrp1-expression in the boundary. *In situ* hybridization of Sfrp1 in frontal sections of E7 chick telencephalon. The expression is restricted to the region between DVR and subpallium at all rostro/caudal levels (A, D: rostral; B, E: medial; C, F: caudal). Scale bars: 500μm.

Analysis of the chick forebrain at E10

A avian wulst
DVR
subpallium
Tbr

B boundary
Blbp

C
C'
BrdU

D ChP
Ttr

E VZ
Emx2

F VZ
Pax6
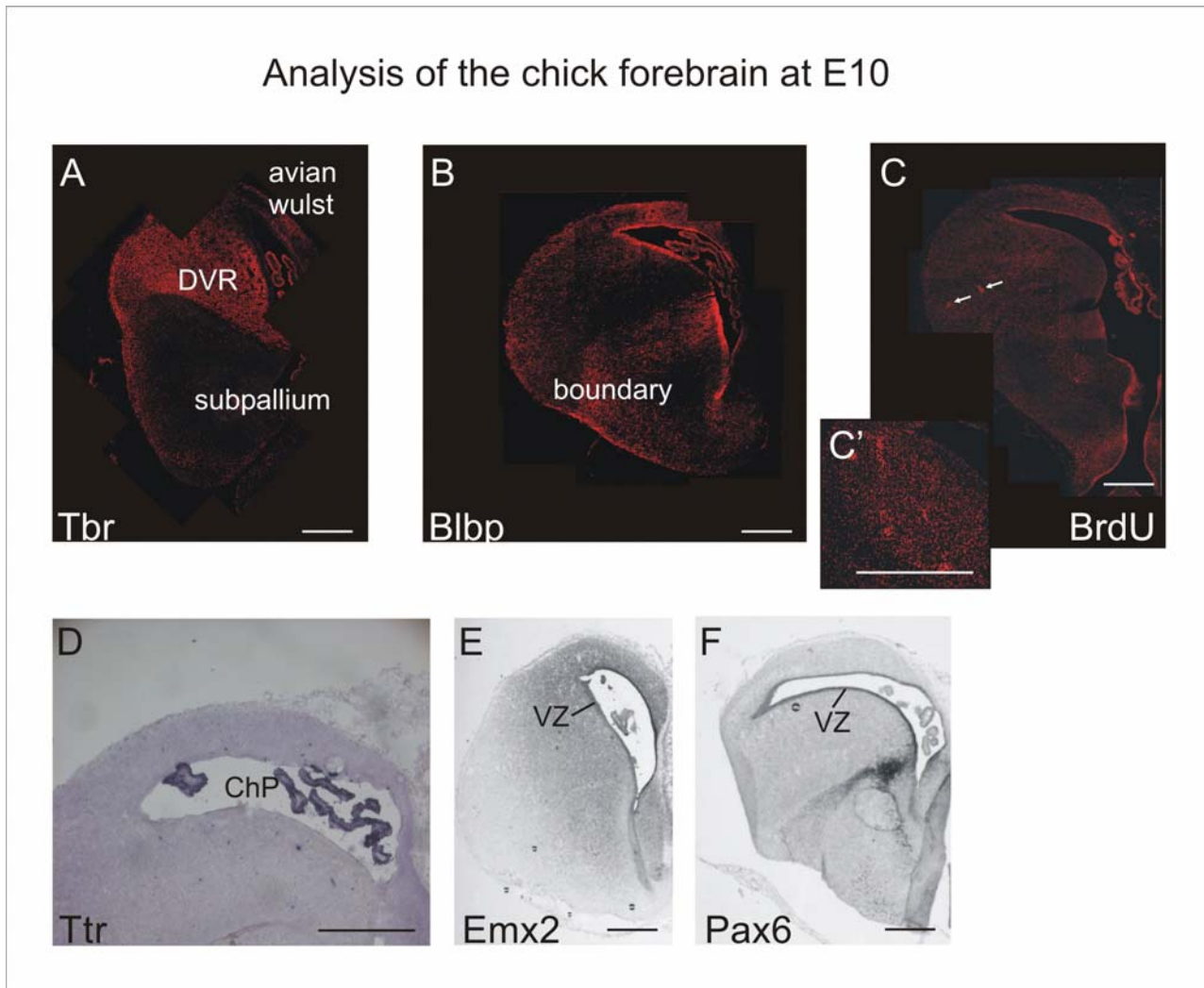
Fig.17 Forebrain analysis at E10. Frontal sections of the chick forebrain immunostained against Tbr, a dorsal marker of the forebrain expressed from precusor cells and postmitotic neurons (A) and against Blbp, a glial cell marker, located in the region of the pallial/subpallial boundary (B). (C) depicts a brain that was treated with BrdU at E6 and sacrificed at E10. Labeled cells migrated into the marginal zone of the DVR and formed cell clusters at E10 (indicated by arrows), which can be detected by staining against BrdU. (C') shows a magnification of nuclei from another section. *In situ* hybridized sections depict Ttr (D), Emx2 (E) and Pax6 (F). Scale bars: 250μm.

Summary of regionalization
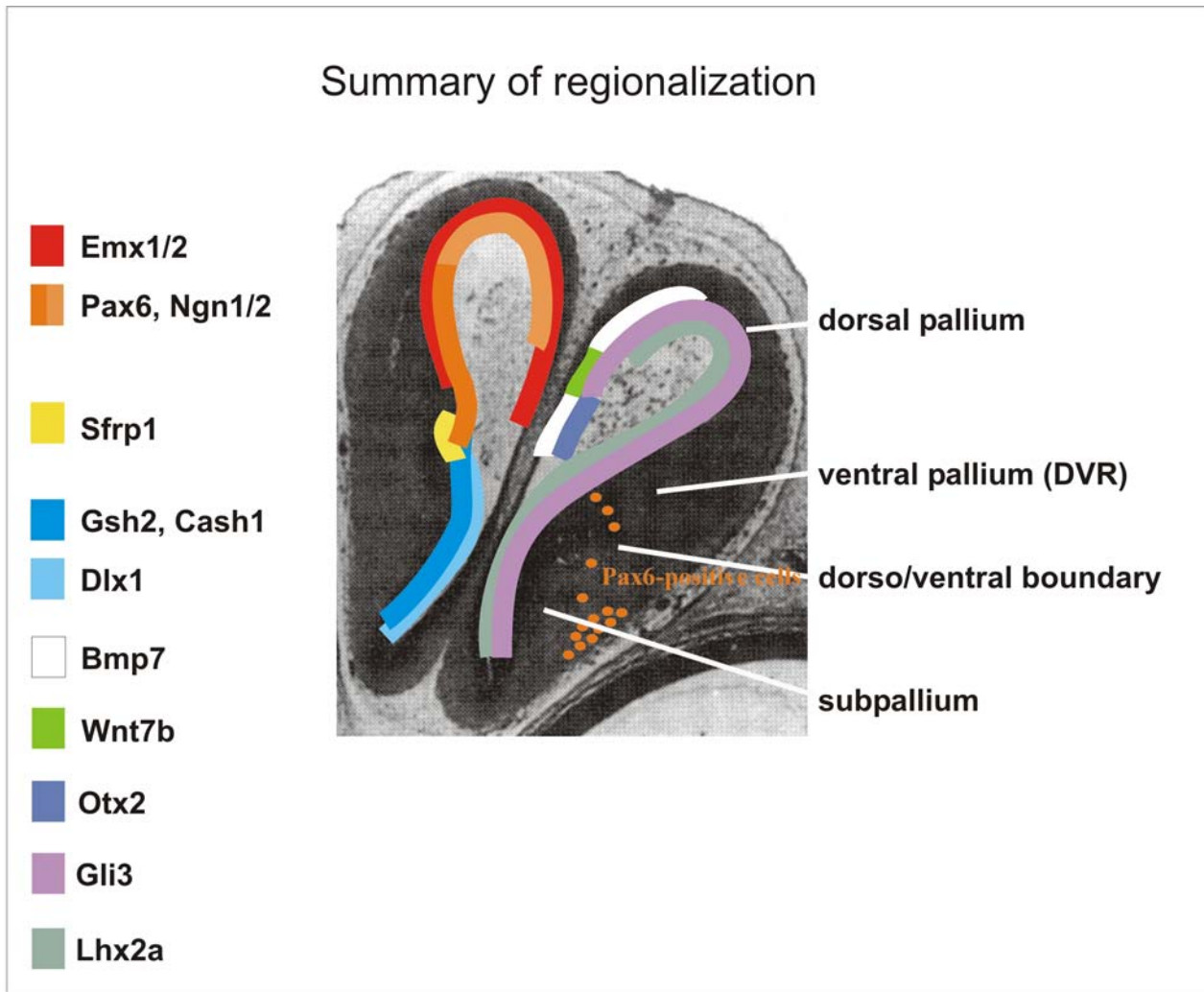
Fig.18 Schematic summary of the regionalization of the developing chick telencephalon at E7. Pax6, Emx1/2 and Ngn1/2 are expressed in the dorsal pallium and the DVR, while Emx1/2 expression extends only partially into the DVR. The subpallium is characterized by Dlx1-, Gsh2- and Cash1-expression. Sfrp1 is expressed in the dorso/ventral boundary-region, delineating the DVR from the subpallium. The midline-territory expresses Wnt7b in the region of the cortical hem. Otx2 and Bmp7 are both strongly expressed in the choroid plexus, while Bmp7-expression gradually decreases dorsally. Gli3 marks the entire forebrain VZ except the ChP and Lhx2a labels the forebrain VZ excluding ChP and hem.
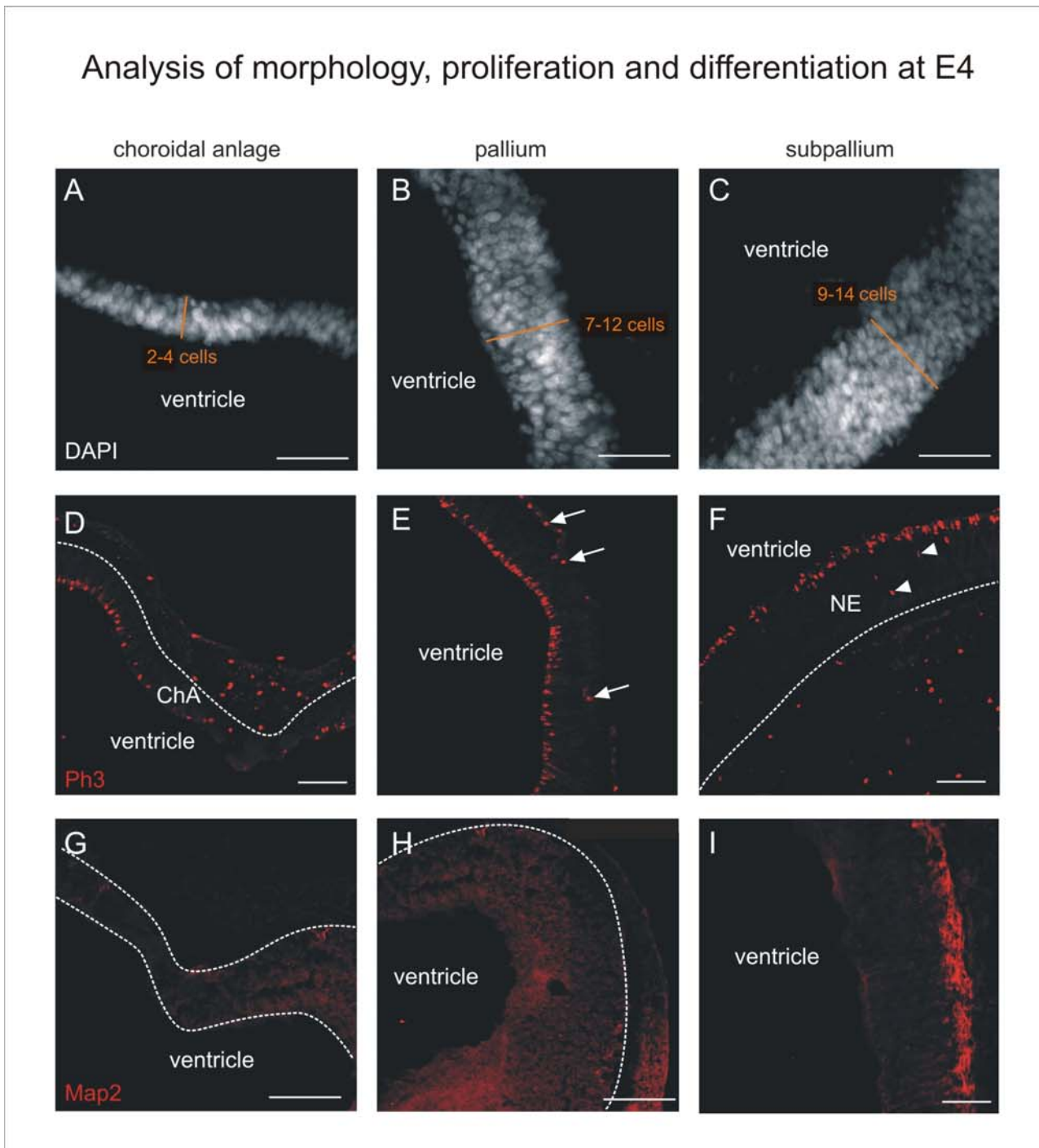
Fig.19 Analysis of morphology, proliferation and differentiation at E4 (HH24/25). A staining for Dapi in 20µm cryosections reveals that the tissue located medio/dorsally comprises of 2-4 cells in thickness (A), whereas the pallium consists of 7-12 cells (B) and the subpallium of 9-14 cells (C). Antibody stainings for PH3 show that the pallial (E) and subpallial neuroepithelium (NE; F) stongly proliferate, whereas only few mitotically active cells can be observed in the choroidal anlage (ChA; D). Arrowheads in (F) indicate subpallial SVZ-cells, whereas arrows in (E) indicate proliferative cells in the pia mater. Differentiation, monitored by Map2, is observed in several embryos in the subpallial region (I), but not in the pallium (H) or choroidal anlage (G). Scale bars: 50µm.

Analysis of morphology, proliferation and differentiation at E6
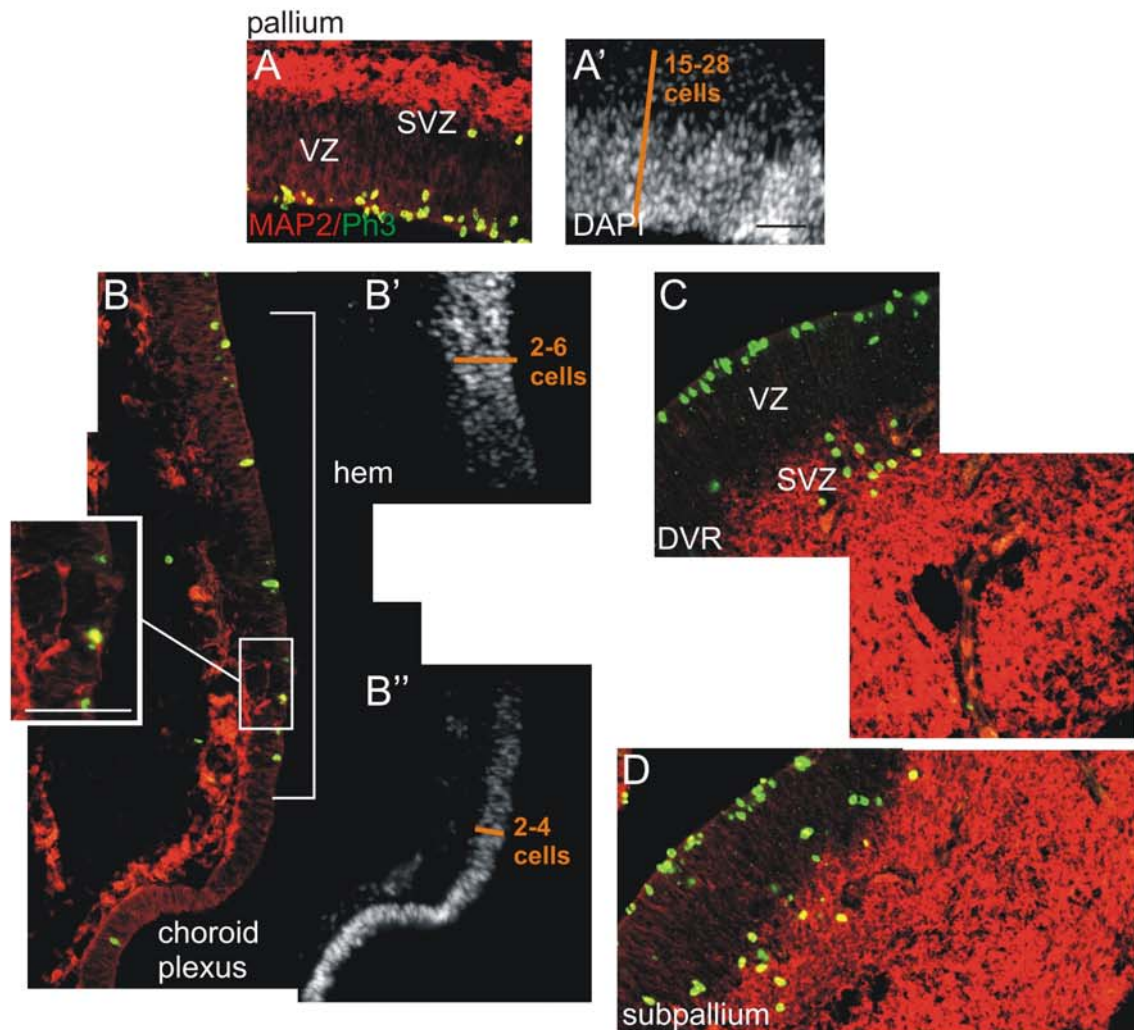
Control E6	ChP (n)	hem (n)	hippocampus (n)	pallium (n)	DVR (n)	subpallium (n)
Thickness	2.4±0.2 (12)	4±0.3 (16)	11.1±0.4 (9)	20.6±1.4 (10)		
Ph3+ cells/area	2.4±0.4 (13)	5.4±1.6 (5)		18.3±1.1 (3)	19.5±1.1(2)	24.5±1.6 (6)

Fig.20 Comparison of proliferation, differentiation and morphology in the different brain regions at E6. Cryosections are stained for PH3 (green; mitotic cells) and Map2 (red; neurons). Nuclei are visualized with Dapi. The pallium (A) exhibits a thickness of about 21 cells, a high rate of proliferation in the VZ and some mitotically active cells in the SVZ. A band of postmitotic neurons is also visible in the pallium. In (B) a part of the midline-region is depicted. The choroid plexus (B, B'') consists of 2 cells in thickness and the hem region contains 4 cells. The proliferation is very low in the choroid plexus and slightly higher in the hem. Differentiated neurons cannot be observed in the ChP but in the hem. In the hem not only a thin band lining the VZ, but also some neurons inside the VZ characterize this region (see inset in B). The region of the DVR (C) as well as the subpallium (D) are characterized by strong proliferation in VZ and SVZ and a large area of differentiated neurons. (E) Quantification of thickness (Dapi+ cells; n=number of counts) and proliferation (PH3+ cells/field of view). Scale bars: 25µm.

Migration in the chick forebrain

A, Infection in the cortex

B, Infection in the DVR

C, Infection in the subpallium

D, Quantification of migration studies

Infection in :	pallium	DVR	pallial/subpallial boundary	subpallium
number of infections:	3	15	5	12
no migration:	0	7	0	0
migration to pallium:		8	2	7
migration to DVR:	0		1	4
radial elongation:	3	0	3	0
migration to subpallium:	0	1	0	

Fig.21 Migrational analysis in the chick forebrain using GFP-adenovirally infected telencephalic slices at E7. In the pallium (P) cells mainly elongate radially towards the pial surface (A). Cells from the DVR (B) and from the subpallium (SP; C) take different routes of migration. They migrate in the subventricular zone (SVZ), the mantel zone (M) and the marginal zone (MZ) tangentially into the pallium (indicated by black and white arrows in B and C). Only very few cells from the DVR turn ventrally and cross into the subpallium (red arrows in B). (D) depicts the quantification of the migration analysis. V, ventricle. Scale bars: 250µm.
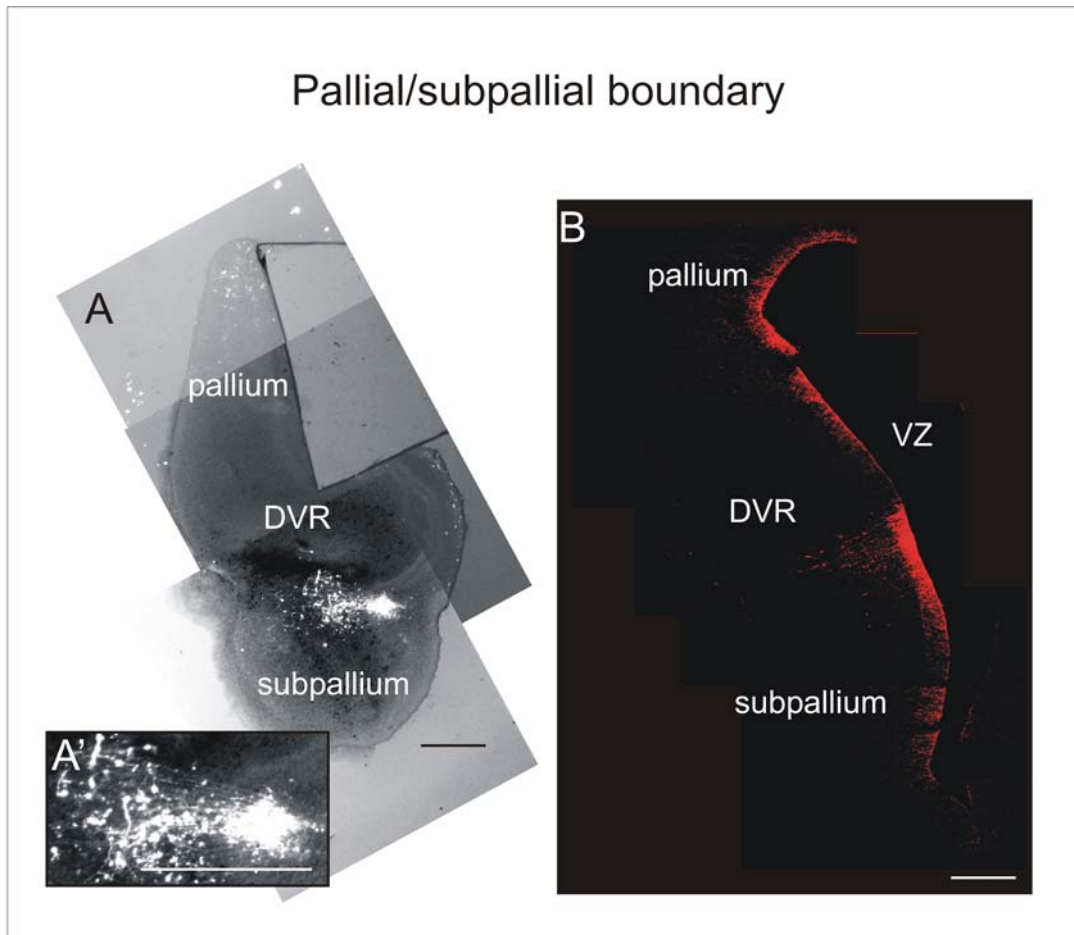
Fig.22 Radially oriented cells in the pallial/subpallial boundary. (A) depicts an GFP-adenovirally infected slice of the forebrain. Many cells infected in the pallial/subpallial boundary achieve a radial shape (A'; higher magnification), which could correspond to the bundle of radial glia cells forming the pallial/subpallial boundary similar to the situation in mammals. In the region of this boundary an antibody-staining against Blbp (B), a radial glia marker, also labels some radially oriented cells. Scale bars: 100μm.
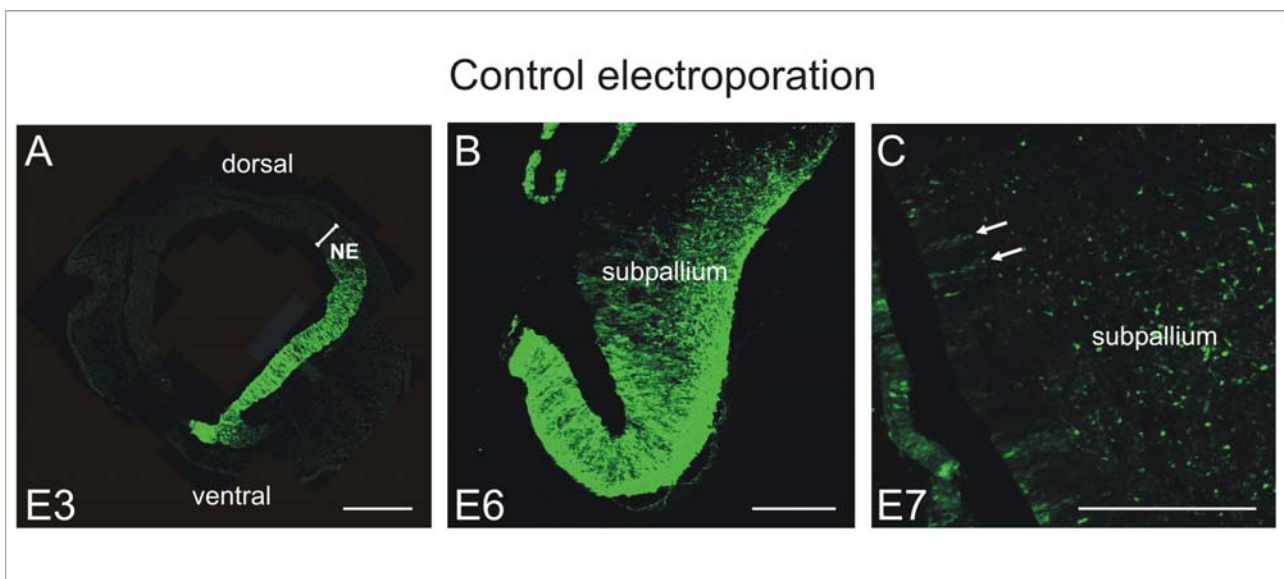
Fig.23 Confocal images of electroporated chick embryos at E2. A control plasmid containing the GFP-gene is transduced and the embryos are sacrificed at E3 (A), at E6 (B) and at E7 (C). At E3 all cells in the transduced neuroepithelium (NE) are strongly labeled, whereas at E6 fewer subpallial cells are GFP-positive and at E7 only very few cells in the VZ express GFP. These cells are arranged in colums (see arrows in C). Scale bars: 250µm.
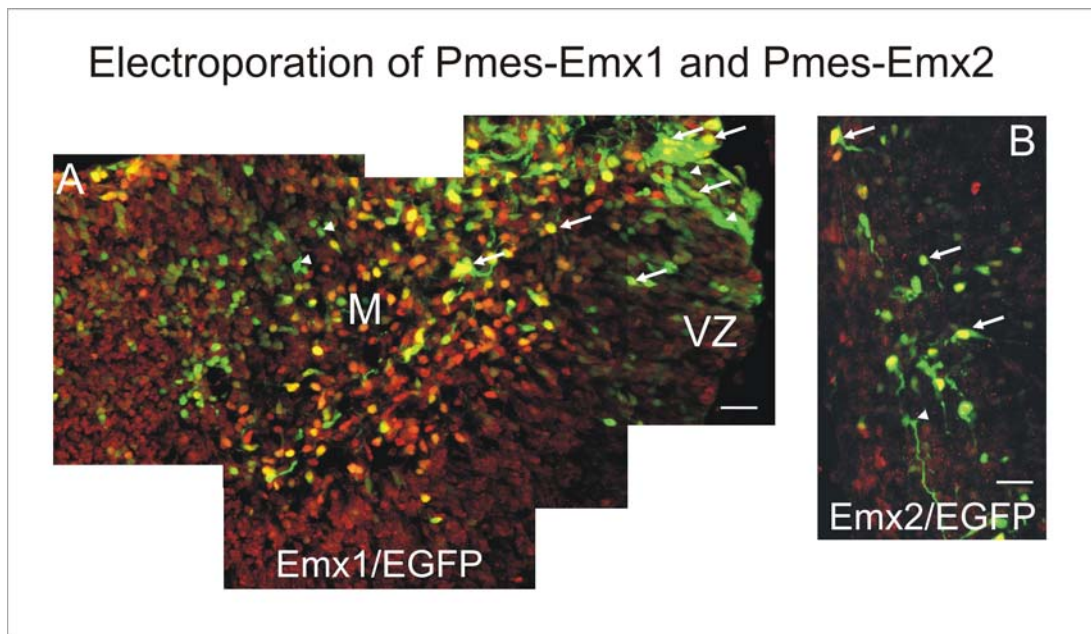
Fig.24 Conformation of electroporation. Electroporation of Pmes-Emx1(A) and Pmes-Emx2 (B) at E2 into the developing subpallium of the forebrain. The presence of Emx-protein at E4, is tested by double-stainings for Emx1 or Emx2 and GFP. This results in a nice colocalization of Emx and GFP (see arrows). Arrowheads indicate cells that only seem to express GFP. Scale bars: 25 μm.
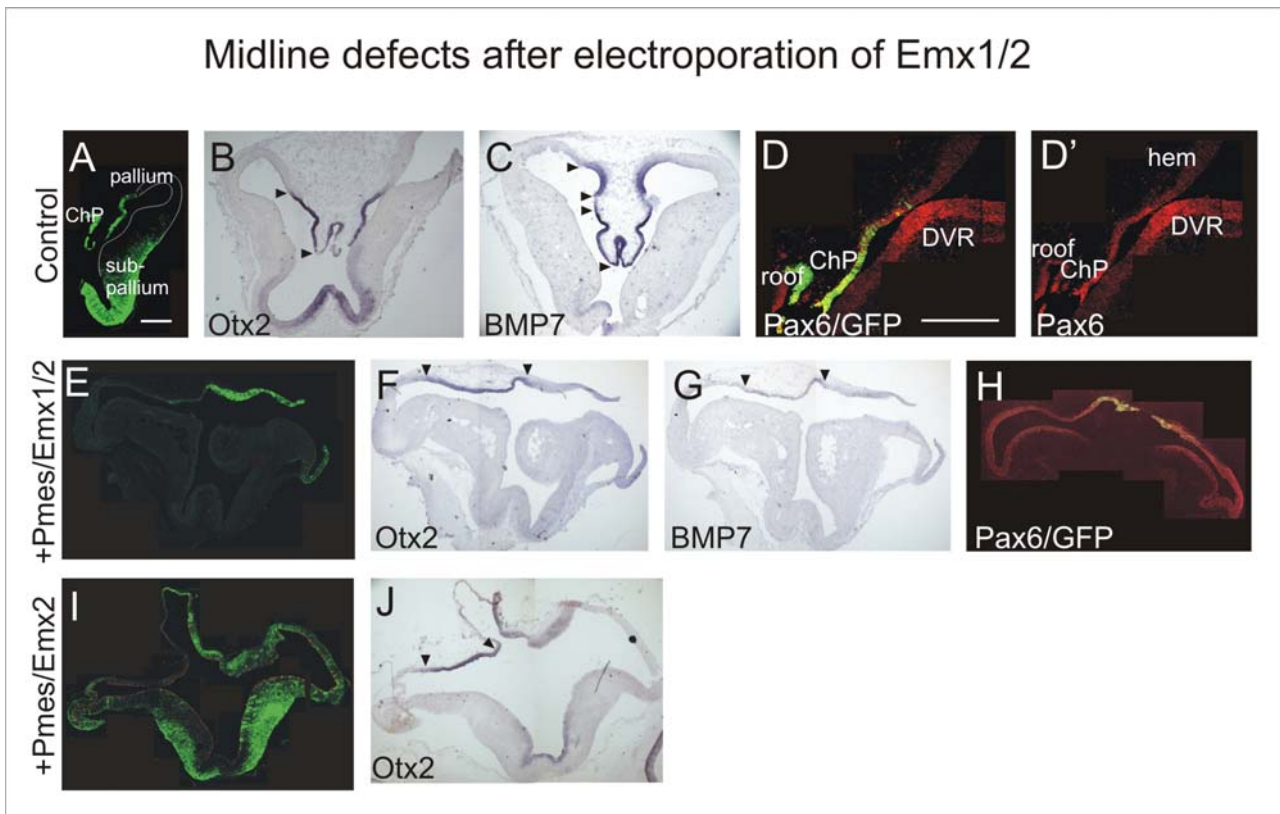
Fig.25 Midline defects caused by ectopic Emx1/2. Strong transduction of Emx1/2 leads to deformations of the forebrain at E6. The tissue of the midline-region does not develop properly, which manifests in no invagination of the presumptive midline-tissue (E) or even in evagination of this region (I). (A, D, E, H, I) show immunostainings for GFP and (I) is additionally labeld for PH3. Sections in (D, D', H) are also immunostained against Pax6. (D') depicts the normal distribution of Pax6-protein, with strong expression in the DVR and low levels in the choroidal roof and dorsal hem. Arrowheads in (B) and (C) depict the region of Otx2- and Wnt7b-expression in control sections. Otx2 (F, J) and Bmp7 (G) are not observed in the region of Emx1/2-overexpression, but are shifted to a region flanking the area of ectopic Emx1/2 (see arrowheads in F, G, J), using *in situ* hybridization for detection. Scale bars: 250μm.
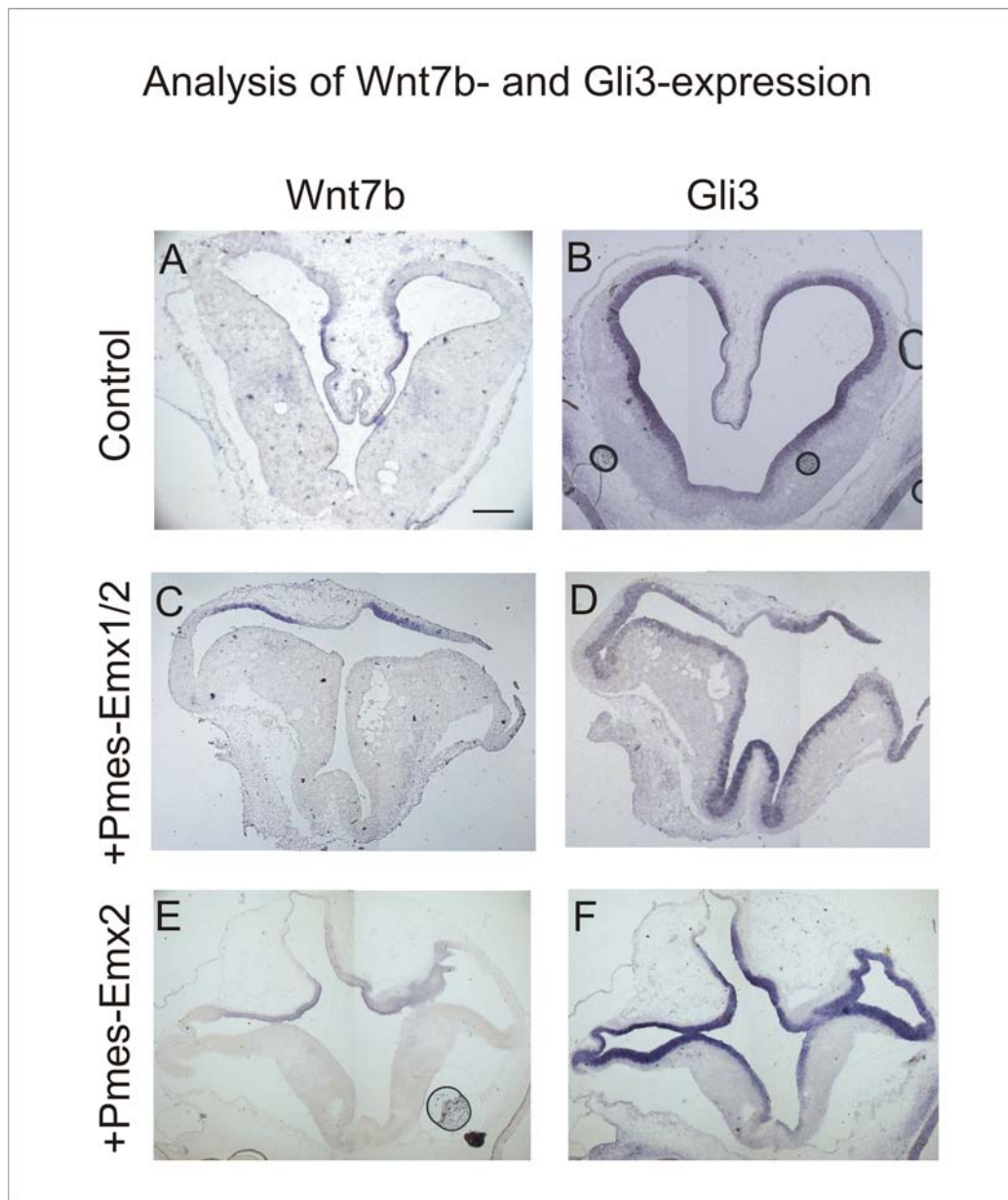
Fig.26 Analysis of Wnt7b and Gli3, genes that are expressed in distinct forebrain regions at E6. (A, B) show the normal distribution of these genes in the forebrain using *in situ* hybridization. Analysis of Wnt7b (C, E) in manipulated brains does not show alterations. The expression is still present in the region located adjacent to the Otx2-positive region. Gli3, a telencephalic marker (B, D, F), which is normally absent in the choroid plexus (B) labels the region of misexpression upon Emx1/2-overexpression, but excludes the region of Otx2-expression (D). In the example of Emx2-overexpression it not only marks the region of Emx2-overexpression, but also the Otx2-positive region (F). Scale bar: 250μm.
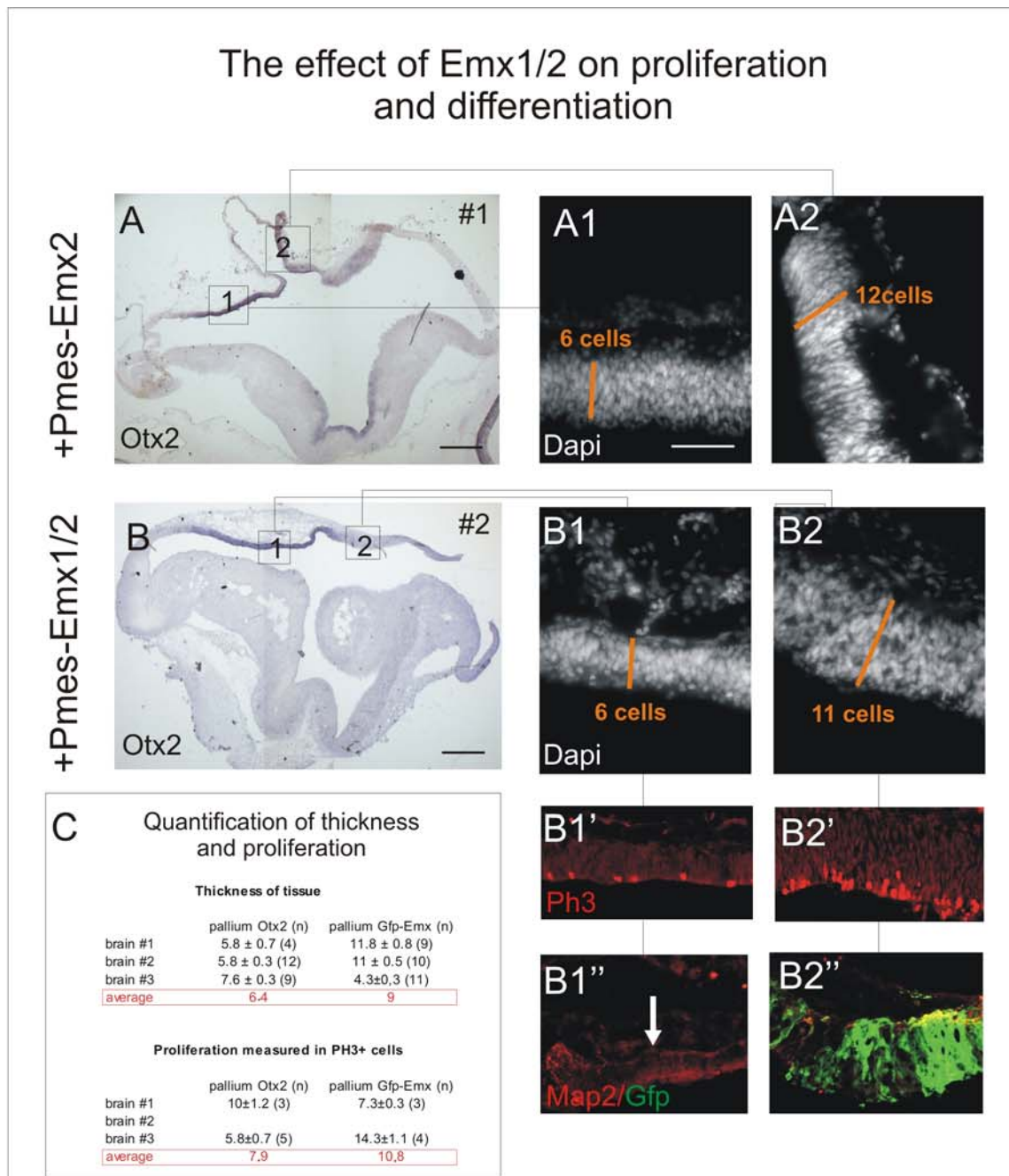
Fig.27 Analysis of thickness of epithelium, cell proliferation and neurogenesis upon Emx1/2-misexpression. Emx-misexpression causes an increase of cell thickness to 12 cells (in A2; by Emx2) and to 11 cells (in B2; by Emx1/2). In the shifted Otx2-positive region an increased thickness of 6 cells (A1, B1) is observed. Proliferation observed by antibody-staining for PH3 is higher in the transduced area (B2') than in the shifted Otx2-positive area (B1'). Differentiation of neurons, monitored by the expression of Map2 (B1'', B2''), showes interruptions at the sites of high Emx-expression (B2''), compared to the normal band lining the VZ. In the region of Otx2 no differentiated band of cells is observed (see arrow in B1''). (C) depicts the quantification of thickness and proliferation. Scale bars (A, B): 250µm; (A1): 25µm.

Brain deformations induced by overexpression of Emx1 or Emx2

A

Pallium

DVR

Subpallium

E6 Pmes-Emx2
Gfp+Ph3

B

Pallium

DVR

Subpallium

E5 Pmes-Emx1
Gfp+Ph3
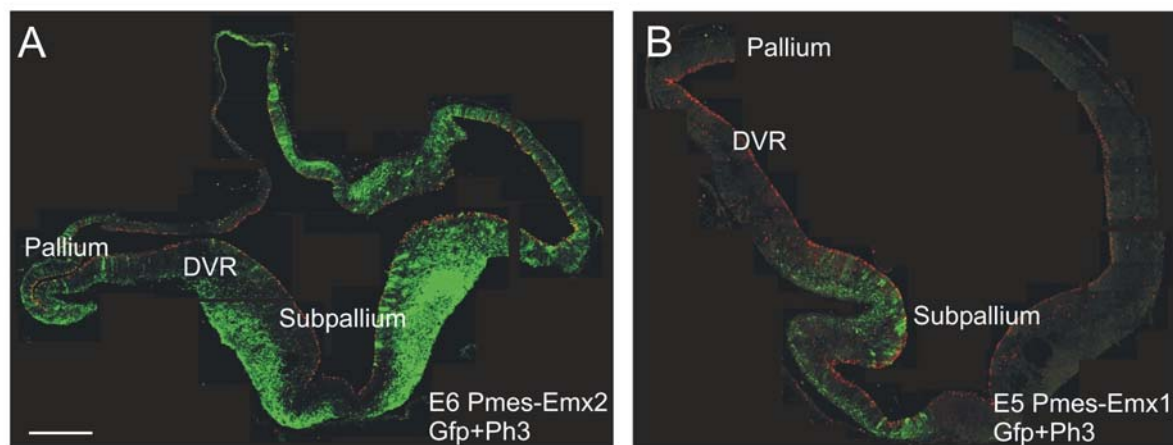
Fig.28 Deformations induced by misexpression of Emx1 or Emx2. Strong folding of the forebrain tissue is observed by transduction of Emx1 (B) or Emx2 (A) into the telencephalic vesicle at E2 of chick embryos, analyzed at E5 or E6. Upon Emx2-overexpression the pallial region shows additional foldings and a midline-region strangely folded to the outside. Whereas the overexpression of Emx1 is also able to induce an additional folding in the subpallium (green: GFP, red: PH3). (A, B) show immunostained sections against GFP and PH3. Scale bar: 250μm.
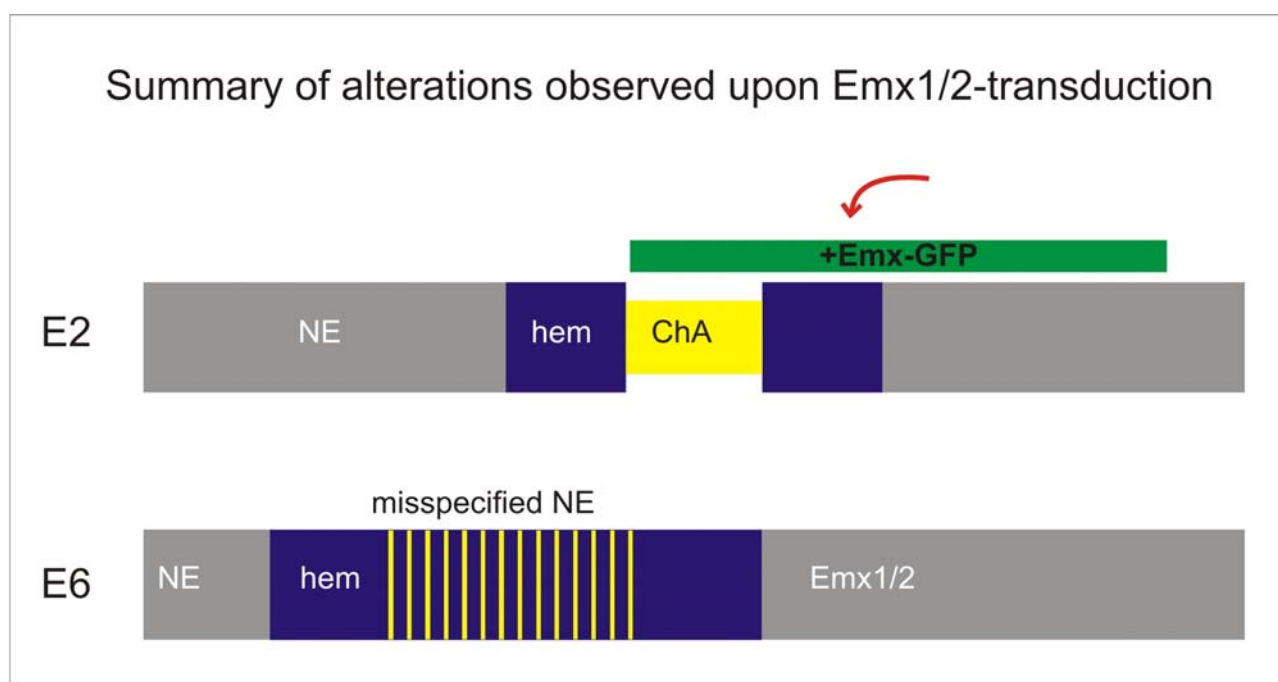
Fig.29 Schematic summary of introduced alterations upon Emx1/2-transduction into the region of the choroidal anlage. The misexpression of Emx1/2 results in a shift of the Otx2-positive ChP-region besides the Emx1/2-expressing area. The medial region of ectopic Emx1/2-expression displays features of the hem-region, while the shifted Otx2-positive region is characterized by ChP- and hem-features. NE, neuroepithelium
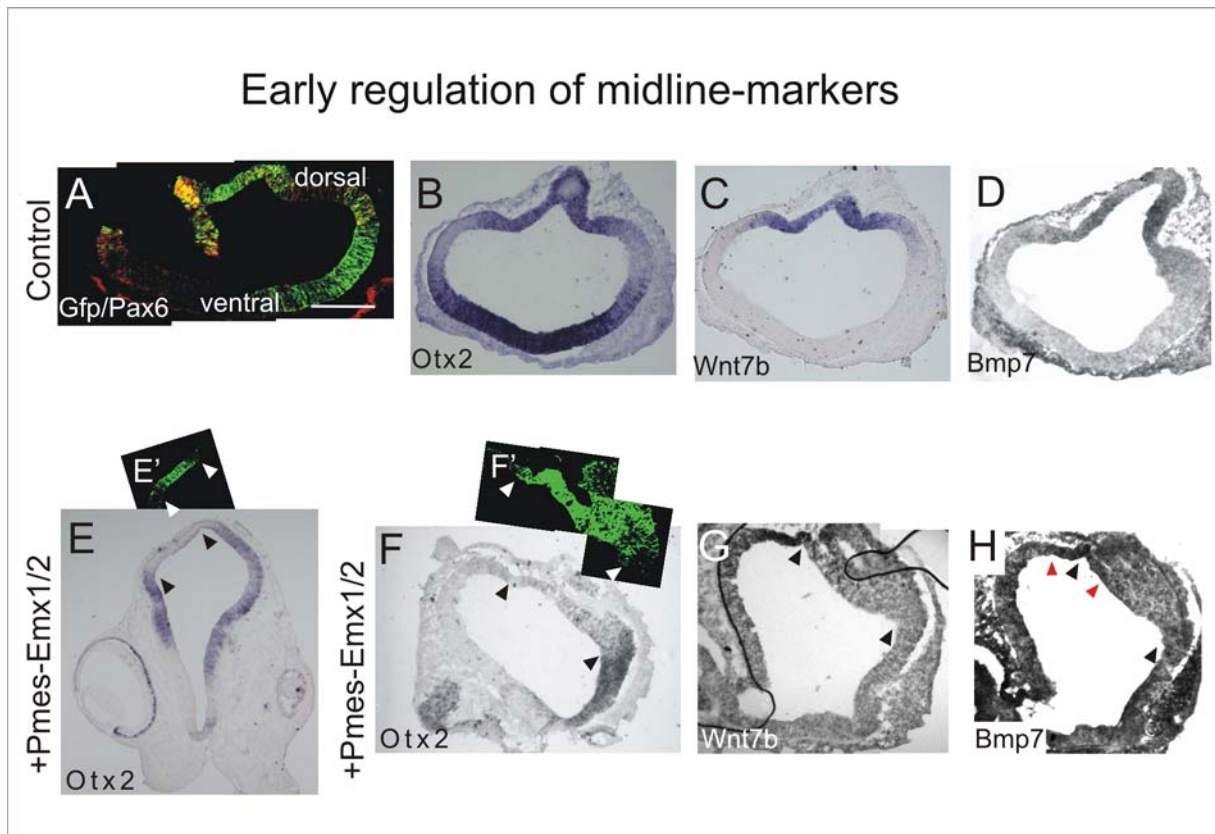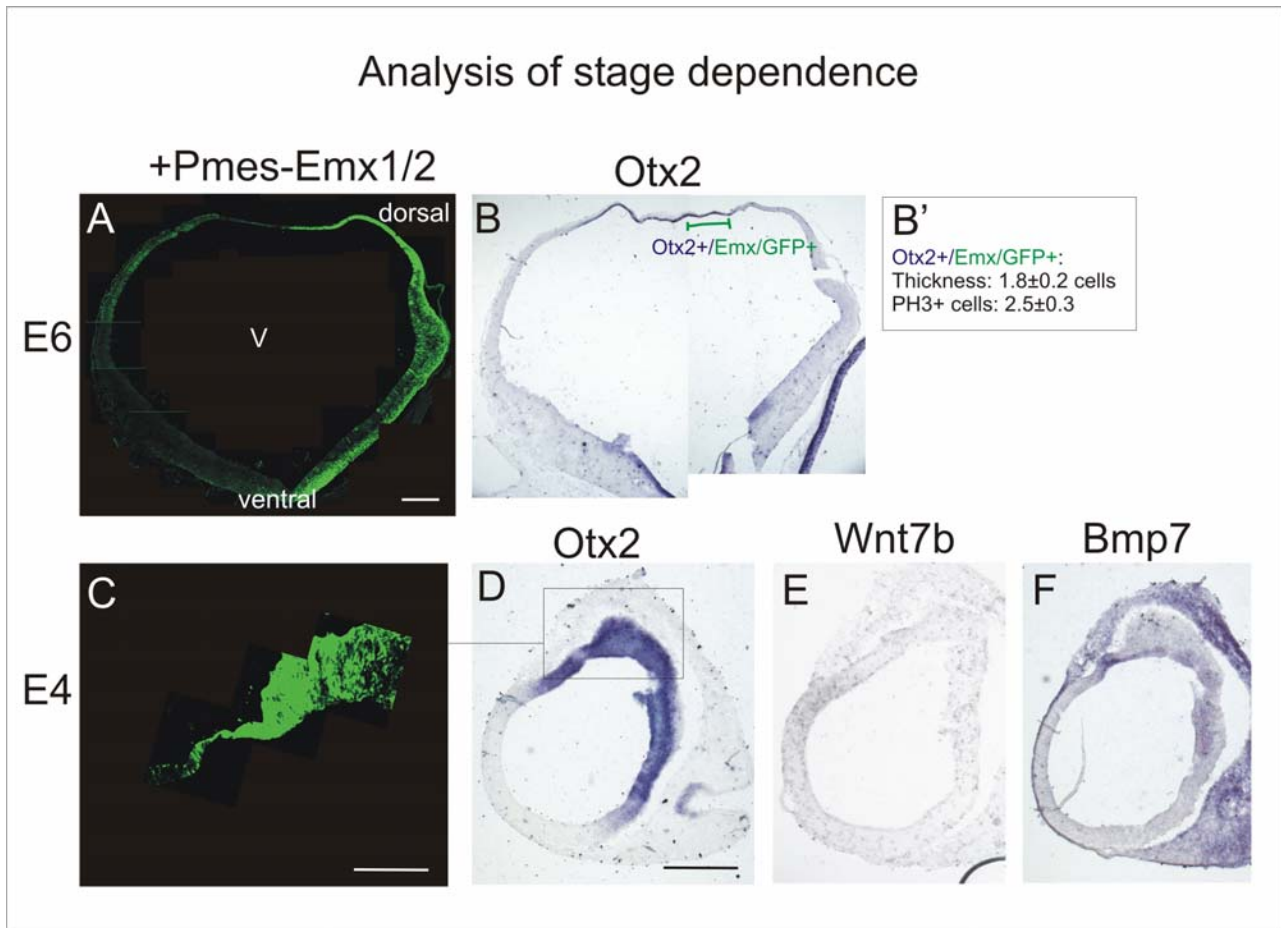
Fig.30 Ectopic Emx1/2-expression alters the pattern at E4. Analysis of the regulation of Otx2 (B, E, F), Wnt7b (C, G) and Bmp7 (D, H) at E4 by *in situ* hybridization. The analysis reveales a downregulation of Otx2 in the region of Emx1/2-misexpression (E, F) as well as of Wnt7b (G). The area of misexpression is indicated by black arrowheads. Bmp7-expression is not downregulated at E4 (see red arrowheads in H). Immunostaining for GFP indicates the region of transduction (A, E', F'). Scale bar: 250μm.

Quantification of proliferation
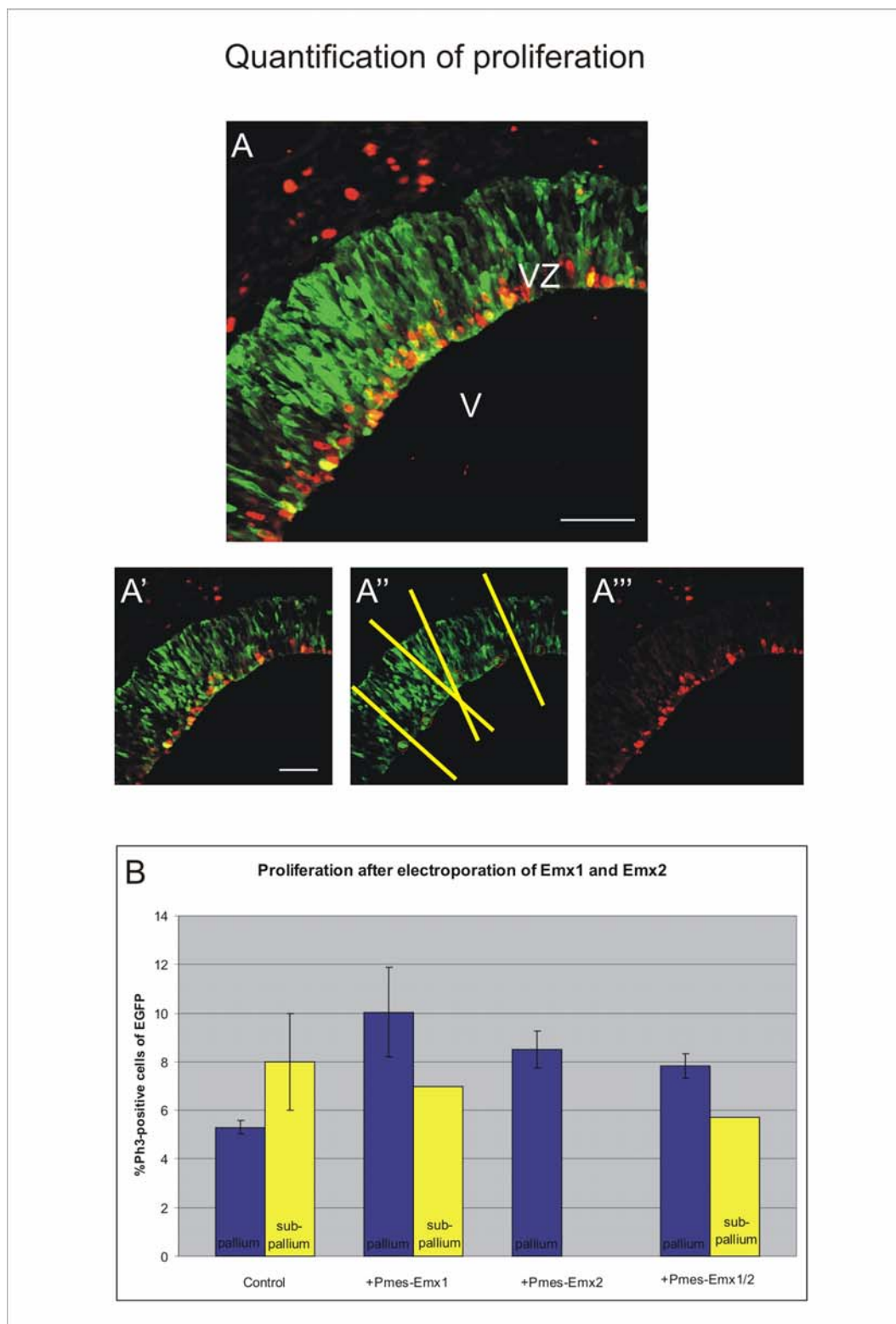
Fig.31 Proliferation analysis at E4. (A, A', A'', A''') show an example for electroporation with the control plasmid, immunostained against GFP (green) and PH3 (red). (B) For the quantification single optical sections are analyzed counting the PH3-positive cells as proportion of all transduced cells. Blue columns represent the brains manipulated in the pallium, whereas the yellow columns represent brains transduced in the subpallial region. The strongest result is obtain by electroporation of Pmes-Emx1 into the pallium. The error bars indicate the SEM. V, ventricle; VZ, ventricular zone. Scale bars: 25μm.
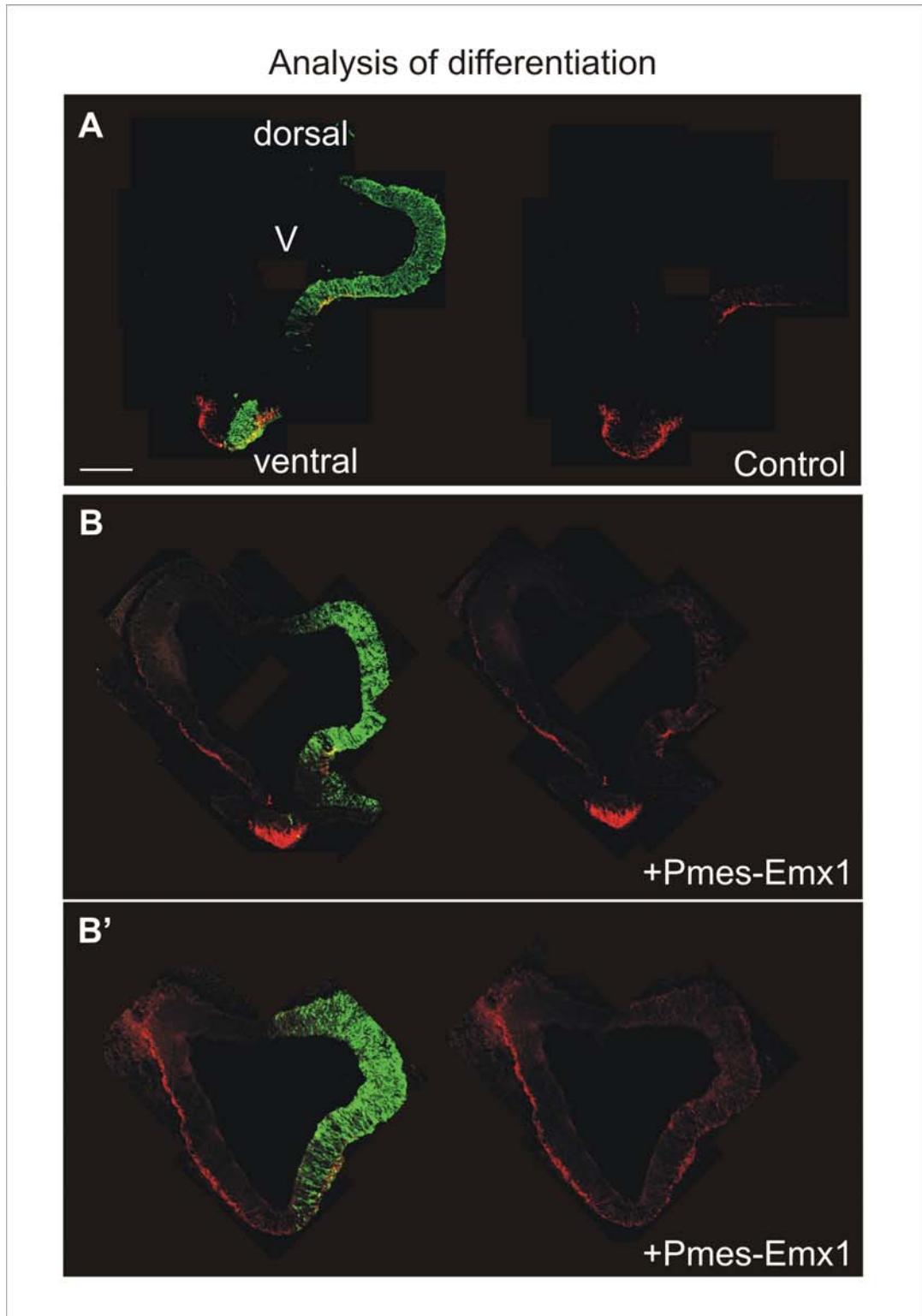
Fig.32 Analysis of differentiation after misexpression of Emx1 in the telencephalon.
Strongly electroporated brains with a GFP-control plasmid (A) and Pmes-Emx1 (B, B') at
two different rostro/caudal levels are stained for Map2 to determine the degree of
differentiation in the manipulted region. Electroporation with the control plasmid (A)
showes only few differentiated neurons in the lateral region of transduction, whereas
Emx1-ovexpression showes even less differented neurons on the side of manipualtion (B,
B'). V, ventricle. Scale bar: 250μm.

Analysis of stage dependence

+Pmes-Emx1/2

A dorsal

E6

v

ventral

Otx2

B

Otx2+/Emx/GFP+

B'

Otx2+/Emx/GFP+:
Thickness: 1.8±0.2 cells
PH3+ cells: 2.5±0.3

C

E4

Otx2

D

**Wnt7b**

E

Bmp7

F

Fig.33 Analysis of stage dependence of gene regulation. When electroporation is performed after HH12 an inhibition of the Otx2-downregulation is observed at E4 and E6. (A, B) depict an example of a forebrain at E6, whereas (C, D, E, F) show an E4 brain electroporated at HH13 and HH14. Otx2 is not downregulated (B, D), whereas Wnt7b (E) can still be downregulated by misexpression of Emx1/2. Bmp7-expression is also not altered (F). Sections in (A, C) are stained for GFP and (B, D, E, F) are *in situ* hybridized. The Otx2/Emx-GFP- positive area exhibits a "ChP-like" pheotype (B'). Scale bars: 250μm.

97
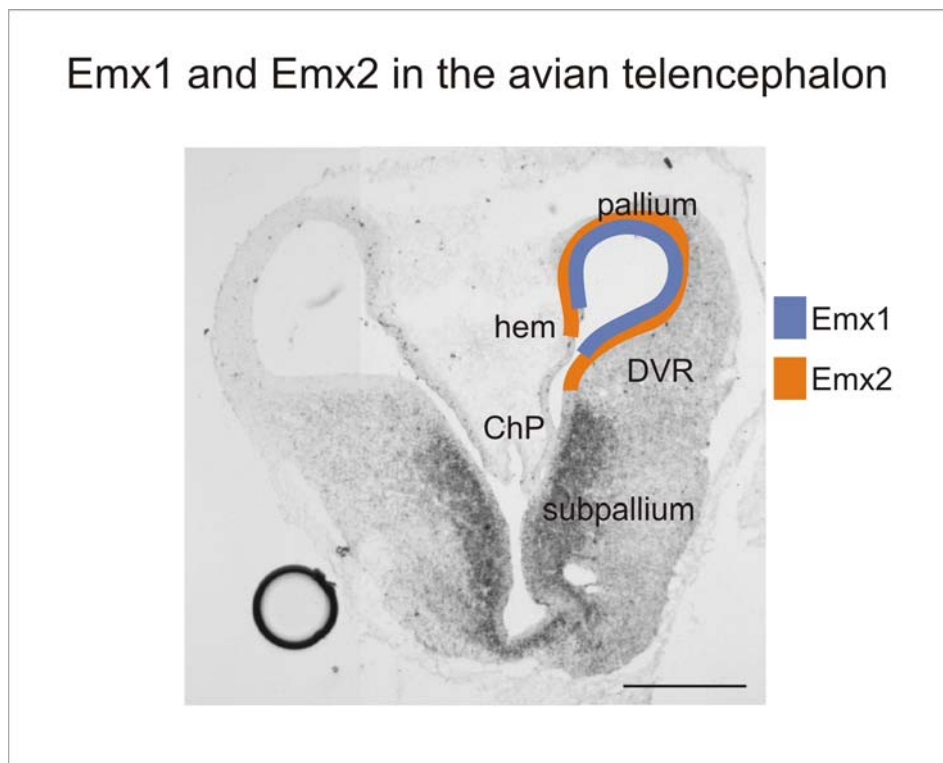
Fig.34 Schematic comparison of the expression pattern of Emx1 and Emx2 at E7. Emx2 is expressed further medially in the region of the cortical hem as well as further laterally in the DVR compared to Emx1. Scale bar: 500μm.

Distribution of Reelin in the mammalian and avian forebrain
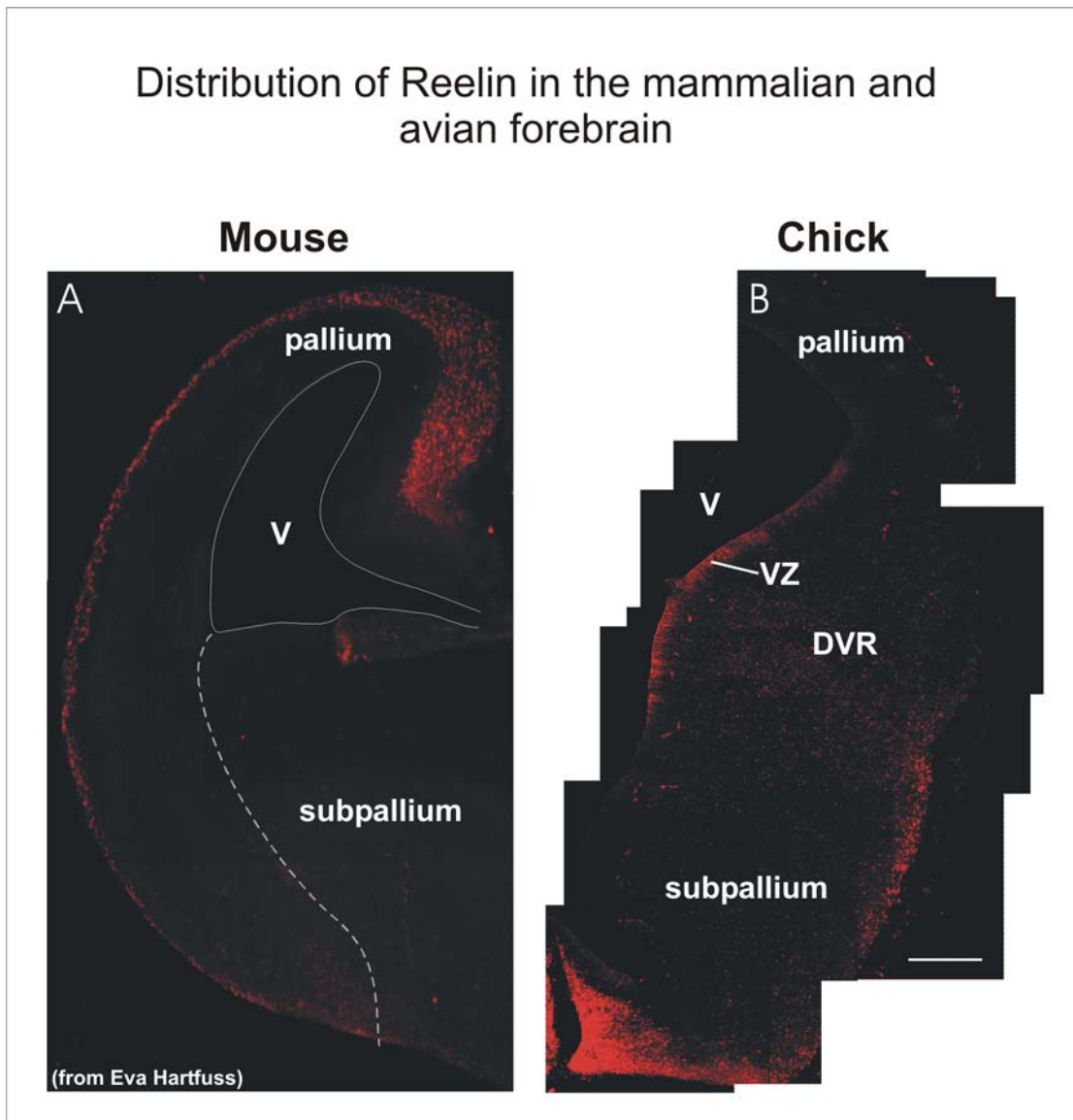
Mouse **Chick**

Fig.35 Reelin in the forebrain. The distribution of Reelin in the mammalian and avian brain shows one major difference. In the mouse forebrain (A) Reelin-positive cells are located in the marginal zone, adjacent to the pial surface. In the chick forebrain (B) Reelin-positive cells are located in the marginal zone but strong expression is detected in the VZ of the DVR and throughout the whole thickness of this region. Also mantel zone cells in the chick subpallium seem to express Reelin more frequently than the mammalian subpallium. Cryosections of 14µm thickness were immunostained for Reelin. V, ventricle; VZ, ventricular zone. Scale bar: 100µm
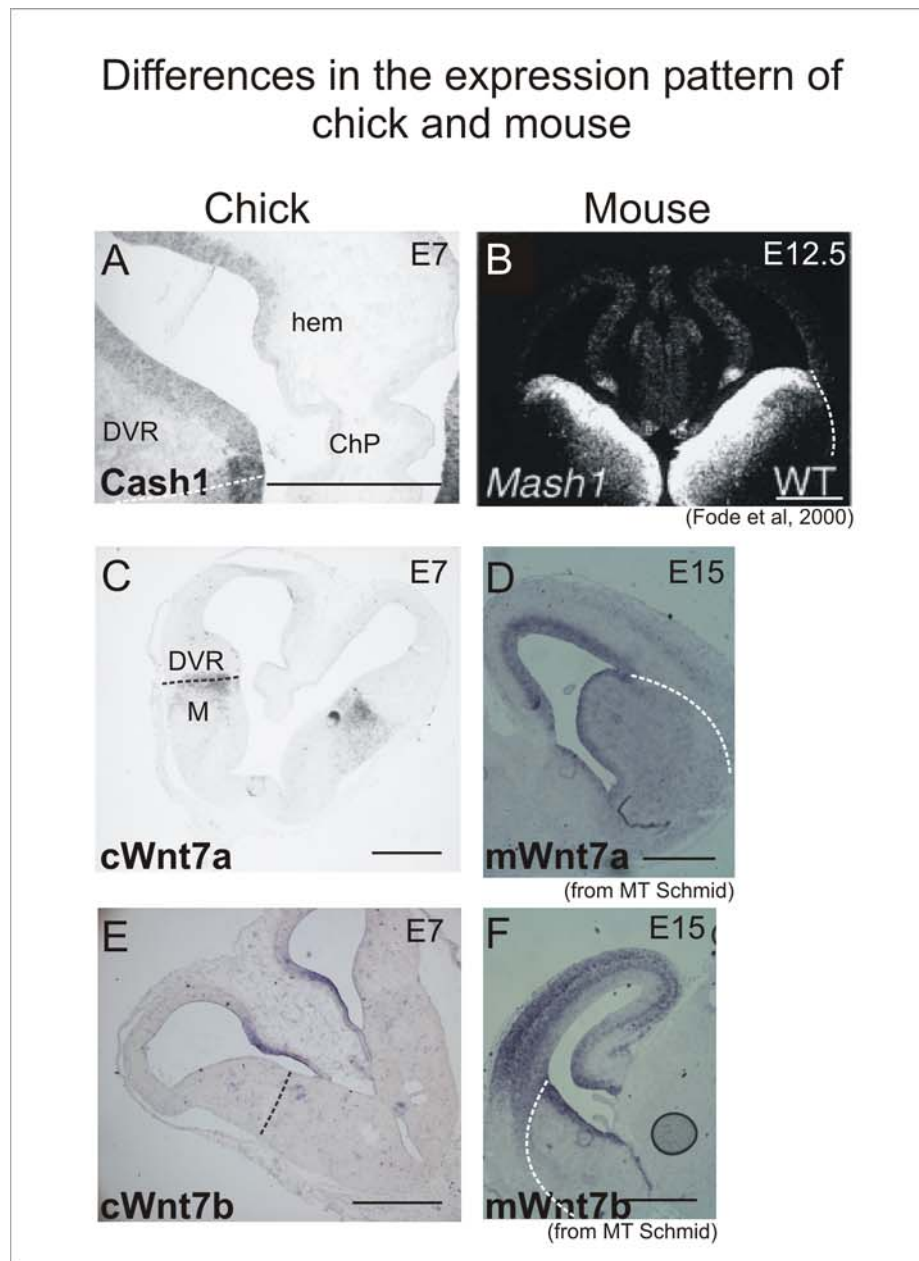
Fig.36 Comparison of transcription factors and secreted signals in chick and mouse forebrains. Some factors are differently expressed in mouse and chick forebrains, shown by *in situ* hybridization. Cash1, the avian homologue of Mash1, is strongly expressed in the subpallium, slightly extends into the region of the DVR and continues to be weakly expressed in the VZ of the pallium, hippocampus and hem. Only the ChP is devoid of Cash1-expression. The mammalian Mash1 also shows strong expression in the subpallium, a clear medial high and lateral low gradient in the pallium and a specifically strong expression in the hem. Chicken Wnt7a marks the region of the pallial/subpallial boundary (indicated by dashed line), whereas mouse Wnt7a is expressed throughout the VZ of the forebrain, excluding the region of the hem. Wnt7b in the chick exclusively labels the region of hem and in the mouse marks the VZ of the hem, the VZ of the subpallium and postmitotic neurons in upper layers in the pallium. Scale bars: 500μm.
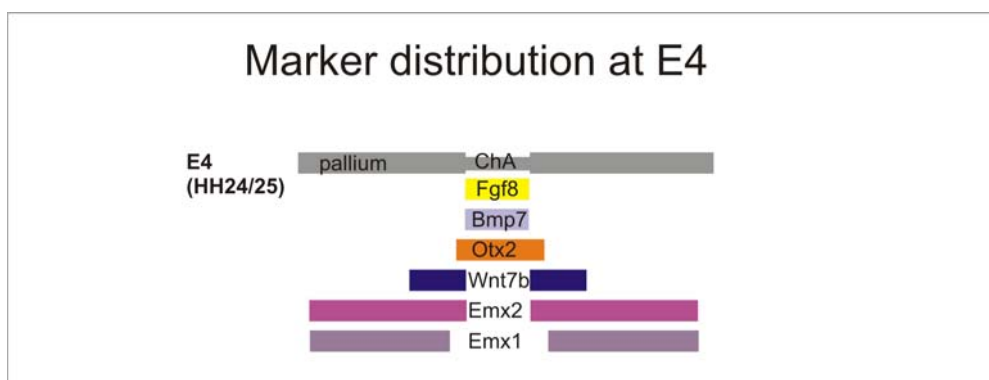
Fig.37 Schematic illustration of the distribution of secreted molecules (Fgf8, Bmp7, Wnt7b) and transcription factors (Otx2, Emx1, Emx2) at E4. The ChA expresses Fgf8, Bmp7 and Otx2, while Wnt7b, Emx1 and Emx2 abut this region.
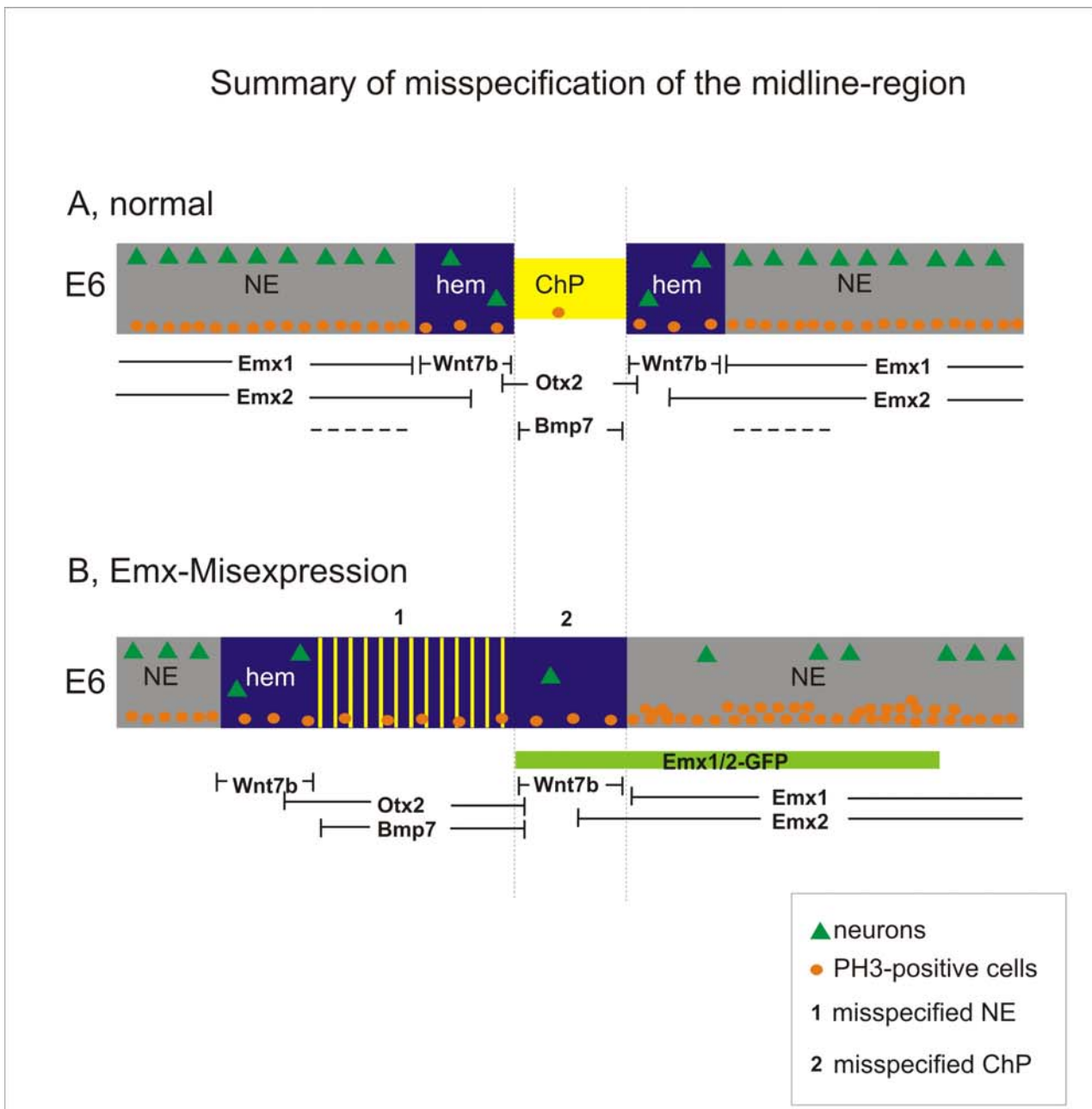
Fig.38 Misspecification of midline-tissue upon Emx1/2-misexpression. (A) Normally, the region of the ChP expresses Otx2 and Bmp7, exhibits a low rate of proliferation (PH3-positive cell; orange), does not contain neurons (green) and is thinner than the adjacent neuroepithelium (NE). The hem expresses Wnt7b, is characterized by an intermediate rate of proliferation and contains few neurons throughout the thickness of the tissue. The NE expresses Emx1 and Emx2, shows a high rate of proliferation and a layer of neurons lining the pial surface. Bmp7 is not detectable in the hem but describes a gradient in the NE. (B) Upon Emx1/2-misexpression (indicated by the green bar), two misspecified regions appear: (1) Misspecified neuroepithelium is characterized by the expression of ChP-markers (Otx2, Bmp7) and no generation of neurons on the one side and a "hem-like" thickness of epithelium as well as a "hem-like" rate of proliferation on the other. (2) The misspecified ChP exhibits a "hem-like" phenotype, with the expression of Wnt7b, an intermediate rate of proliferation, the thickness of the hem and few neurons.
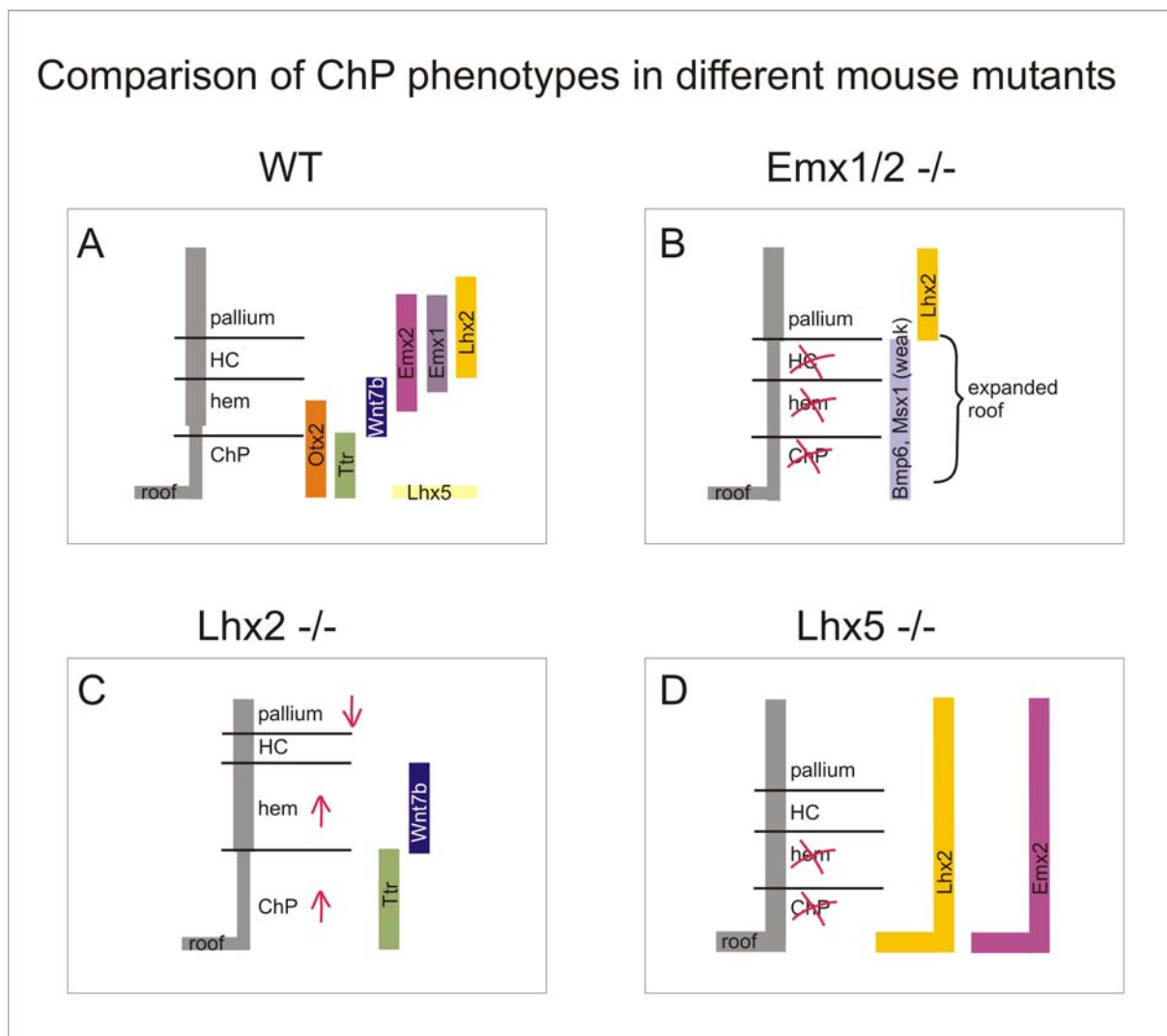
Fig.39 Comparison of marker expression in the midline-region of different mouse mutants.
Wildtype (A), Emx1/2-mutant (B), Lhx2-mutant (C) and Lhx5-mutant (D). The Emx1/2-mutant exhibits an enlarged choroidal roof, coinciding with the loss of hippocampus (HC), cortical hem and ChP (B). A loss of the Lhx2-gene induces an enlargement of ChP- and hem-regions, while the pallial region shortens (C). The Lhx5-mutation results in a loss of choroidal roof, ChP and hem and the tissue appears amorph (D).
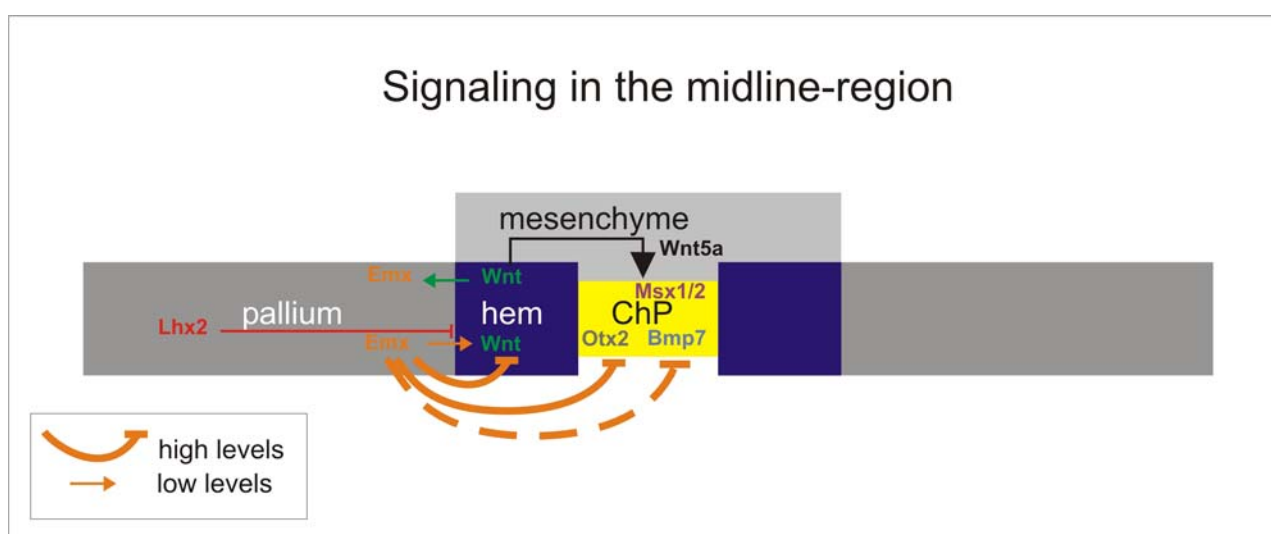
Fig.40 Model for signaling in the midline-region. Lhx2 restricts the region of the hem (red). Wnt-signals (green) induce Emx-genes (orange) to proliferate, which in a feed-back loop enlarge the medial region and thus also the region of the Wnt-expressing hem. The ChP requires the expression of Otx2, Bmp7 and Msx1/2, as well as Wnt-signaling from the cortical hem for a proper differentiation. The Wnt-signaling might be accomplished through the mesenchyme by Wnt5a (black). Misexpressing high levels of Emx1/2 in the midline-region demonstrated a direct downregulation of Otx2 and Wnt7b (see thick orange line) and a secondary downregulation of Bmp7 (see thick orange dashed line).

10 References

Abel, T. and Lattal, K. M. (2001). Molecular mechanisms of memory acquisition, consolidation and retrieval. *Curr Opin Neurobiol* **11**, 180-7.

Aboitiz, F. (1999). Comparative development of the mammalian isocortex and the reptilian dorsal ventricular ridge. Evolutionary considerations. *Cereb Cortex* **9**, 783-91.

Aboitiz, F., Morales, D. and Montiel, J. (2003). The evolutionary origin of the mammalian isocortex: towards an integrated developmental and functional approach. *Behav Brain Sci* **26**, 535-52; discussion 552-85.

Acampora, D., Avantaggiato, V., Tuorto, F., Briata, P., Corte, G. and Simeone, A. (1998). Visceral endoderm-restricted translation of Otx1 mediates recovery of Otx2 requirements for specification of anterior neural plate and normal gastrulation. *Development* **125**, 5091-104.

Acampora, D., Avantaggiato, V., Tuorto, F. and Simeone, A. (1997). Genetic control of brain morphogenesis through Otx gene dosage requirement. *Development* **124**, 3639-50.

Acampora, D., Mazan, S., Lallemand, Y., Avantaggiato, V., Maury, M., Simeone, A. and Brulet, P. (1995). Forebrain and midbrain regions are deleted in Otx2-/- mutants due to a defective anterior neuroectoderm specification during gastrulation. *Development* **121**, 3279-90.

Altmann, C. R. and Brivanlou, A. H. (2001). Neural patterning in the vertebrate embryo. *Int Rev Cytol* **203**, 447-82.

Anderson, S. A., Eisenstat, D. D., Shi, L. and Rubenstein, J. L. (1997). Interneuron migration from basal forebrain to neocortex: dependence on Dlx genes. *Science* **278**, 474-6.

Ariëns Kappers, C. H., CG; Crosby, EC. (1936). Comparative anatomy of the nervous system of vertebrates, including man. *Reprint. New York: Hafner, 1960.*

Bar, I., Lambert de Rouvroit, C. and Goffinet, A. M. (2000). The evolution of cortical development. An hypothesis based on the role of the Reelin signaling pathway. *Trends Neurosci* **23**, 633-8.

Bell, E., Ensini, M., Gulisano, M. and Lumsden, A. (2001). Dynamic domains of gene expression in the early avian forebrain. *Dev Biol* **236**, 76-88.

Bernier, B., Bar, I., D'Arcangelo, G., Curran, T. and Goffinet, A. M. (2000). Reelin mRNA expression during embryonic brain development in the chick. *J Comp Neurol* **422**, 448-63.

Birge, W. J. (1961). Tissue interactions associated with the differentiation of presumptive spongioblasts of the chick neural tube. *Anat Rec* **140**, 345-57.

Birge, W. J. (1962). Induced Choroid plexus development in the chick metencephalon. *J.Copmp. Neurol.* **118**, 89-95.

Bishop, K. M., Garel, S., Nakagawa, Y., Rubenstein, J. L. and O'Leary, D. D. (2003). Emx1 and Emx2 cooperate to regulate cortical size, lamination, neuronal differentiation, development of cortical efferents, and thalamocortical pathfinding. *J Comp Neurol* **457**, 345-60.

Bishop, K. M., Goudreau, G. and O'Leary, D. D. (2000). Regulation of area identity in the mammalian neocortex by Emx2 and Pax6. *Science* **288**, 344-9.

Bishop, K. M., Rubenstein, J. L. and O'Leary, D. D. (2002). Distinct actions of Emx1, Emx2, and Pax6 in regulating the specification of areas in the developing neocortex. *J Neurosci* **22**, 7627-38.

Boncinelli, E. (1999). Homeobox genes in development. *Adv Neurol* **79**, 81-94.

Bottcher, R. T. and Niehrs, C. (2004). Fibroblast Growth Factor Signalling during early vertebrate development. *Endocr Rev*.

Boulder Committee. (1970). Embryonic vertebrate central nervous system: revised terminology. *Anat Rec* **166**, 257-261.

Briata, P., Di Blas, E., Gulisano, M., Mallamaci, A., Iannone, R., Boncinelli, E. and Corte, G. (1996). EMX1 homeoprotein is expressed in cell nuclei of the developing cerebral cortex and in the axons of the olfactory sensory neurons. *Mech Dev* **57**, 169-80.

Brittis, P. A., Meiri, K., Dent, E. and Silver, J. (1995). The earliest patterns of neuronal differentiation and migration in the mammalian central nervous system. *Exp Neurol* **134**, 1-12.

Bulchand, S., Grove, E. A., Porter, F. D. and Tole, S. (2001). LIM-homeodomain gene Lhx2 regulates the formation of the cortical hem. *Mech Dev* **100**, 165-75.

Cadigan, K. M. and Nusse, R. (1997). Wnt signaling: a common theme in animal development. *Genes Dev* **11**, 3286-305.

Cameron, R. S. and Rakic, P. (1991). Glial cell lineage in the cerebral cortex: a review and synthesis. *Glia* **4**, 124-37.

Cavallaro, T., Martone, R. L., Stylianopoulou, F. and Herbert, J. (1993). Differential expression of the insulin-like growth factor II and transthyretin genes in the developing rat choroid plexus. *J Neuropathol Exp Neurol* **52**, 153-62.

Caviness, V. S., Jr., Takahashi, T. and Nowakowski, R. S. (1995). Numbers, time and neocortical neuronogenesis: a general developmental and evolutionary model. *Trends Neurosci* **18**, 379-83.

Cecchi, C. (2002). Emx2: a gene responsible for cortical development, regionalization and area specification. *Gene* **291**, 1-9.

Chan, C. H., Godinho, L. N., Thomaidou, D., Tan, S. S., Gulisano, M. and Parnavelas, J. G. (2001). Emx1 is a marker for pyramidal neurons of the cerebral cortex. *Cereb Cortex* **11**, 1191-8.

Chapman, S. C., Brown, R., Lees, L., Schoenwolf, G. C. and Lumsden, A. (2004). Expression analysis of chick Wnt and frizzled genes and selected inhibitors in early chick patterning. *Dev Dyn* **229**, 668-76.

Chapman, S. C., Schubert, F. R., Schoenwolf, G. C. and Lumsden, A. (2002). Analysis of spatial and temporal gene expression patterns in blastula and gastrula stage chick embryos. *Dev Biol* **245**, 187-99.

Chapouton, P., Gartner, A. and Götz, M. (1999). The role of Pax6 in restricting cell migration between developing cortex and basal ganglia. *Development* **126**, 5569-79.

Chapouton, P., Schuurmans, C., Guillemot, F. and Götz, M. (2001). The transcription factor neurogenin 2 restricts cell migration from the cortex to the striatum. *Development* **128**, 5149-59.

Chenn, A. and McConnell, S. K. (1995). Cleavage orientation and the asymmetric inheritance of Notch1 immunoreactivity in mammalian neurogenesis. *Cell* **82**, 631-41.

Chenn, A. and Walsh, C. A. (2002). Regulation of cerebral cortical size by control of cell cycle exit in neural precursors. *Science* **297**, 365-9.

Cobos, I., Puelles, L. and Martinez, S. (2001a). The avian telencephalic subpallium originates inhibitory neurons that invade tangentially the pallium (dorsal ventricular ridge and cortical areas). *Dev Biol* **239**, 30-45.

Cobos, I., Shimamura, K., Rubenstein, J. L., Martinez, S. and Puelles, L. (2001b). Fate map of the avian anterior forebrain at the four-somite stage, based on the analysis of quail-chick chimeras. *Dev Biol* **239**, 46-67.

Cooper, J. A. (1987). Effects of cytochalasin and phalloidin on actin. *J Cell Biol* **105**, 1473-8.

Crossley, P. H., Martinez, S., Ohkubo, Y. and Rubenstein, J. L. (2001). Coordinate expression of Fgf8, Otx2, Bmp4, and Shh in the rostral prosencephalon during development of the telencephalic and optic vesicles. *Neuroscience* **108**, 183-206.

de Bergeyck, V., Naerhuyzen, B., Goffinet, A. M. and Lambert de Rouvroit, C. (1998). A panel of monoclonal antibodies against reelin, the extracellular matrix protein defective in reeler mutant mice. *J Neurosci Methods* **82**, 17-24.

DeDiego, I., Smith-Fernandez, A. and Fairen, A. (1994). Cortical cells that migrate beyond area boundaries: characterization of an early neuronal population in the lower intermediate zone of prenatal rats. *Eur J Neurosci* **6**, 983-97.

Denaxa, M., Chan, C. H., Schachner, M., Parnavelas, J. G. and Karagogeos, D. (2001). The adhesion molecule TAG-1 mediates the migration of cortical interneurons from the ganglionic eminence along the corticofugal fiber system. *Development* **128**, 4635-44.

Deng, C. and Rogers, L. J. (2000). Organization of intratelencephalic projections to the visual Wulst of the chick. *Brain Res* **856**, 152-62.

Dono, R. (2003). Fibroblast growth factors as regulators of central nervous system development and function. *Am J Physiol Regul Integr Comp Physiol* **284**, R867-81.

Duan, W., Achen, M. G., Richardson, S. J., Lawrence, M. C., Wettenhall, R. E., Jaworowski, A. and Schreiber, G. (1991). Isolation, characterization, cDNA cloning and gene expression of an avian transthyretin. Implications for the evolution of structure and function of transthyretin in vertebrates. *Eur J Biochem* **200**, 679-87.

Feng, L., Hatten, M. E. and Heintz, N. (1994). Brain lipid-binding protein (BLBP): a novel signaling system in the developing mammalian CNS. *Neuron* **12**, 895-908.

Fernandez, A. S., Pieau, C., Reperant, J., Boncinelli, E. and Wassef, M. (1998). Expression of the Emx-1 and Dlx-1 homeobox genes define three molecularly distinct domains in the telencephalon of mouse, chick, turtle and frog embryos: implications for the evolution of telencephalic subdivisions in amniotes. *Development* **125**, 2099-111.

Figdor, M. C. and Stern, C. D. (1993). Segmental organization of embryonic diencephalon. *Nature* **363**, 630-4.

Finkelstein, R. and Boncinelli, E. (1994). From fly head to mammalian forebrain: the story of otd and Otx. *Trends Genet* **10**, 310-5.

Fode, C., Ma, Q., Casarosa, S., Ang, S. L., Anderson, D. J. and Guillemot, F. (2000). A role for neural determination genes in specifying the dorsoventral identity of telencephalic neurons. *Genes Dev* **14**, 67-80.

Ford-Perriss, M., Abud, H. and Murphy, M. (2001). Fibroblast growth factors in the developing central nervous system. *Clin Exp Pharmacol Physiol* **28**, 493-503.

Frowein, J., Campbell, K. and Götz, M. (2002). Expression of Ngn1, Ngn2, Cash1, Gsh2 and Sfrp1 in the developing chick telencephalon. *Mech Dev* **110**, 249-52.

Furuta, Y., Piston, D. W. and Hogan, B. L. (1997). Bone morphogenetic proteins (BMPs) as regulators of dorsal forebrain development. *Development* **124**, 2203-12.

Gangemi, R. M., Daga, A., Marubbi, D., Rosatto, N., Capra, M. C. and Corte, G. (2001). Emx2 in adult neural precursor cells. *Mech Dev* **109**, 323-9.

Garda, A. L., Puelles, L., Rubenstein, J. L. and Medina, L. (2002). Expression patterns of Wnt8b and Wnt7b in the chicken embryonic brain suggest a correlation with forebrain patterning centers and morphogenesis. *Neuroscience* **113**, 689-98.

Ghattas, I. R., Sanes, J. R. and Majors, J. E. (1991). The encephalomyocarditis virus internal ribosome entry site allows efficient coexpression of two genes from a recombinant provirus in cultured cells and in embryos. *Mol Cell Biol* **11**, 5848-59.

Gilbert, S., F. Developmental biology: Sinauer.

Götz, M., Hartfuss, E. and Malatesta, P. (2002). Radial glial cells as neuronal precursors: a new perspective on the correlation of morphology and lineage restriction in the developing cerebral cortex of mice. *Brain Res Bull* **57**, 777-88.

Graham, A., Heyman, I. and Lumsden, A. (1993). Even-numbered rhombomeres control the apoptotic elimination of neural crest cells from odd-numbered rhombomeres in the chick hindbrain. *Development* **119**, 233-45.

Graham, F. a. P., L. (1991). Manipulation of adenovirus vectors. *Methodes in Molecular Biology: Gene Transfer and Expression Protocols 7. Eds:Murray E, Humana Press, Clifton.*

Greenhouse, J. J., Petropoulos, C. J., Crittenden, L. B. and Hughes, S. H. (1988). Helper-independent retrovirus vectors with Rous-associated virus type O long terminal repeats. *J Virol* **62**, 4809-12.

Grove, E. A., Tole, S., Limon, J., Yip, L. and Ragsdale, C. W. (1998). The hem of the embryonic cerebral cortex is defined by the expression of multiple Wnt genes and is compromised in Gli3-deficient mice. *Development* **125**, 2315-25.

Grove, E. A., Williams, B. P., Li, D. Q., Hajihosseini, M., Friedrich, A. and Price, J. (1993). Multiple restricted lineages in the embryonic rat cerebral cortex. *Development* **117**, 553-61.

Gulisano, M., Broccoli, V., Pardini, C. and Boncinelli, E. (1996). Emx1 and Emx2 show different patterns of expression during proliferation and differentiation of the developing cerebral cortex in the mouse. *Eur J Neurosci* **8**, 1037-50.

Guo, H., Christoff, J. M., Campos, V. E., Jin, X. L. and Li, Y. (2000). Normal corpus callosum in Emx1 mutant mice with C57BL/6 background. *Biochem Biophys Res Commun* **276**, 649-53.

Hamburger, V. a. H., HL. (1951). A series of of normal stages in the development of the chick embryo. *Journal of Morphophology* **68**, 49-95.

Hartfuss, E., Forster, E., Bock, H. H., Hack, M. A., Leprince, P., Luque, J. M., Herz, J., Frotscher, M. and Götz, M. (2003). Reelin signaling directly affects radial glia morphology and biochemical maturation. *Development* **130**, 4597-609.

Hartfuss, E., Galli, R., Heins, N. and Götz, M. (2001). Characterization of CNS precursor subtypes and radial glia. *Dev Biol* **229**, 15-30.

Hebert, J. M., Mishina, Y. and McConnell, S. K. (2002). BMP signaling is required locally to pattern the dorsal telencephalic midline. *Neuron* **35**, 1029-41.

Heins, E. (2004). Intrinsic fate determinants of neural and multipotent CNS precursor cells. *PhD Thesis*.

Heins, N., Cremisi, F., Malatesta, P., Gangemi, R. M., Corte, G., Price, J., Goudreau, G., Gruss, P. and Götz, M. (2001). Emx2 promotes symmetric cell divisions and a multipotential fate in precursors from the cerebral cortex. *Mol Cell Neurosci* **18**, 485-502.

Heins, N., Malatesta, P., Cecconi, F., Nakafuku, M., Tucker, K. L., Hack, M. A., Chapouton, P., Barde, Y. A. and Götz, M. (2002). Glial cells generate neurons: the role of the transcription factor Pax6. *Nat Neurosci* **5**, 308-15.

Hendzel, M. J., Wei, Y., Mancini, M. A., Van Hooser, A., Ranalli, T., Brinkley, B. R., Bazett-Jones, D. P. and Allis, C. D. (1997). Mitosis-specific phosphorylation of histone H3 initiates primarily within pericentromeric heterochromatin during G2 and spreads in an ordered fashion coincident with mitotic chromosome condensation. *Chromosoma* **106**, 348-60.

Hevner, R. F., Neogi, T., Englund, C., Daza, R. A. and Fink, A. (2003). Cajal-Retzius cells in the mouse: transcription factors, neurotransmitters, and birthdays suggest a pallial origin. *Brain Res Dev Brain Res* **141**, 39-53.

Heyers, D., Kovjanic, D. and Redies, C. (2003). Cadherin expression coincides with birth dating patterns in patchy compartments of the developing chicken telencephalon. *J Comp Neurol* **460**, 155-66.

Hirth, F., Therianos, S., Loop, T., Gehring, W. J., Reichert, H. and Furukubo-Tokunaga, K. (1995). Developmental defects in brain segmentation caused by mutations of the homeobox genes orthodenticle and empty spiracles in Drosophila. *Neuron* **15**, 769-78.

Houart, C., Westerfield, M. and Wilson, S. W. (1998). A small population of anterior cells patterns the forebrain during zebrafish gastrulation. *Nature* **391**, 788-92.

Hughes, S. and Kosik, E. (1984). Mutagenesis of the region between env and src of the SR-A strain of Rous sarcoma virus for the purpose of constructing helper-independent vectors. *Virology* **136**, 89-99.

Hughes, S. H., Greenhouse, J. J., Petropoulos, C. J. and Sutrave, P. (1987). Adaptor plasmids simplify the insertion of foreign DNA into helper-independent retroviral vectors. *J Virol* **61**, 3004-12.

Hynes, R. O. (1992). Integrins: versatility, modulation, and signaling in cell adhesion. *Cell* **69**, 11-25.

Ikeya, M., Lee, S. M., Johnson, J. E., McMahon, A. P. and Takada, S. (1997). Wnt signalling required for expansion of neural crest and CNS progenitors. *Nature* **389**, 966-70.

Ingham, P. W. and McMahon, A. P. (2001). Hedgehog signaling in animal development: paradigms and principles. *Genes Dev* **15**, 3059-87.

Ishii, Y., Nakamura, S. and Osumi, N. (2000). Demarcation of early mammalian cortical development by differential expression of fringe genes. *Brain Res Dev Brain Res* **119**, 307-20.

Jacques, T. S., Relvas, J. B., Nishimura, S., Pytela, R., Edwards, G. M., Streuli, C. H. and ffrench-Constant, C. (1998). Neural precursor cell chain migration and division are regulated through different beta1 integrins. *Development* **125**, 3167-77.

Janis, L. S., Cassidy, R. M. and Kromer, L. F. (1999). Ephrin-A binding and EphA receptor expression delineate the matrix compartment of the striatum. *J Neurosci* **19**, 4962-71.

Jaroszeski, M. J., Gilbert, R., Nicolau, C. and Heller, R. (1999). In vivo gene delivery by electroporation. *Adv Drug Deliv Rev* **35**, 131-137.

Jessell, T. M. (2000). Neuronal specification in the spinal cord: inductive signals and transcriptional codes. *Nat Rev Genet* **1**, 20-9.

Joyner, A. L. (1996). Engrailed, Wnt and Pax genes regulate midbrain--hindbrain development. *Trends Genet* **12**, 15-20.

Joyner, A. L., Liu, A. and Millet, S. (2000). Otx2, Gbx2 and Fgf8 interact to position and maintain a mid-hindbrain organizer. *Curr Opin Cell Biol* **12**, 736-41.

Karten, H. (1969). The organization of the avian telencephalon and some speculations on the phylogeny of the amniote telencephalon. *Ann N Y Acad Sci* **167**, 164-179.

Kim, A. S., Anderson, S. A., Rubenstein, J. L., Lowenstein, D. H. and Pleasure, S. J. (2001). Pax-6 regulates expression of SFRP-2 and Wnt-7b in the developing CNS. *J Neurosci* **21**, RC132.

Kurtz, A., Zimmer, A., Schnutgen, F., Bruning, G., Spener, F. and Muller, T. (1994). The expression pattern of a novel gene encoding brain-fatty acid binding protein correlates with neuronal and glial cell development. *Development* **120**, 2637-49.

Lambert de Rouvroit, C. and Goffinet, A. M. (1998). The reeler mouse as a model of brain development. *Adv Anat Embryol Cell Biol* **150**, 1-106.

Lavdas, A. A., Grigoriou, M., Pachnis, V. and Parnavelas, J. G. (1999). The medial ganglionic eminence gives rise to a population of early neurons in the developing cerebral cortex. *J Neurosci* **19**, 7881-8.

Lee, K. J. and Jessell, T. M. (1999). The specification of dorsal cell fates in the vertebrate central nervous system. *Annu Rev Neurosci* **22**, 261-94.

Lee, S. M., Tole, S., Grove, E. and McMahon, A. P. (2000). A local Wnt-3a signal is required for development of the mammalian hippocampus. *Development* **127**, 457-67.

Li, H., Babiarz, J., Woodbury, J., Kane-Goldsmith, N. and Grumet, M. (2004). Spatiotemporal heterogeneity of CNS radial glial cells and their transition to restricted precursors. *Dev Biol* **271**, 225-38.

Lohman, A. S., WJAJ. (1990). The dorsal ventricular ridge and cortex of reptiles in historical and phylogenetic perspective. *In: The neocortex: ontogeny and phylogeny (Finlay BL, Innocenti G, Scheich H, eds)* **New York: Plenum**, 59-74.

Lumsden, A. and Krumlauf, R. (1996). Patterning the vertebrate neuraxis. *Science* **274**, 1109-15.

Mallamaci, A., Iannone, R., Briata, P., Pintonello, L., Mercurio, S., Boncinelli, E. and Corte, G. (1998). EMX2 protein in the developing mouse brain and olfactory area. *Mech Dev* **77**, 165-72.

Mallamaci, A., Mercurio, S., Muzio, L., Cecchi, C., Pardini, C. L., Gruss, P. and Boncinelli, E. (2000a). The lack of Emx2 causes impairment of Reelin signaling and defects of neuronal migration in the developing cerebral cortex. *J Neurosci* **20**, 1109-18.

Mallamaci, A., Muzio, L., Chan, C. H., Parnavelas, J. and Boncinelli, E. (2000b). Area identity shifts in the early cerebral cortex of Emx2-/- mutant mice. *Nat Neurosci* **3**, 679-86.

Marazzi, G., Wang, Y. and Sassoon, D. (1997). Msx2 is a transcriptional regulator in the BMP4-mediated programmed cell death pathway. *Dev Biol* **186**, 127-38.

Marin, O. and Rubenstein, J. L. (2001). A long, remarkable journey: tangential migration in the telencephalon. *Nat Rev Neurosci* **2**, 780-90.

Marin, O. and Rubenstein, J. L. (2003). Cell migration in the forebrain. *Annu Rev Neurosci* **26**, 441-83.

Martin, S. J., Grimwood, P. D. and Morris, R. G. (2000). Synaptic plasticity and memory: an evaluation of the hypothesis. *Annu Rev Neurosci* **23**, 649-711.

Matsunami, H. and Takeichi, M. (1995). Fetal brain subdivisions defined by R- and E-cadherin expressions: evidence for the role of cadherin activity in region-specific, cell-cell adhesion. *Dev Biol* **172**, 466-78.

McConnell, S. K. (1988). Development and decision-making in the mammalian cerebral cortex. *Brain Res* **472**, 1-23.

McConnell, S. K. (1989). The determination of neuronal fate in the cerebral cortex. *Trends Neurosci* **12**, 342-9.

McConnell, S. K. and Kaznowski, C. E. (1991). Cell cycle dependence of laminar determination in developing neocortex. *Science* **254**, 282-5.

McLaughlin, D. P., J; Mason, J;. (2000). *Wnt8b* regulates cellular proliferation in the adult dentate gyrus. *Soc Neurosci*, 228.1.

Medina, L. and Reiner, A. (2000). Do birds possess homologues of mammalian primary visual, somatosensory and motor cortices? *Trends Neurosci* **23**, 1-12.

Megason, S. G. and McMahon, A. P. (2002). A mitogen gradient of dorsal midline Wnts organizes growth in the CNS. *Development* **129**, 2087-98.

Mellitzer, G., Xu, Q. and Wilkinson, D. G. (1999). Eph receptors and ephrins restrict cell intermingling and communication. *Nature* **400**, 77-81.

Mione, M. C., Cavanagh, J. F., Harris, B. and Parnavelas, J. G. (1997). Cell fate specification and symmetrical/asymmetrical divisions in the developing cerebral cortex. *J Neurosci* **17**, 2018-29.

Mir, L. M., Bureau, M. F., Rangara, R., Schwartz, B. and Scherman, D. (1998). Long-term, high level in vivo gene expression after electric pulse-mediated gene transfer into skeletal muscle. *C R Acad Sci III* **321**, 893-9.

Miyata, T., Kawaguchi, A., Okano, H. and Ogawa, M. (2001). Asymmetric inheritance of radial glial fibers by cortical neurons. *Neuron* **31**, 727-41.

Moore, K., Persaud, TVN. (1993). Before We Are Born: Essentials of Embryology and Birth Defects.: Saunders, Philadelphia.

Morest, D. K. (1970). A study of neurogenesis in the forebrain of opossum pouch young. *Z Anat Entwicklungsgesch* **130**, 265-305.

Mullen, R. J., Buck, C. R. and Smith, A. M. (1992). NeuN, a neuronal specific nuclear protein in vertebrates. *Development* **116**, 201-11.

Murakami, S. and Arai, Y. (2002). Migration of LHRH neurons into the spinal cord: evidence for axon-dependent migration from the transplanted chick olfactory placode. *Eur J Neurosci* **16**, 684-92.

Muzio, L., DiBenedetto, B., Stoykova, A., Boncinelli, E., Gruss, P. and Mallamaci, A. (2002). Emx2 and Pax6 control regionalization of the pre-neuronogenic cortical primordium. *Cereb Cortex* **12**, 129-39.

Muzio, L. and Mallamaci, A. (2003). Emx1, emx2 and pax6 in specification, regionalization and arealization of the cerebral cortex. *Cereb Cortex* **13**, 641-7.

Nadarajah, B., Brunstrom, J. E., Grutzendler, J., Wong, R. O. and Pearlman, A. L. (2001). Two modes of radial migration in early development of the cerebral cortex. *Nat Neurosci* **4**, 143-50.

Nadarajah, B. and Parnavelas, J. G. (2002). Modes of neuronal migration in the developing cerebral cortex. *Nat Rev Neurosci* **3**, 423-32.

Nelson, W. J. and Nusse, R. (2004). Convergence of Wnt, beta-catenin, and cadherin pathways. *Science* **303**, 1483-7.

Neumann, E., Kakorin, S., and Toensing, K. (1999). Fundamentals of electroporative delivery of drugs and genes. *Bioelectrochem. Bioenerg.* **48**, 3-16.

Noctor, S. C., Martinez-Cerdeno, V., Ivic, L. and Kriegstein, A. R. (2004). Cortical neurons arise in symmetric and asymmetric division zones and migrate through specific phases. *Nat Neurosci* **7**, 136-44.

Nowakowski, R. S., Lewin, S. B. and Miller, M. W. (1989). Bromodeoxyuridine immunohistochemical determination of the lengths of the cell cycle and the DNA-synthetic phase for an anatomically defined population. *J Neurocytol* **18**, 311-8.

Panchision, D. M., Pickel, J. M., Studer, L., Lee, S. H., Turner, P. A., Hazel, T. G. and McKay, R. D. (2001). Sequential actions of BMP receptors control neural precursor cell production and fate. *Genes Dev* **15**, 2094-110.

Peifer, M. and Polakis, P. (2000). Wnt signaling in oncogenesis and embryogenesis--a look outside the nucleus. *Science* **287**, 1606-9.

Pellegrini, M., Mansouri, A., Simeone, A., Boncinelli, E. and Gruss, P. (1996). Dentate gyrus formation requires Emx2. *Development* **122**, 3893-8.

Polleux, F., Giger, R. J., Ginty, D. D., Kolodkin, A. L. and Ghosh, A. (1998). Patterning of cortical efferent projections by semaphorin-neuropilin interactions. *Science* **282**, 1904-6.

Polleux, F., Morrow, T. and Ghosh, A. (2000). Semaphorin 3A is a chemoattractant for cortical apical dendrites. *Nature* **404**, 567-73.

Puelles, L., Kuwana, E., Puelles, E., Bulfone, A., Shimamura, K., Keleher, J., Smiga, S. and Rubenstein, J. L. (2000). Pallial and subpallial derivatives in the embryonic chick and mouse telencephalon, traced by the expression of the genes Dlx-2, Emx-1, Nkx-2.1, Pax-6, and Tbr-1. *J Comp Neurol* **424**, 409-38.

Qian, X., Goderie, S. K., Shen, Q., Stern, J. H. and Temple, S. (1998). Intrinsic programs of patterned cell lineages in isolated vertebrate CNS ventricular zone cells. *Development* **125**, 3143-52.

Qian, X., Shen, Q., Goderie, S. K., He, W., Capela, A., Davis, A. A. and Temple, S. (2000). Timing of CNS cell generation: a programmed sequence of neuron and glial cell production from isolated murine cortical stem cells. *Neuron* **28**, 69-80.

Rakic, P. (1995). A small step for the cell, a giant leap for mankind: a hypothesis of neocortical expansion during evolution. *Trends Neurosci* **18**, 383-8.

Redies, C. (2000). Cadherins in the central nervous system. *Prog Neurobiol* **61**, 611-48.

Redies, C., Kovjanic, D., Heyers, D., Medina, L., Hirano, S., Suzuki, S. T. and Puelles, L. (2002). Patch/matrix patterns of gray matter differentiation in the telencephalon of chicken and mouse. *Brain Res Bull* **57**, 489-93.

Reid, C. B., Liang, I. and Walsh, C. (1995). Systematic widespread clonal organization in cerebral cortex. *Neuron* **15**, 299-310.

Roelink, H. (2000). Hippocampus formation: an intriguing collaboration. *Curr Biol* **10**, R279-81.

Rubenstein, J. L., Shimamura, K., Martinez, S. and Puelles, L. (1998). Regionalization of the prosencephalic neural plate. *Annu Rev Neurosci* **21**, 445-77.

Sauer, F. C. (1935). Mitosis in the neural tube. *J.Comp.Neurol.* **62**, 377-405.

Shimamura, K., Hartigan, D. J., Martinez, S., Puelles, L. and Rubenstein, J. L. (1995). Longitudinal organization of the anterior neural plate and neural tube. *Development* **121**, 3923-33.

Shimamura, K. and Rubenstein, J. L. (1997). Inductive interactions direct early regionalization of the mouse forebrain. *Development* **124**, 2709-18.

Shinozaki, K., Miyagi, T., Yoshida, M., Miyata, T., Ogawa, M., Aizawa, S. and Suda, Y. (2002). Absence of Cajal-Retzius cells and subplate neurons associated with defects of tangential cell migration from ganglionic eminence in Emx1/2 double mutant cerebral cortex. *Development* **129**, 3479-92.

Shinozaki, K., Yoshida, M., Nakamura, M., Aizawa, S. and Suda, Y. (2004). Emx1 and Emx2 cooperate in initial phase of archipallium development. *Mech Dev* **121**, 475-89.

Simeone, A., Acampora, D., Gulisano, M., Stornaiuolo, A. and Boncinelli, E. (1992a). Nested expression domains of four homeobox genes in developing rostral brain. *Nature* **358**, 687-90.

Simeone, A., Gulisano, M., Acampora, D., Stornaiuolo, A., Rambaldi, M. and Boncinelli, E. (1992b). Two vertebrate homeobox genes related to the Drosophila empty spiracles gene are expressed in the embryonic cerebral cortex. *Embo J* **11**, 2541-50.

Smart, I. H. (1976). A pilot study of cell production by the ganglionic eminences of the developing mouse brain. *J Anat* **121**, 71-84.

Smart, I. H. (1985). Differential growth of the cell production systems in the lateral wall of the developing mouse telencephalon. *J Anat* **141**, 219-29.

Smart, I. H., Dehay, C., Giroud, P., Berland, M. and Kennedy, H. (2002). Unique morphological features of the proliferative zones and postmitotic compartments of the neural epithelium giving rise to striate and extrastriate cortex in the monkey. *Cereb Cortex* **12**, 37-53.

Smith, J. L. and Schoenwolf, G. C. (1997). Neurulation: coming to closure. *Trends Neurosci* **20**, 510-7.

Solloway, M. J. and Robertson, E. J. (1999). Early embryonic lethality in Bmp5;Bmp7 double mutant mice suggests functional redundancy within the 60A subgroup. *Development* **126**, 1753-68.

Somiari, S., Glasspool-Malone, J., Drabick, J. J., Gilbert, R. A., Heller, R., Jaroszeski, M. J. and Malone, R. W. (2000). Theory and in vivo application of electroporative gene delivery. *Mol Ther* **2**, 178-87.

Song, Q., Mehler, M. F. and Kessler, J. A. (1998). Bone morphogenetic proteins induce apoptosis and growth factor dependence of cultured sympathoadrenal progenitor cells. *Dev Biol* **196**, 119-27.

Stern, C. D. (2001). Initial patterning of the central nervous system: how many organizers? *Nat Rev Neurosci* **2**, 92-8.

Stoykova, A., Fritsch, R., Walther, C. and Gruss, P. (1996). Forebrain patterning defects in Small eye mutant mice. *Development* **122**, 3453-65.

Stoykova, A., Götz, M., Gruss, P. and Price, J. (1997). Pax6-dependent regulation of adhesive patterning, R-cadherin expression and boundary formation in developing forebrain. *Development* **124**, 3765-77.

Stoykova, A., Hatano, O., Gruss, P. and Götz, M. (2003). Increase in reelin-positive cells in the marginal zone of Pax6 mutant mouse cortex. *Cereb Cortex* **13**, 560-71.

Striedter, G. F. (1997). The telencephalon of tetrapods in evolution. *Brain Behav Evol* **49**, 179-213.

Striedter, G. F. and Beydler, S. (1997). Distribution of radial glia in the developing telencephalon of chicks. *J Comp Neurol* **387**, 399-420.

Striedter, G. F. and Keefer, B. P. (2000). Cell migration and aggregation in the developing telencephalon: pulse-labeling chick embryos with bromodeoxyuridine. *J Neurosci* **20**, 8021-30.

Sturrock, R. R. (1979). A morphological study of the development of the mouse choroid plexus. *J Anat* **129**, 777-93.

Sussel, L., Marin, O., Kimura, S. and Rubenstein, J. L. (1999). Loss of Nkx2.1 homeobox gene function results in a ventral to dorsal molecular respecification within the basal telencephalon: evidence for a transformation of the pallidum into the striatum. *Development* **126**, 3359-70.

Swartz, M., Eberhart, J., Mastick, G. S. and Krull, C. E. (2001a). Sparking new frontiers: using in vivo electroporation for genetic manipulations. *Dev Biol* **233**, 13-21.

Swartz, M. E., Eberhart, J., Pasquale, E. B. and Krull, C. E. (2001b). EphA4/ephrin-A5 interactions in muscle precursor cell migration in the avian forelimb. *Development* **128**, 4669-80.

Takahashi, T., Goto, T., Miyama, S., Nowakowski, R. S. and Caviness, V. S., Jr. (1999). Sequence of neuron origin and neocortical laminar fate: relation to cell cycle of origin in the developing murine cerebral wall. *J Neurosci* **19**, 10357-71.

Takeichi, M. (1995). Morphogenetic roles of classic cadherins. *Curr Opin Cell Biol* **7**, 619-27.

Takiguchi-Hayashi, K., Sekiguchi, M., Ashigaki, S., Takamatsu, M., Hasegawa, H., Suzuki-Migishima, R., Yokoyama, M., Nakanishi, S. and Tanabe, Y. (2004). Generation of reelin-positive marginal zone cells from the caudomedial wall of telencephalic vesicles. *J Neurosci* **24**, 2286-95.

Tan, S. S., Kalloniatis, M., Sturm, K., Tam, P. P., Reese, B. E. and Faulkner-Jones, B. (1998). Separate progenitors for radial and tangential cell dispersion during development of the cerebral neocortex. *Neuron* **21**, 295-304.

Tanabe, Y. and Jessell, T. M. (1996). Diversity and pattern in the developing spinal cord. *Science* **274**, 1115-23.

Terry, K., Magan, H., Baranski, M. and Burrus, L. W. (2000). Sfrp-1 and sfrp-2 are expressed in overlapping and distinct domains during chick development. *Mech Dev* **97**, 177-82.

Theil, T., Aydin, S., Koch, S., Grotewold, L. and Ruther, U. (2002). Wnt and Bmp signalling cooperatively regulate graded Emx2 expression in the dorsal telencephalon. *Development* **129**, 3045-54.

Timmer, J. R., Wang, C. and Niswander, L. (2002). BMP signaling patterns the dorsal and intermediate neural tube via regulation of homeobox and helix-loop-helix transcription factors. *Development* **129**, 2459-72.

Tissir, F., Lambert de Rouvroit, C. and Goffinet, A. M. (2002). The role of reelin in the development and evolution of the cerebral cortex. *Braz J Med Biol Res* **35**, 1473-84.

Tole, S., Goudreau, G., Assimacopoulos, S. and Grove, E. A. (2000). Emx2 is required for growth of the hippocampus but not for hippocampal field specification. *J Neurosci* **20**, 2618-25.

Toresson, H., Potter, S. S. and Campbell, K. (2000). Genetic control of dorsal-ventral identity in the telencephalon: opposing roles for Pax6 and Gsh2. *Development* **127**, 4361-71.

Tsai, H. M., Garber, B. B. and Larramendi, L. M. (1981a). 3H-thymidine autoradiographic analysis of telencephalic histogenesis in the chick embryo: I. Neuronal birthdates of telencephalic compartments in situ. *J Comp Neurol* **198**, 275-92.

Tsai, H. M., Garber, B. B. and Larramendi, L. M. (1981b). 3H-thymidine autoradiographic analysis of telencephalic histogenesis in the chick embryo: II. Dynamics of neuronal migration, displacement, and aggregation. *J Comp Neurol* **198**, 293-306.

Valverde, F., De Carlos, J. A. and Lopez-Mascaraque, L. (1995). Time of origin and early fate of preplate cells in the cerebral cortex of the rat. *Cereb Cortex* **5**, 483-93.

Wallis, D. E. and Muenke, M. (1999). Molecular mechanisms of holoprosencephaly. *Mol Genet Metab* **68**, 126-38.

Walther, C. and Gruss, P. (1991). Pax-6, a murine paired box gene, is expressed in the developing CNS. *Development* **113**, 1435-49.

Weaver, J. C., and Chimadzev, Y. A. (1996). Theory of electroporation: A review. *Bioelectrochem. Bioenerg.* **41**, 135-160.

Wichterle, H., Garcia-Verdugo, J. M., Herrera, D. G. and Alvarez-Buylla, A. (1999). Young neurons from medial ganglionic eminence disperse in adult and embryonic brain. *Nat Neurosci* **2**, 461-6.

Wichterle, H., Turnbull, D. H., Nery, S., Fishell, G. and Alvarez-Buylla, A. (2001). In utero fate mapping reveals distinct migratory pathways and fates of neurons born in the mammalian basal forebrain. *Development* **128**, 3759-71.

Wilson, S. W. and Houart, C. (2004). Early steps in the development of the forebrain. *Dev Cell* **6**, 167-81.

Wilson, S. W. and Rubenstein, J. L. (2000). Induction and dorsoventral patterning of the telencephalon. *Neuron* **28**, 641-51.

Wodarz, A. and Nusse, R. (1998). Mechanisms of Wnt signaling in development. *Annu Rev Cell Dev Biol* **14**, 59-88.

Wolpert, L. (1969). Positional information and the spatial pattern of cellular differentiation. *J Theor Biol* **25**, 1-47.

Wray, S. (2001). Development of luteinizing hormone releasing hormone neurones. *J Neuroendocrinol* **13**, 3-11.

Yoshida, M., Suda, Y., Matsuo, I., Miyamoto, N., Takeda, N., Kuratani, S. and Aizawa, S. (1997). Emx1 and Emx2 functions in development of dorsal telencephalon. *Development* **124**, 101-11.

Yun, K., Fischman, S., Johnson, J., Hrabe de Angelis, M., Weinmaster, G. and Rubenstein, J. L. (2002). Modulation of the notch signaling by Mash1 and Dlx1/2 regulates sequential specification and differentiation of progenitor cell types in the subcortical telencephalon. *Development* **129**, 5029-40.

Yun, K., Potter, S. and Rubenstein, J. L. (2001). Gsh2 and Pax6 play complementary roles in dorsoventral patterning of the mammalian telencephalon. *Development* **128**, 193-205.

Zeltser, L. M., Larsen, C. W. and Lumsden, A. (2001). A new developmental compartment in the forebrain regulated by Lunatic fringe. *Nat Neurosci* **4**, 683-4.

Zhao, G. Q. (2003). Consequences of knocking out BMP signaling in the mouse. *Genesis* **35**, 43-56.

Zhao, Y., Sheng, H. Z., Amini, R., Grinberg, A., Lee, E., Huang, S., Taira, M. and Westphal, H. (1999). Control of hippocampal morphogenesis and neuronal differentiation by the LIM homeobox gene Lhx5. *Science* **284**, 1155-8.

11 Thanks and acknowledgements

12 Curriculum vitae

Personal data: **Julia von Frowein**
Date and place of birth: 23th November 1973, Munich, Germany

School:
September 1980 - July 1984   Primary School at the Oselstraße, Munich
September 1984 - July 1991   High School, Elsa-Brändström-Gymnasium, Munich
August 1991 - July 1992   Red-Bluff-Union High School, California, USA
September 1992 - July 1994   Elsa-Brändström-Gymnasium, Munich
                                    Grade: Abitur

University:
October 1994 - January 2000   University, study of biology at the Ludwig-Maximilian-University, Munich, Germany

April 1999 - January 2000   Diploma thesis at the Max-Planck-Institute of Neurobiology, Martinsried, in the group of Dr. Magdalena Götz, "How are neurons specified in certain regions of the brain? *In-vitro*-analyses of the regionspecific influence on neurons and their precursors in the telencephalon of the mouse."

26.1.2000   Diploma of biology (Master of Science), Ludwig-Maximilian-University, Munich, Germany

February 2000 - December 2004 PhD-student in the group of PD Dr. Magdalena Götz at the Max-Planck-Institute of Neurobiology, Martinsried, Germany
Move to the GSF/Institute for Stem cell Research, Neuherberg, Germany
"The role of Emx1 and Emx2 in the developing chick telencephalon"

Publications:

Frowein, J. (2000). How are neurons specified in certain regions of the brain? *In-vitro*-analyses of the regionspecific influence on neurons and their precursors in the telencephalon of the mouse. *Diplomathesis*

Frowein J.v., Campbell K., Götz M. (2002) Expression of Ngn1 and 2, Gsh2 and Sfrp1 in the developing chick telencephalon. *Mech.Dev.* 110, 249-252.

127